COMPUTATIONAL FLUID DYNAMICS ANALYSIS OF THE EFFECTS OF RODENT ACTIVITIES IN VENTILATED CAGES

By

JATIN LAMBA

A THESIS PRESENTED TO THE GRADUATE SCHOOL
OF THE UNIVERSITY OF FLORIDA IN PARTIAL FULFILLMENT
OF THE REQUIREMENTS FOR THE DEGREE OF
MASTER OF SCIENCE

UNIVERSITY OF FLORIDA

2005

This document is dedicated to my family for their unwavering support

ACKNOWLEDGMENTS

I would first like to thank my advisor, Dr. H. A. Ingley. Dr. Ingley shared his knowledge with me and always motivated me to do better. I would also like to thank Dr. S. A. Sherif and Dr. J. Chung for acting as my committee members and for the time and support they provided.

I would also like to thank my friends especially, Ashutosh Pandey and Rohit Sharma.

Above all I would like to express my gratitude to my parents and brothers for their unwavering support and blessings.

TABLE OF CONTENTS

page

ACKNOWLEDGMENTS iv

LIST OF TABLES vii

LIST OF FIGURES viii

NOMENCLATURE xii

ABSTRACT xv

CHAPTER

1 INTRODUCTION 1

2 LITERATURE REVIEW 5

3 APPROACH 20

4 RESULTS AND DISCUSSION 26

5 SUMMARY AND CONCLUSIONS 53

6 RECOMMENDATIONS 56

APPENDIX

A MESH CAGE PROFILES 57

B CONTOURS OF DIFFERENT SPECIES 59

C CALCULATIONS FOR POWER CONSUMPTION AND SAVINGS 80

D CALCULATIONS FOR VERIFICATION OF MASS FLOW RATE 82

E CASES THAT DID NOT WORK 84

F GOVERNING EQUATIONS 86

LIST OF REFERENCES 88

BIOGRAPHICAL SKETCH 90

LIST OF TABLES

Table page

2-1 Effect of cage ventilation and frequency of cage changes on microenvironment.....9

2.2 Response time needed for CO_2 concentrations to reach above 3%.....11

2-3 Ammonia concentrations in IVC2S & IVC1 for negative pressure.....13

2-4 Ammonia concentrations in IVC2S & IVC1 for positive pressure.....14

2-5 Comparisons of CO_2, and NH_3, concentrations.....19

2-6 Results of CO_2, and NH_3, concentrations.....19

3-1 Model definitions.....24

3-2 Discretization scheme.....25

3-3 Variable definitions.....25

4-1 Results from CFD simulations.....49

4-2 CO_2 and NH_3 concentrations Vs. ACPH for center of cage case.....49

4-3 Comparison of NH_3 concentrations for different cases at 60 ACPH.....51

4-4 Comparisons of NH_3 concentrations against results reported by Pandey (2005) at 100 ACPH.....51

4-5 Comparisons of NH_3 concentrations against results reported by Pandey (2005) at 60 ACPH.....52

LIST OF FIGURES

Figure page

2-1 Effect of 1% and 3% CO_2 on mice preference 6

2-2 Effect of airspeeds on mice preference 7

2-3 Effect of air change rates on preference of mice 8

2-4 Cage microenvironment 10

2-5 CO_2 concentrations in different types of sealed filter top cages 11

2-6 Schematic diagram of Hasegawa apparatus 15

2-7 CO_2 concentrations in FVMIS cages 16

2-8 Geometry of Allentown cage 17

2-9 Contours of CO_2 for corner bottom at 100 ACPH 18

2-10 Contours of CO_2 for whole bottom at 100 ACPH 18

3-1 Mice positioned at the outer walls of the cage 22

3-2 Mice positioned along the y axis 22

3-3 Mice positioned at the center of the cage 23

3-4 Meshing scheme used in the LM case 24

4-1 Outside wall case 27

4-2 Center of cage case 27

4-3 Four mice case 28

4-4 Velocity profiles for center of cage at 100 ACPH 29

4-5 Contours of mole fraction of CO_2 for center of cage (100 ACPH) 30

4-6 Contours of mole fraction of NH_3 for center of cage (100 ACPH) 31

4-7 Top view of contours of mole fraction of NH_3 for center of cage (100 ACPH) 31
4-8 Velocity profiles for four mice at 60 ACPH 32
4-9 Contours of mole fraction of CO_2 for four mice (60 ACPH) 33
4-10 Contours of mole fraction of NH_3 for four mice (60 ACPH) 33
4-11 Top view of contours of mole fraction of NH3 for four mice (60 ACPH) 34
4-12 Velocity profiles for outside wall at 60 ACPH 35
4-13 Contours of mole fraction of CO_2 for outside wall (60 ACPH) 36
4-14 Contours of mole fraction of NH_3 for outside wall (60 ACPH) 36
4-15 Top view of contours of mole fraction of NH_3 for outside wall (60 ACPH) 37
4-16 Velocity profiles for center of cage case at 20 ACPH 38
4-17 Contours of mole fraction CO_2 for center of cage (20 ACPH) 39
4-18 Contours of mole fraction of NH_3 for center of cage (20 ACPH) 40
4-19 Top view of contours of mole fraction of NH_3 for center of cage (20 ACPH) 40
4-20 Velocity profiles for outside wall at 40 ACPH 41
4-21 Contours of mole fraction of CO_2 for outside wall (40 ACPH) 42
4-22 Contours of mole fraction of NH_3 for outside wall (40 ACPH) 42
4-23 Top view of contours of mole fraction of NH_3 for outside wall (40 ACPH) 43
4-24 Velocity profiles for center of cage at 60 ACPH 44
4-25 Contours of mole fraction of CO_2 for center of cage (60 ACPH) 45
4-26 Contours of mole fraction of NH_3 for center of cage (60 ACPH) 45
4-27 Top view of contours of mole fraction of NH_3 for center of cage (60 ACPH) 46
4-28 Velocity profiles for center of cage case at 40 ACPH 47
4-29 Contours of mole fraction of CO_2 for center of cage case (40 ACPH) 47
4-30 Contours of mole fraction of NH_3 for center of cage case (40 ACPH) 48
4-31 Top view of contours of mole fraction of NH_3 for center of cage case (40 ACPH) 48

4-32 CO_2 concentrations Vs. ACPH....50
4-33 NH_3 concentrations Vs. ACPH....50
A-1 Mesh used for CC case....57
A-2 Mesh used for OW case....58
B-1 Contours of CO_2 for CC in X-Y-Z plane (100 ACPH)....59
B-2 Contours of CO_2 for CC in X-Y plane (100 ACPH)....60
B-3 Contours of CO_2 for CC in Z-X plane (100 ACPH)....60
B-4 Contours of NH_3 for CC in X-Y-Z plane (100 ACPH)....61
B-5 Contours of NH_3 for CC in X-Y plane (100 ACPH)....61
B-6 Contours of NH_3 for CC in Z-X plane (100 ACPH)....62
B-7 Contours of CO_2 for LM in X-Y plane (60 ACPH)....62
B-8 Contours of CO_2 for LM in X-Y-Z plane (60 ACPH)....63
B-9 Contours of CO_2 for LM in Z-X plane (60 ACPH)....63
B-10 Contours of NH_3 for LM in X-Y plane (60 ACPH)....64
B-11 Contours of NH_3 for LM in X-Y-Z plane (60 ACPH)....64
B-12 Contours of NH_3 for LM in Z-X plane (60 ACPH)....65
B-13 Contours of CO_2 for OW in X-Y-Z plane (60 ACPH)....65
B-14 Contours of CO_2 for OW in X-Y plane (60 ACPH)....66
B-15 Contours of CO_2 for OW in Z-X plane (60 ACPH)....66
B-16 Contours of NH_3 for OW in X-Y plane (60 ACPH)....67
B-17 Contours of NH_3 for OW in Z-X plane (60 ACPH)....67
B-18 Contours of NH_3 for OW in X-Y-Z plane (60 ACPH)....68
B-19 Contours of CO_2 for CC in X-Y plane (20 ACPH)....68
B-20 Contours of CO_2 for CC in X-Y-Z plane (20 ACPH)....69
B-21 Contours of CO_2 for CC in Z-X plane (20 ACPH)....69

B-22 Contours of NH_3 for CC in X-Y plane (20 ACPH) 70
B-23 Contours of NH_3 for CC in X-Y-Z plane (20 ACPH) 70
B-24 Contours of NH_3 for CC in Z-X plane (20 ACPH) 71
B-25 Contours of CO_2 for OW in X-Y-Z plane (40 ACPH) 71
B-26 Contours of CO_2 for OW in Z-X plane (40 ACPH) 72
B-27 Contours of CO_2 for OW in X-Y plane (40 ACPH) 72
B-28 Contours of NH_3 for OW in X-Y-Z plane (40 ACPH) 73
B-29 Contours of NH_3 for OW in Z-X plane (40 ACPH) 73
B-30 Contours of NH_3 for OW in X-Y plane (40 ACPH) 74
B-31 Contours of CO_2 for CC in X-Y plane (60 ACPH) 74
B-32 Contours of CO_2 for CC in Z-X plane (60 ACPH) 75
B-33 Contours of NH_3 for CC in X-Y plane (60 ACPH) 75
B-34 Contours of NH_3 for CC in X-Y-Z plane (60 ACPH) 76
B-35 Contours of NH_3 for CC in Z-X plane (60 ACPH) 76
B-36 Contours of CO_2 for CC in X-Y plane (40 ACPH) 77
B-37 Contours of CO_2 for CC in X-Y-Z plane (40 ACPH) 77
B-38 Contours of CO_2 for CC in Z-X plane (40 ACPH) 78
B-39 Contours of NH_3 for CC in X-Y plane (40 ACPH) 78
B-40 Contours of NH_3 for CC in X-Y-Z plane (40 ACPH) 79
B-41 Contours of NH_3 for CC in Z-X plane (40 ACPH) 79
E-1 Single mouse in Y- direction 84
E-2 Two mice in the center of cage in X- direction 84
E-3 Four mice in the center of cage in Y- direction 85
E-4 Four mice in the center of cage in X- direction 85

NOMENCLATURE

CFD	Computational Fluid Dynamics
ACPH	Air Changes per hour
CO_2	Carbon dioxide
NH_3	Ammonia
W	Weight of each mouse
V	Volume of each mouse
d	Diameter of each mouse
L	Length of each mouse
OW	Outside wall case
LM	Four mice case
CC	Center cage case
Q_1	Flow rate in $feet^3$ per minute for 100 ACPH
Q_2	Flow rate in $feet^3$ per minute for 60 ACPH
Q_3	Flow rate in $feet^3$ per minute for 40 ACPH
Q_4	Flow rate in $feet^3$ per minute for 20 ACPH
P_1	Power at 100 ACPH for 140 cages
P_2	Power at 60 ACPH for 140 cages
P_3	Power at 40 ACPH for 140 cages
P_4	Power at 20 ACPH for 140 cages
P_5	Power at 30 ACPH for 140 cages

S_1 Savings per year at 60 ACPH

S_2 Savings per year at 40 ACPH

S_3 Savings per year at 20 ACPH

S_4 Savings per year at 30 ACPH

K Turbulent kinetic energy

v Velocity

M Number of elements in the system

N Number of species

div Divergence

Greek

ε Dissipation rate

μ Viscosity

ρ Density of each mouse

τ_{ij} Shear Stress

g_i Body force in the i^{th} coordinates

δ_{ij} Krockner delta

σ_ε Empirical constants

$c_{\varepsilon 1}$ Empirical constants

$c_{\varepsilon 2}$ Empirical constants

J_{ij} Mass molecular flux of species i in j^{th} direction

D_i Diffusion Coefficient

Z_i Mass fraction of i^{th} element

Y_i Mass fraction of species

μ_T Turbulent exchange coefficient

μ_{ij} Number of kilograms of element i in a kilogram of species j

w_i Mass rate of creation of species i

Abstract of Thesis Presented to the Graduate School
of the University of Florida in Partial Fulfillment of the
Requirements for the Degree of Master of Science

COMPUTATIONAL FLUID DYNAMICS ANALYSIS OF THE EFFECTS OF RODENT ACTIVITIES IN VENTILATED CAGES

By

Jatin Lamba

December 2005

Chair: Herbert Ingley III
Major Department: Mechanical and Aerospace Engineering

The purpose of this study was to perform a computational fluid dynamics analysis to study the effects of rodent activities on selected air quality indicators (e.g., carbon dioxide, ammonia and humidity) in a ventilated rodent cage. The individually ventilated cage system is the most widely used method for rodent housing. Various studies have been performed to develop the optimum ventilation performance in the ventilated rodent cage. These studies have included variables such as ventilation rates, the structure of the cage and various other parameters as they affect the microenvironment variables of temperature, relative humidity, ammonia and carbon dioxide. *The Guide for Care and Use of Laboratory Animals*, The Institute of Laboratory Animal Resources and the *American Society of Heating Refrigerating and Air Conditioning Engineers Applications and Fundamentals Handbook* provide guidelines for these microenvironment variables.

Computational fluid dynamics (CFD) was used for analyzing the rodent cage environment. A conventional Allentown rodent cage PC7115RT was used for the CFD

modeling. Various locations in the cage were analyzed in the GAMBIT software. The rodents were modeled as half cylinders generally representing the size of rodents for the analyses. The cylinders were then treated as sources of carbon dioxide. FLUENT software was used to determine the effects of these sources on the microenvironment of the cage.

The results for 100 and 60 ACPH agreed with the previously published experimental and CFD results. The prevailing concentrations of CO_2 and NH_3 for the case with two mice positioned near the inlet nozzle of the cage were 970 ppm and 6 ppm respectively at 100 ACPH and 4300 ppm and 27 ppm respectively at 20 ACPH. The average concentrations of CO_2 and NH_3 for the case with four mice positioned along the y-axis were 1350 ppm and 9 ppm respectively at 60 ACPH. The most prevalent concentrations of CO_2 and NH_3 for the case with two mice bodies positioned at the outer walls opposite to each other away from the nozzle were 1000 ppm and 11 ppm respectively at 60 ACPH.

The CO_2 and NH_3 concentrations increased with a decrease in air change rates. From the plots it could be seen that 30 ACPH is an optimum air change rate in terms of acceptable cage environment conditions and savings as compared to 100 ACPH. With further CFD studies it may be possible to produce a design that could effectively ventilate rodent cages.

CHAPTER 1
INTRODUCTION

At present the use of rodents as research subjects is playing an extremely significant role in medical research. Laboratory mice have been a major component of medical research since the 1880's.The microenvironment as defined by the levels of carbon dioxide, ammonia, temperature, and humidity must be maintained properly for research and the well being of the animals. In order to provide proper care for the animals, criteria for the needs of the animals are required (Institute of Laboratory Animal Resources, 1996). As there is no specified acceptable CO_2 concentration for mice so assuming acceptable CO_2 concentrations for humans that is 5000 ppm as a standard. The acceptable NH_3 concentration specified by the guide for ventilated cages is 25 ppm.

Guidelines for experiments with rodents are provided by the *Guide for Care and Use of Laboratory Animals*, the Institute of Laboratory Animal Resources and the *American Society of Heating Refrigerating and Air Conditioning Engineers Applications and Fundamentals Handbooks*. The guide recognizes computational fluid dynamics as a technique for studying the optimum performance of ventilated cages.

The two major types of rodent caging systems in use today are static and ventilated cages. The static cages with filter tops have been known to provide a protective barrier for rodents and thereby reduce the transcage coupling of microenvironment contaminants. Studies have shown these cages effectively reduce cross-contamination by particulate materials. However studies have also shown that the use of filter top cages can

cause large accumulations of carbon dioxide, ammonia and relative humidity which have adverse effects on the health of rodents and thereby, their performance in medical studies.

Ventilated cages help in reducing the high levels of carbon dioxide, ammonia and humidity in the cages. This technology has led to a significant increase in the use of ventilated cages as a method of housing research mice.

Various designs are being utilized to provide ventilation to rodent cages. The basic difference between them is in the way the air is introduced into the cages. Air can be supplied directly by a portable blower and filter through a coupling attached to the cage. The top of the cage and the base of the cage can be used to provide air to the cage. Automatic watering may be combined with the system if air is provided at the base of the cage. Automatic watering saves labor (White, 2001).

An indirect method of supplying air is by using individually mounted rack blowers. The blower supplies air at high velocity over the filter on the cage, which pushes the air through the filter into the cage. This method reduces the chance of contamination that may be caused due to inadequate disinfection of cage couplings used in ventilation. Filters should be changed regularly as the length of use affects the resistance provided by the cage, which can affect the ventilation efficiency (A Guide to Research Rodent Housing).

Captured exhaust is another method of providing air to ventilated system. Air can be pulled directly into the cage through a filtered cage connection. A vacuum port above the filter top can also be used to pull in exhaust air. The port is not directly connected to the exhaust of the cage and it does not capture all the exhaust air from the cage. This

method provides reduction in heat load, and moisture (A Guide to Research Rodent Housing).

Pandey (2005) conducted a computational fluid dynamics analysis of ventilated cages. A conventional Allentown cage PC 7115RT was used for the study. The cage was analyzed for two different air change rates for carbon dioxide, ammonia, relative humidity, and temperature. The corners of the cages were selected as latrine areas and were also considered as sources of carbon dioxide due to mice respiration. For the second case the whole bottom of the cage was selected as a source of carbon dioxide, ammonia, and relative humidity. However, mice bodies were not included in the geometry and the bottom of the cage was taken as a source of carbon dioxide, ammonia, heat, and humidity for one case.

The geometry of a conventional Allentown rodent cage PC 7115RT was also used in the current study. Computational fluid dynamics was used to construct the cage and determine the flow of air in the cage. FLUENT 6.2.16 and Gambit 2.2.30 provided the computational software for these analyses. Gambit was used to construct the geometry of cage and also to specify the rodent position. The geometry was then analyzed in FLUENT for the concentration distribution of microenvironment variables like carbon dioxide, and ammonia. In the current study cylinders generally representing the size of the rodents simulated mice bodies. The cylinders were treated as source of carbon dioxide. Different positions of mice and latrines were then analyzed. A study of the effects of rodent activity on microenvironment variables in the ventilated cages could help in improving the performance of these cages.

Three different locations were analyzed for the study. For the first case two mice were located in the center of the cage near the inlet nozzle. This case was analyzed for 20, 40, 60, and 100 ACPH. The mice bodies were positioned next to each other to reduce the complexity of the model. This case was analyzed for 40 and 60 ACPH. Two mice were positioned opposite to each other along the outer wall of the cage for the second case. For the third case two half cylinders were positioned a small distance away from the center of the cage. The two half cylinders were double the length of the other mice bodies analyzed in the study. The two half cylinders represented four mice present in the cage. This case was analyzed for 60 ACPH.

CHAPTER 2
LITERATURE REVIEW

This chapter reviews literature relevant to the microenvironment parameters such as carbon dioxide, ammonia, temperature, and relative humidity for ventilated rodent cages.

Krohn et al. (2003B) studied the effect of the presence of CO_2 in rodent cages. The presence of CO_2 on heart rate and blood pressure of the mice was studied by considering concentrations of 1%, 3% and 5% of CO_2 in the air in the cages. Figure: 2.1 (Krohn et al., 2003B) shows the effects of CO_2 on mice. The figure shows the distribution of dwelling time of mice at day and night in ventilated cages and in cages with 1% and 3% concentrations of CO_2. It can be seen that for the case of 1% CO_2, there is very little difference between the dwelling times of mice in ventilated and ones with fixed concentration of CO_2. However, for the case of 3% CO_2, the mice prefer ventilated cages.

The study showed that rodents were not affected at levels up to 3% CO_2 but were affected significantly at concentrations of CO_2 above 3% in the air.

In another study, Krohn et al. (2003A) analyzed the effect of air speed in ventilated cages. The study was conducted for air speeds less than 0.2 m/s and greater than 0.5 m/s and how these air speeds affect the performance of rats. Figure 2-2 (Krohn et al., 2003A) shows the distribution of dwelling time of mice in ventilated cages in comparison to low air speeds and high air speeds. It can be seen that the mice prefer to stay in cages with high air velocity than lower air velocity.

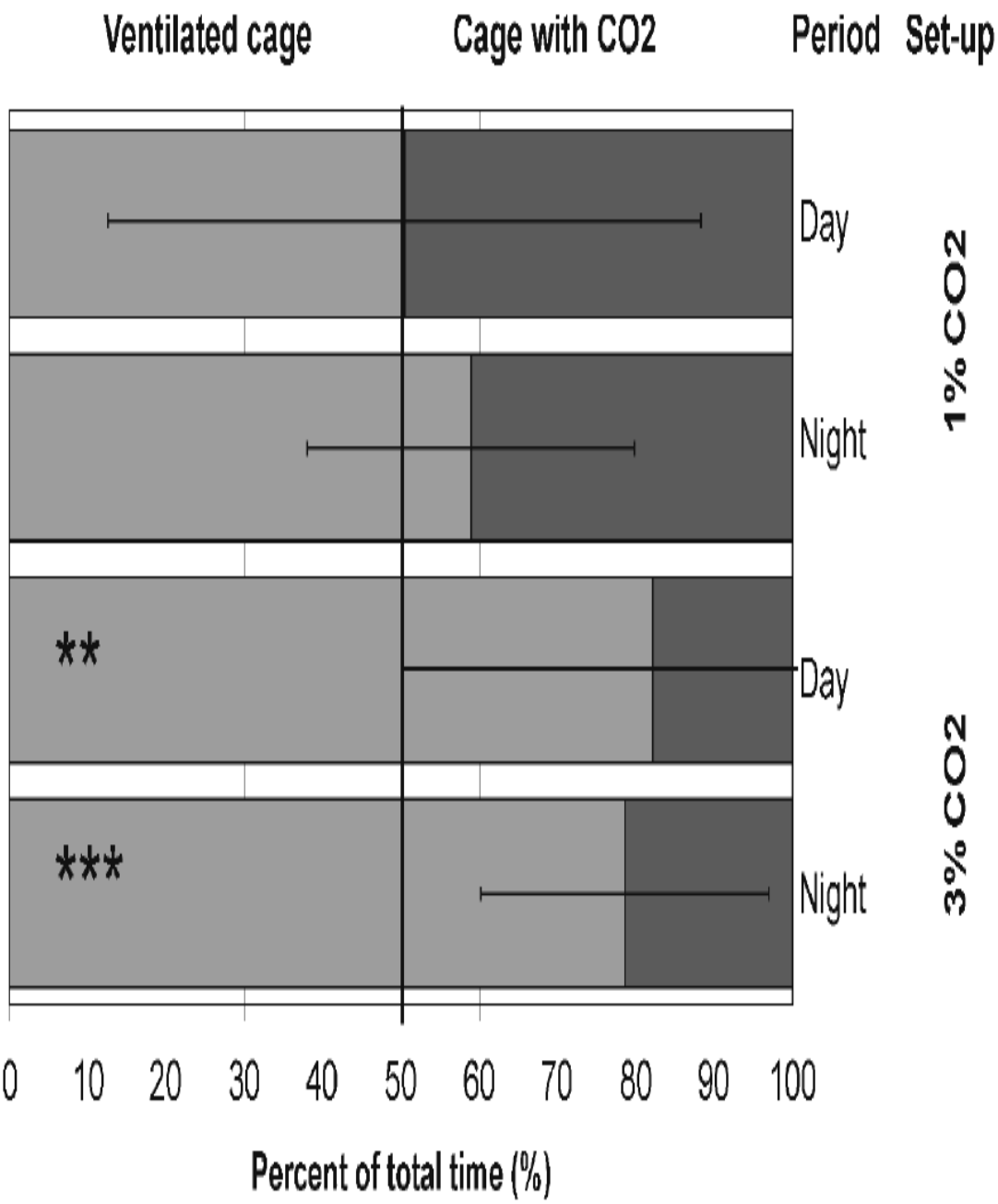

Figure 2-1. Effect of 1% and 3% CO_2 on mice preference (Krohn et al., 2003B)

The effect of 50, 80 and 120 air changes on rats was also analyzed by Krohn et al (2003A). It can be seen from Figure 2-3 (Krohn et al., 2003A) that mice prefer to dwell in cages with an 80 ACPH over cages with ACPH 50 and 120 respectively. The dwelling time of mice in cages with 120 ACPH is greater than that of cages with ACPH of 50. Thus preferred ACPH in cages lays around 80 ACPH.

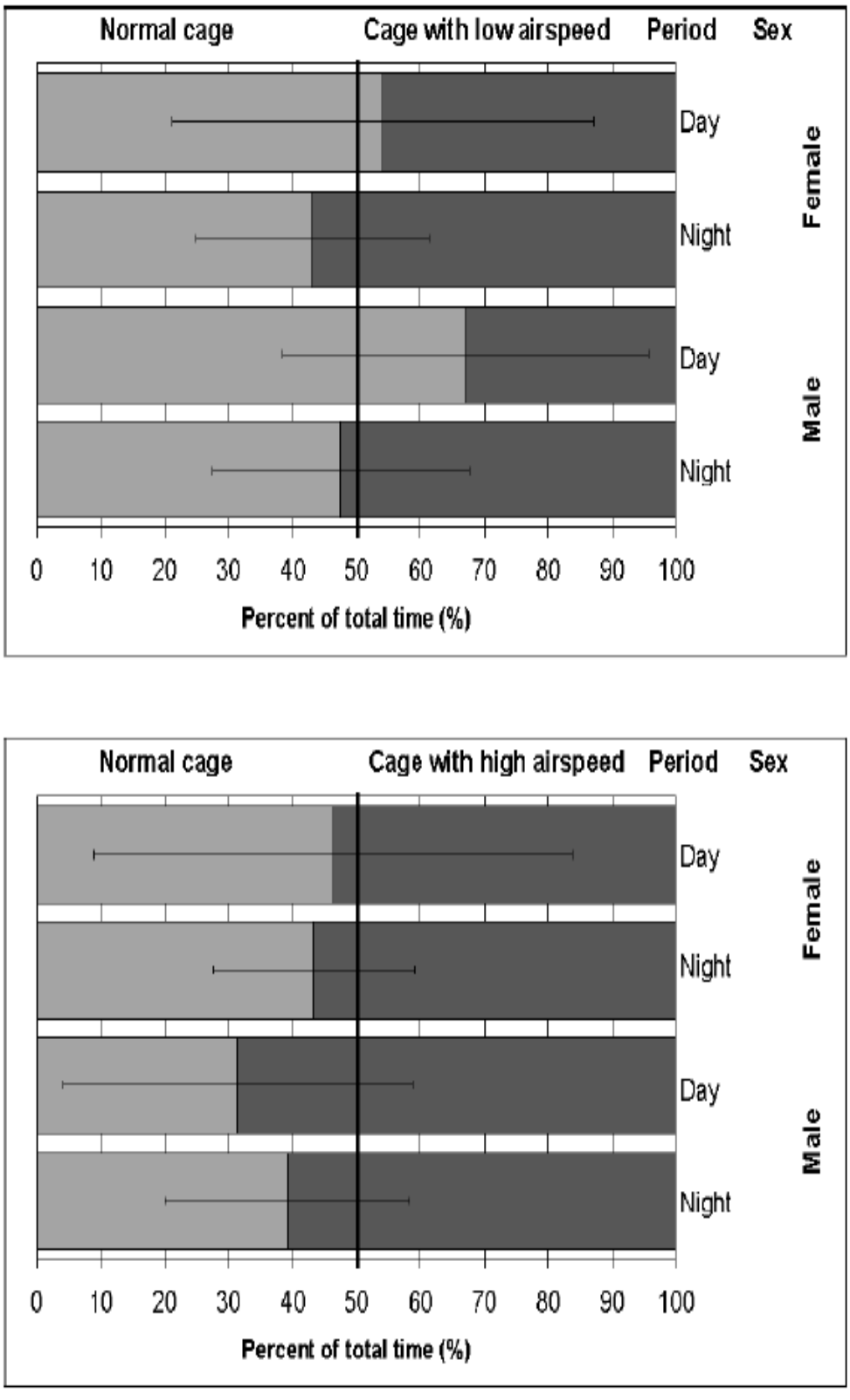

Figure 2-2. Effect of airspeeds on mice preference (Krohn et al., 2003A)

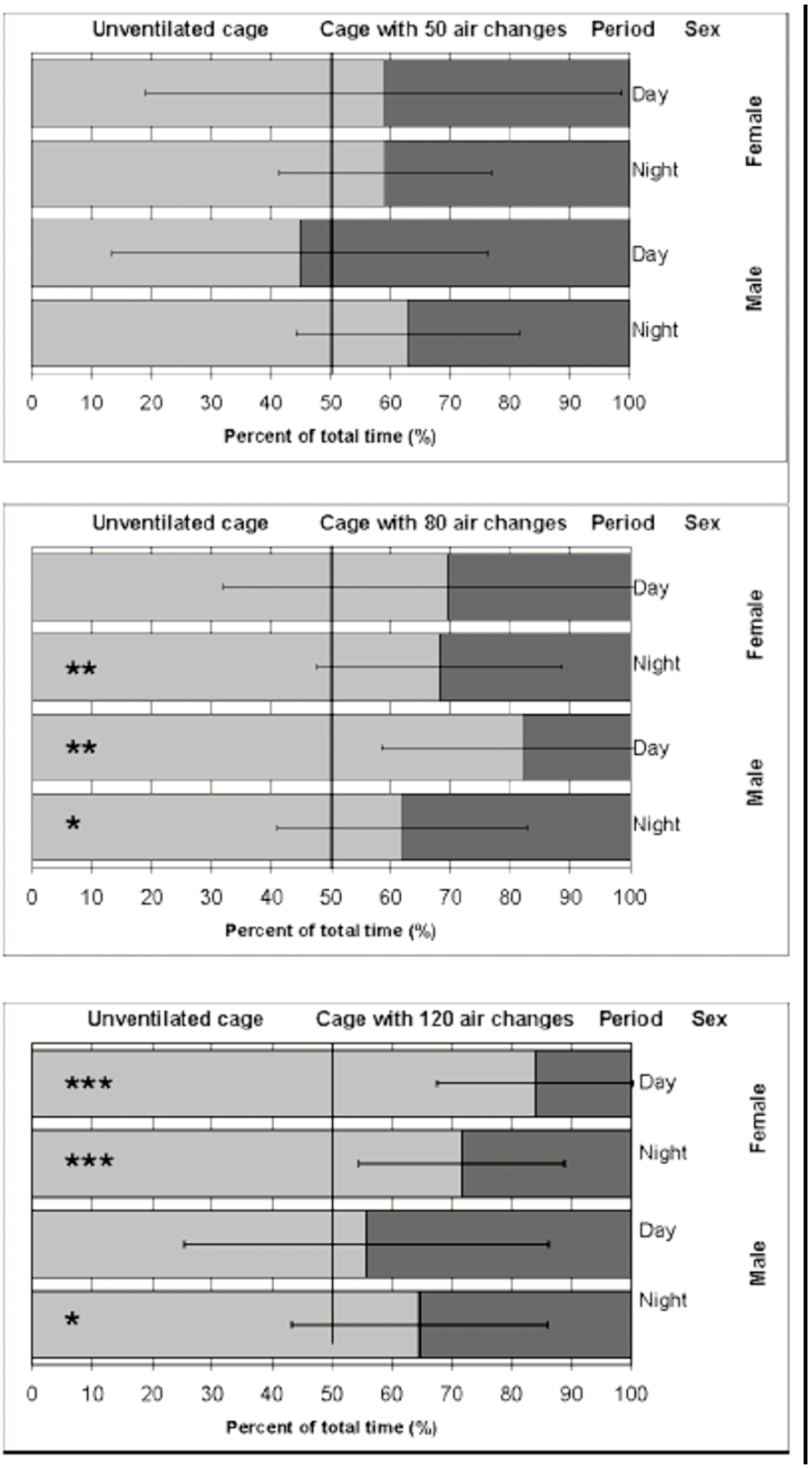

Figure 2-3. Effect of air change rates on preference of mice (Krohn et al., 2003A)

Reeb et al. (2001) studied the health of mice and the microenvironment of cages for bed changing frequencies of 7, 14 and 21 days, for ventilation rates of 30, 60 and 100 air changes per hour. The concentrations of ammonia, CO_2 and relative humidity and temperature changes were analyzed over a period of 4 months. Three mice each were housed in all the cages. Maxi-Miser PIV cages were used for the study. Table: 2.1 (Reeb et al., 2001) show the effect of ventilation rates and the frequency of cage changes on the microenvironment of the cage. It can be seen that the concentration of ammonia decreases with the decrease in the frequency of cage changes. However, the concentration of ammonia was lower at higher ventilation rates. The relative humidity of the air in the cages did not vary significantly with either the change in ventilation rates or the frequency of cage changes. The concentration of CO_2 increased with the decrease in the frequency of cage changes. Figure 2.4 (Reeb et al., 2001) shows the effect of air change rates on ammonia and relative humidity based on the results from Table 2-1.

Table 2-1. Effect of cage ventilation and frequency of cage changes on microenvironment

	Frequency of cage change, days [mean ± SEM (*n*)*]		
	7	14	21
Ammonia (ppm)			
30 air changes/h	26.3 ± 5.7[‡a] (12)	62.8 ± 17.6[a] (5)	73.0 ± 15.4[a] (4)
60 air changes/h	1.5 ± 0.2[‡b] (14)	14.6 ± 6.7[b] (10)	26.9 ± 19.1[b] (9)
100 air changes/h	1.1 ± 0.2[§b] (13)	3.7 ± 1.5[b] (8)	15.4 ± 7.4[b] (6)
Relative humidity (%)			
30 air changes/h	57 ± 1[a]	52 ± 2	57 ± 4
60 air changes/h	48 ± 2[b]	53 ± 4	52 ± 3
100 air changes/h	48 ± 2[b]	51 ± 3	46 ± 2
Carbon dioxide (ppm)			
30 air changes/h	2190 ± 185[a]	1475 ± 90	2050 ± 215[a]
60 air changes/h	1310 ± 145[b]	1775 ± 300	1415 ± 240[a,b]
100 air changes/h	1110 ± 110[b]	1575 ± 270	945 ± 200[b]
Temperature (°C)			
30 air changes/h	24.4 ± 0.2	24.4 ± 0.3	24.8 ± 0.6
60 air changes/h	24.1 ± 0.4	24.1 ± 0.6	23.4 ± 0.5
100 air changes/h	23.2 ± 0.3	23.2 ± 0.2	24.1 ± 0.5

*(*n*) is the number of measurements and applies to all parameters; [‡]Value is significantly different from 14 and 21 day conditions in same row ($P < 0.05$); [§] Value is significantly different from 21 day condition in same row ($P < 0.05$); [a] Within a column, values with different superscript letters differ significantly ($P < 0.05$)

(Reeb et al., 2001)

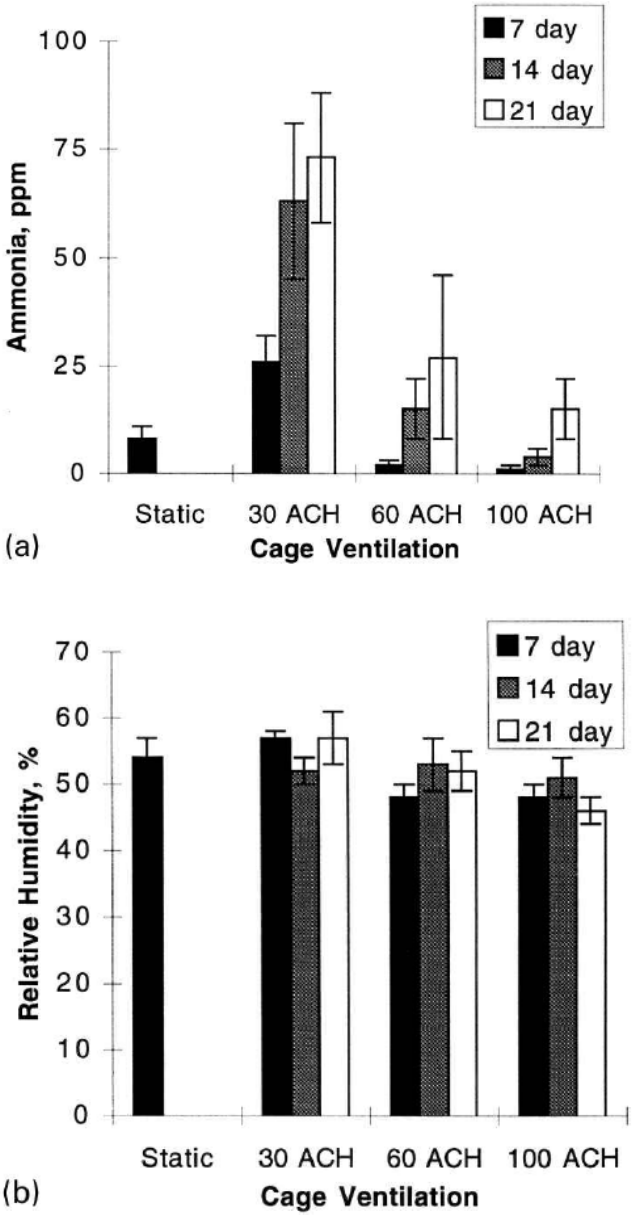

Figure 2-4. Cage microenvironment (Reeb et al., 2001)

Krohn and Hansen (2002) conducted a study to estimate the time required for CO_2 concentrations to reach 3% of the cage volume. CO_2 levels were measured over time in different types of individually ventilated cages when no ventilation was provided to the cages. Seven different types of commercially available cages were used for the study. A standard mouse per air volume ratio of 20 gram/liter was reached by providing a number of 8-10 month old rats. Table: 2.2 (Krohn and Hansen 2002) shows the response time

required for CO_2 concentrations to exceed the 3% concentration in different cages. Figure: 2.5 (Krohn and Hansen. 2002) graphically represent the change in CO_2 concentration in different types of cages over a period of time. It can be seen that for standard static filter top, US filter top, and ventirack type of cages, the concentration of CO_2 never exceeded 3% of the total cage volume.

Table 2.2. Response time needed for CO_2 concentrations to reach above 3%

	Standard static filter top (Tecniplast)	US filter top (Tecniplast)	VentiRack (Biozone)	SealSafe filter top (Tecniplast)	Bio.A.S with internal WB (Ehret)	Bio.A.S with external WB (Ehret)	Quantum-Air Maxi-Seal System (Arrowmight)
Cage volume (l)	11	9	6	9	12	9	6.5
Response time (min)	Unlimited	Unlimited	Unlimited	45 ± 7	27 ± 7	23 ± 9	27 ± 16

WB = water bottle

(Krohn and Hansen, 2002)

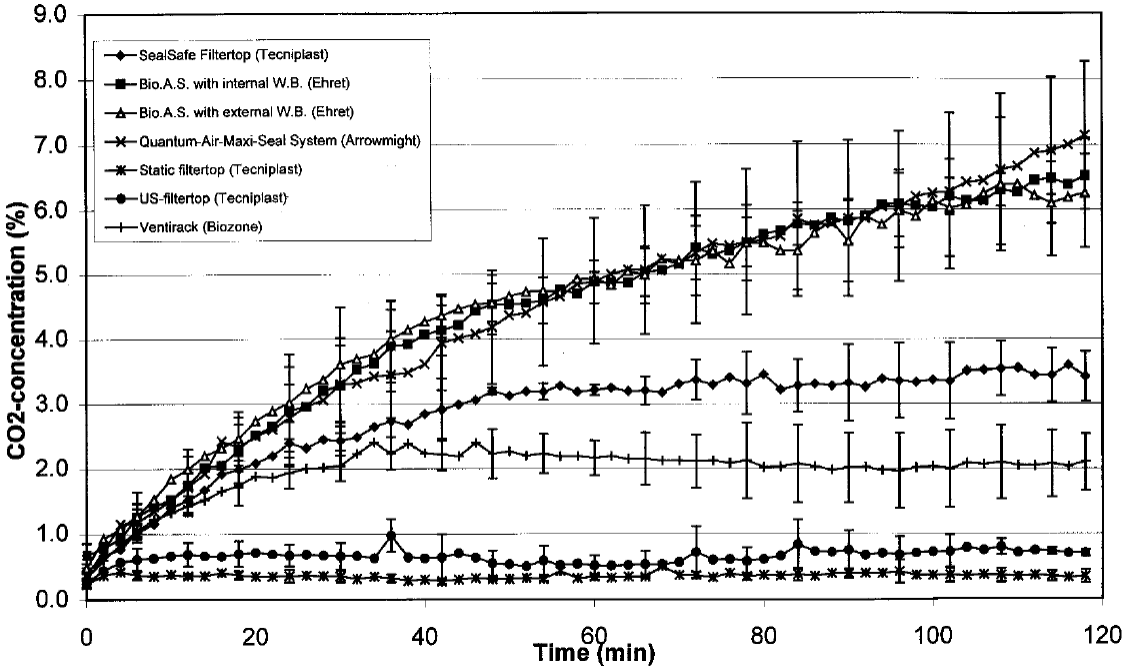

Figure 2-5. CO_2 concentrations in different types of sealed filter top cages (Krohn and Hansen, 2002)

Smith et al. (2004) compared different types of bedding and the effect of these types of bedding on selected micro environmental parameters such as ammonia, carbon

dioxide, relative humidity, and temperature. Results were compared for Nestpaks and loose bedding. C57BL/6J mice and NOD/Ltd mice were used for the study. The results showed that the effect on temperature and relative humidity by bedding type were minimal. The type of bedding significantly affected ammonia concentrations. The cages with hardwood bedding had lower concentrations of ammonia. The study also showed that ventilated cages have significantly lower ammonia concentrations.

Hoglund and Renstrom. (2001) conducted a study to measure the concentrations of ammonia in two different types of individually ventilated cages. BioZone VentiRack, IVC1, and Techniplast SealSafe, IVC2S were the two types of ventilated systems used for the study. The systems were analyzed for negative and positive pressure in the cages for a period of 10 days. Table: 2.3 (Hoglund and Renstrom. 2001) shows the ammonia concentration for negative pressure in both type cages. Table: 2.4 (Hoglund and Renstrom. 2001) shows the ammonia concentration for positive pressure in both types of cages. At the end of 10 days the results showed the ammonia concentration to be lower than 10 ppm in both types of cages. The ammonia concentration was found to be higher in cases where urine had accumulated in the cages.

Memarzedah et al. (2004) conducted a study to compare the environment in static and ventilated cages for different velocities and ventilation designs. The different types of cages used were ventilated cages with exhaust air forced through filters, ventilated cages with forced air inlets and a static cage. The results showed that ventilated cages had higher air velocities, lower relative humidity and lower carbon dioxide and ammonia concentrations.

Table 2-3. Ammonia concentrations in IVC2S & IVC1 for negative pressure

Cage position	1	2	3	4	5	6	7
IVC2S NH_3 (ppm)							
1	1* (3)		1.5 (3)	7.5	11* (3)		7 (3)
2		3.5 (3)		3 (3)		4.5 (1)	
3	0 (3)		3.5 (3)		2 (3)	15* (3)	6.5 (3)
4		2 (3)		2.5 (3)		3 (3)	
5	8* (3)		20* (3)		5.5* (3)		8.5* (3)
6		2.5 (3)		6* (3)			
7							
IVC2S NH_3 (ppm)							
1	8.5 (1)		9 (2)	12	5 (3)	20* (3)	
2		5 (3)	40* (3)	6.5 (3)		5 (3)	
3	4 (3)		10 (3)		5 (3)		
4		7 (1)		6 (3)		20 (3)	
5	7 (3)		6 (3)		4.5 (3)		
6		5.5 (3)		7 (3)		6 (3)	
7	5 (3)		6 (3)		8 (2)		

Figures within parentheses are number of animals in each cage. *Cages where wet corners were noted. Cages in position 4:1 were reference cages that contained no animals. IVC = individually ventilated cage

(Hoglund and Renstrom. 2001)

Table 2-4. Ammonia concentrations in IVC2S & IVC1 for positive pressure

Cage position	1	2	3	4	5	6	7
IVC1 NH_3 (ppm)							
1	0 (3)		1.5 (3)	4	5.5* (3)		1.5 (3)
2		6.5 (3)		1.0 (3)		1.0 (3)	
3	2.5 (3)		1.5 (3)		1.0 (3)		2.0 (3)
4		1.5 (3)		3.5 (3)		1.5 (3)	
5	6* (3)		7.5 (3)		3.5 (3)		3.5 (3)
6		1.5 (3)		5 (3)			
7							
IVC2S NH_3 (ppm)							
1	2 (1)		1.5 (3)	4.5	0.5 (3)		
2		0 (3)		1 (3)		1 (3)	
3	0.5 (3)		2.0* (3)		1 (3)		
4		4.5 (1)		4.0 (3)		5.5* (3)	
5	15* (3)		1 (3)		1.5 (3)		
6		1 (3)		0.5 (3)		6* (3)	
7	0 (3)		2 (3)		2 (2)		

Figures within parentheses are number of animals in each cage. *Cages where wet corners were noted. Cages in position 1:4 were reference cages that contained no animals. IVC=individually ventilated cage

(Hoglund and Renstrom. 2001)

Hasegawa et al. (1997) analyzed the relationship between carbon dioxide concentrations, oxygen and air change rate in forced-air-ventilated micro-isolation systems (FVMIS). Three 8-week-old Wistar strain male rats were used for the study. Figure: 2.6 (Hasegawa et al., 1997) shows the apparatus used for the study.

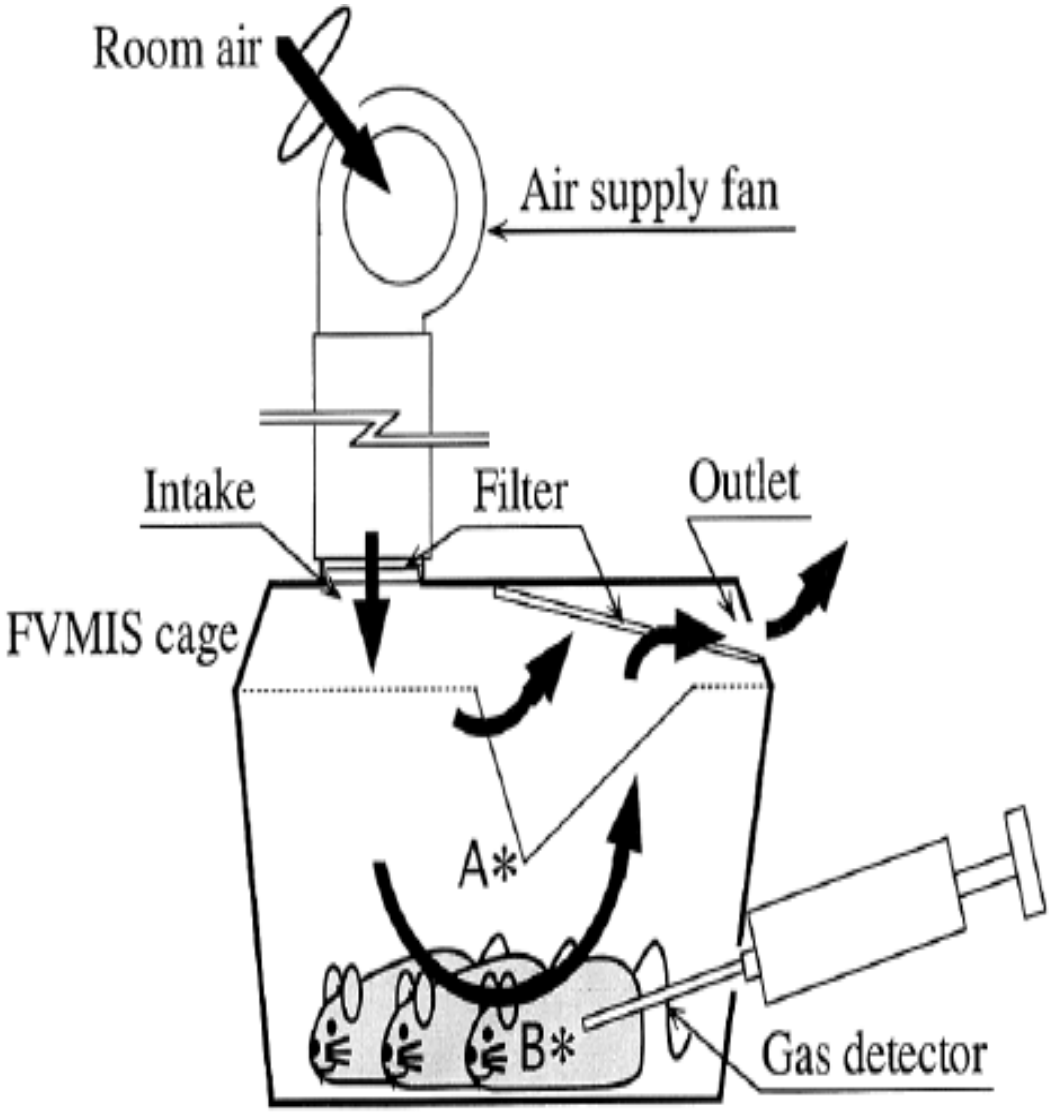

Figure 2-6. Schematic diagram of Hasegawa apparatus (Hasegawa et al., 1997)

Air change rates were varied from 10 ACPH to 120 ACPH and temperature, relative humidity, CO_2 and O_2 were analyzed in the cages. It was noted that with an increase in air change rates, CO_2 concentrations decreased significantly. As no standard

CO_2 concentration in microenvironment of laboratory animals was specified, 5000 ppm was considered as a standard for the study. The air change rate required to maintain the level of CO_2 similar to conventional housing that is less than 5000 ppm (parts per million) was 60 ACPH. Figure: 2.7 (Hasegawa et al., 1997) shows the CO_2 concentration in FVMIS cages at different air changes per hour

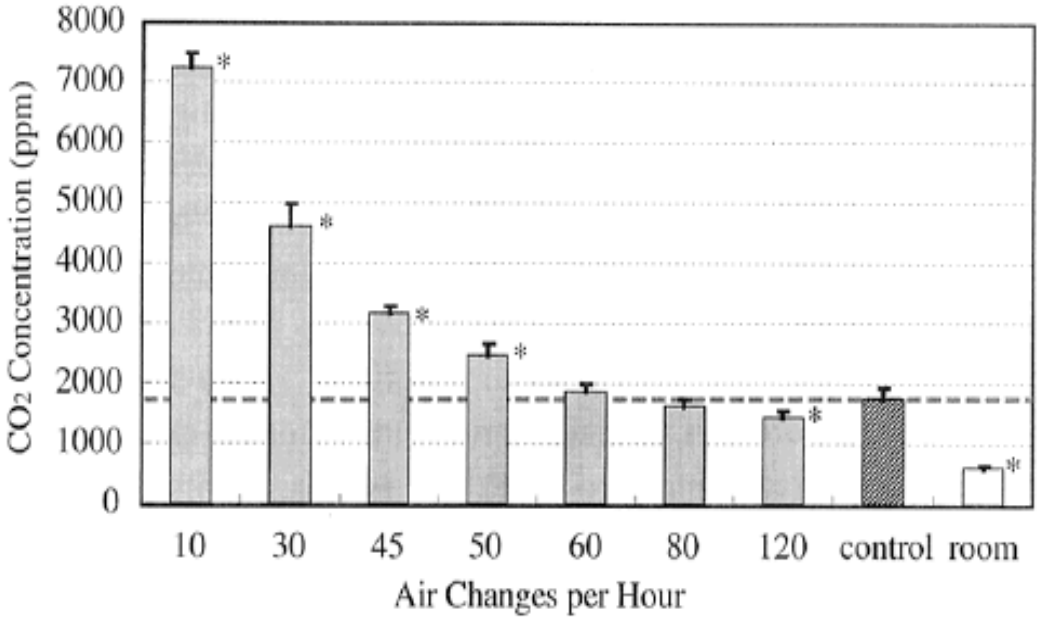

Figure 2-7. CO_2 concentrations in FVMIS cages (Hasegawa et al., 1997)

Pandey (2005) conducted computational fluid dynamics analyses of ventilated cages. Air velocity profiles and concentration distributions for carbon dioxide, ammonia, and water vapor were obtained from the study. A conventional Allentown cage PC 7115RT was analyzed by Pandey. The cage was assumed to house 5 ICR mice. However, the actual mouse geometry was not simulated. The bottom of cage was assumed as a source of carbon dioxide, ammonia, and water vapor in one case, and in the other case small areas at the corners of the cage were considered sources of carbon dioxide, ammonia, and water vapor for second case. The height of cage was reduced by 1” to

compensate for the bedding. The cage geometry was constructed using GAMBIT software. Figure: 2.8 (Pandey, 2005) shows the geometry of the Allentown cage.

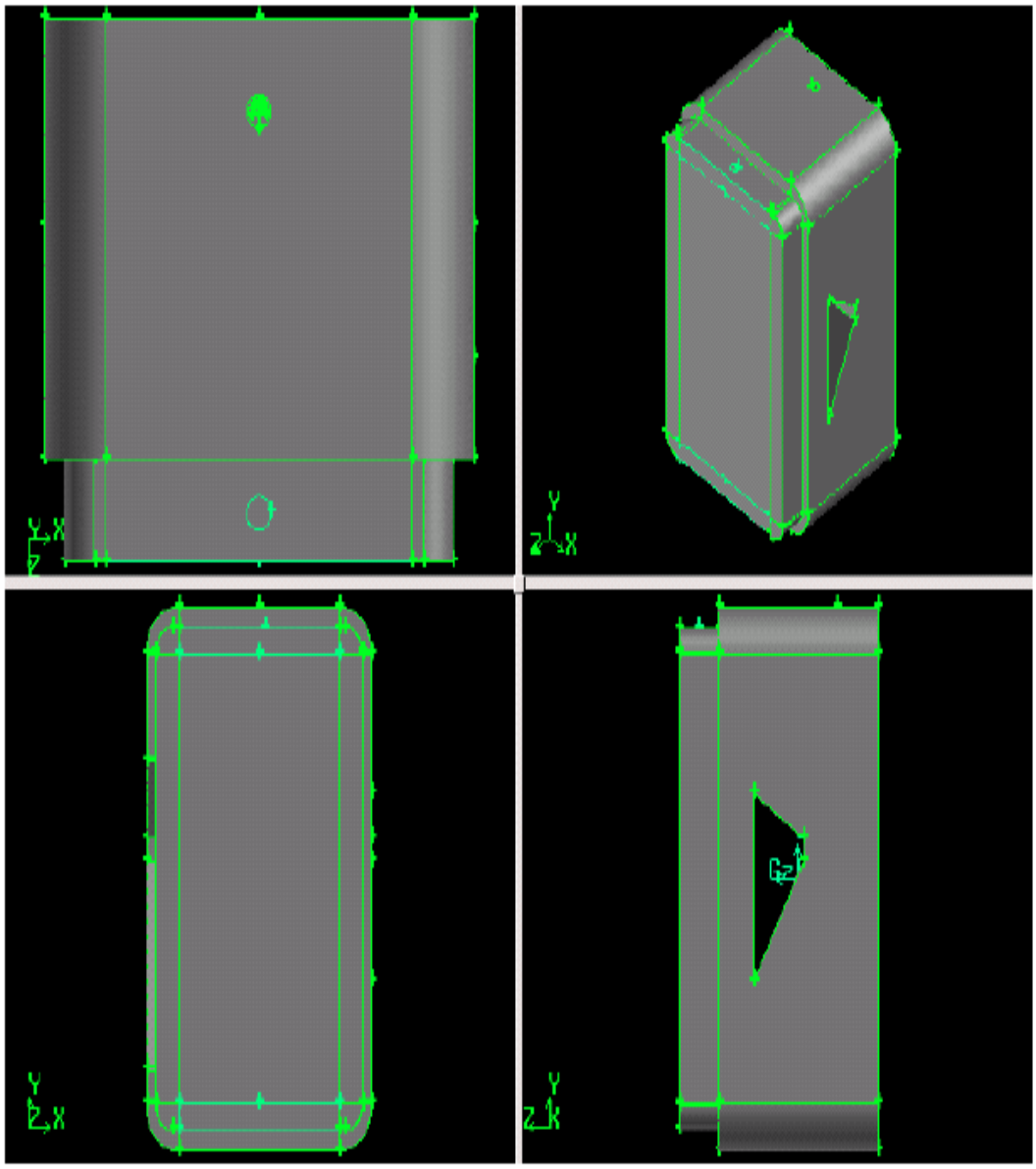

Figure 2-8. Geometry of Allentown cage (Pandey, 2005)

The analyses show that the higher concentrations of CO_2 and NH_3 were towards the opposite corners of the inlet nozzle for both the cases. Figure 2-9: (Pandey, 2005) shows the contours of CO_2 for the corner bottom case. Figure 2-10: (Pandey, 2005) shows the contours of CO_2 for the whole bottom case.

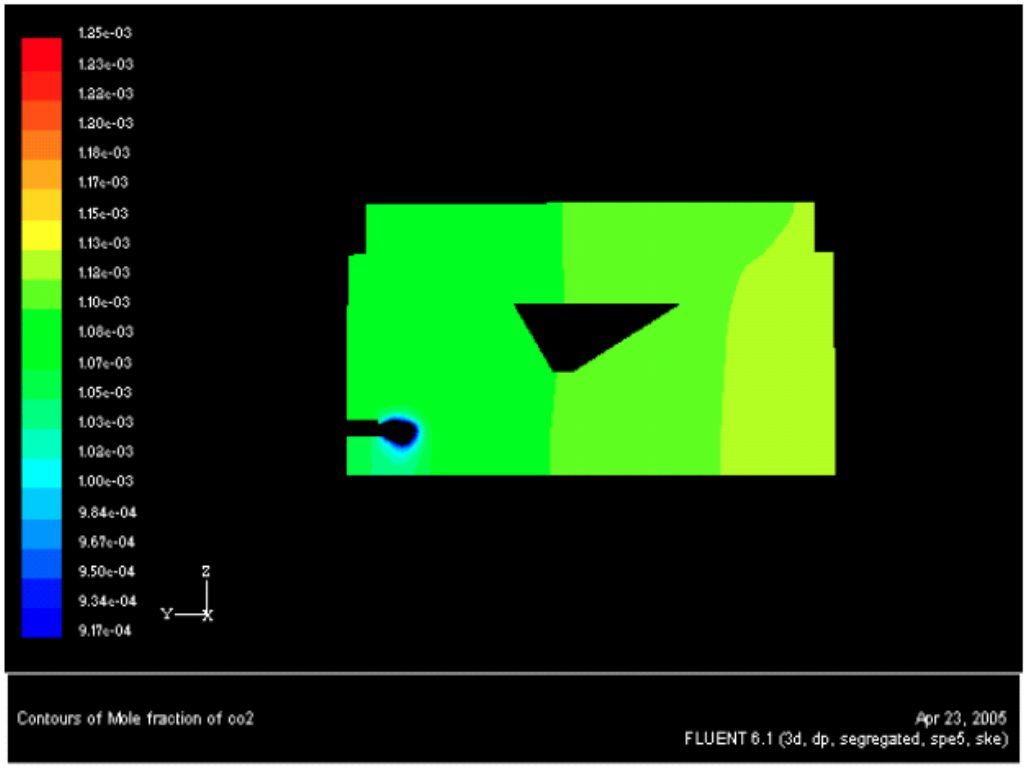

Figure 2-9. Contours of CO_2 for corner bottom at 100 ACPH (Pandey, 2005)

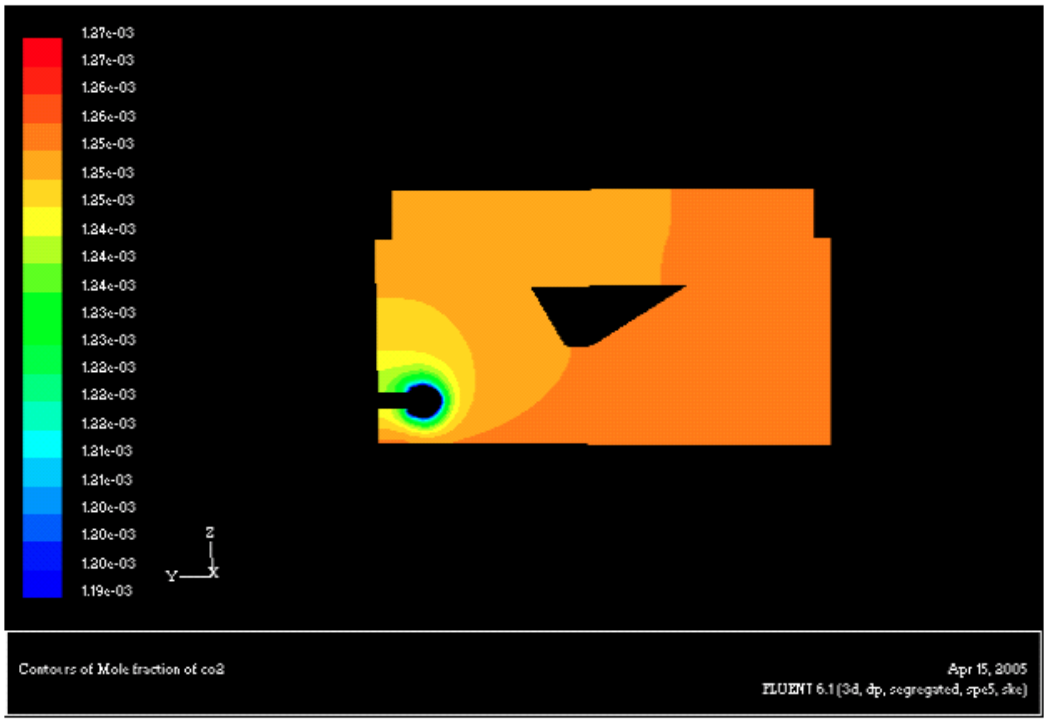

Figure 2-10. Contours of CO_2 for whole bottom at 100 ACPH (Pandey, 2005)

The analyses were carried out for 60 and 100 air changes per hour. The results were validated with the study conducted by Heurkamp et al. (1994). Table: 2.5 (Pandey, 2005) shows validated results. Table: 2.6 (Pandey, 2005) shows the concentrations of ammonia, and carbon dioxide, for 60 ACPH and 100 ACPH for both whole bottom and corner bottom cases.

Table 2-5. Comparisons of CO_2, and NH_3, concentrations

Species	WB (100 ACPH)	CB (100 ACPH)	Huerkamp, M.J., Lehner, N.D.M., (1994) at 112 ACPH
NH_3	8.5 ppm	6.5 ppm	6±8 ppm
CO_2	1190 ppm	1020 ppm	1050±200 ppm

(Pandey, 2005)

Table 2-6. Results of CO_2, and NH_3, concentrations

Species	WB (100 ACPH)	WB (60 ACPH)	CB (100 ACPH)	CB (60 ACPH)
NH_3	8.5 ppm	14.3 ppm	6.5 ppm	13 ppm
CO_2	1190 ppm	2160 ppm	1020 ppm	1920 ppm

WB= Whole Bottom Case, CB= Corner Bottom

(Pandey, 2005)

The study conducted by Pandey (2005) is most pertinent to the current study. The current study is an extension of Pandey's work.

CHAPTER 3
APPROACH

The mice in a rodent cage are sources of sensible and latent heat, water vapor and carbon dioxide. The fecal matter produced by mice, acts as a source of ammonia and moisture. The concentrations of ammonia, and carbon dioxide were analyzed in the ventilated cage to study the effects of rodent activities on the cage microenvironment. To study the cage environment for mice, parameters like the geometry of the cage, bedding, number of mice, and position of the mice must be modeled. Modeling of the physical properties such as flow profiles and concentration distribution inside the cage microenvironment was carried out using FLUENT software.

A conventional Allentown PC 7115RT was used as a model for the study. The cage geometry was modeled using GAMBIT software. For this study, it was assumed that ICR mice, weighing 30 grams, were present in the cage. The mouse body was modeled as a cylinder. The size of this cylinder was calculated based on the following assumptions

Density of mouse (ρ) = 1 gm/cm^3

Weight of mouse (W) = 30 gm

The volume of each mouse is equal to

$V = W/\rho = 30$ cm^3 3-1

The diameter (d) of each mouse was assumed to be 2.54 cm (1 inch). The length of each mouse (L) is thus equal to

$$L = \frac{\Pi d^2}{4V} = 2.5 \text{ inches} \quad 3\text{-}2$$

The type of cage bedding in the current analysis was assumed to be a typical corncob bedding of one inch depth. Corncob bedding is porous in nature and is known to reduce the concentration of ammonia. However the bedding offers resistance to the momentum of the fluid. To model the bedding in the cage, the height of the cage was reduced by one inch.

To reduce the complexity of the analysis, the mice bodies were assumed to be stationary. To further reduce the complexity of the model, mice were modeled as half cylinders. The mouse body was considered to be a source of CO_2 with CO_2 coming out uniformly from the half cylinder. In one case the mice were positioned parallel to the length of the cage. For the second case, they were positioned perpendicular to the length of the cage. Figure 3-1 shows the two cylinders positioned along the x-axis at the outer walls of the cage and away from the inlet air nozzle. Figure 3-2 shows the two cylinders positioned along the y-axis. The cylinders in this case are twice the length of one mouse. This is the geometry that was used to model four mice in the cage. Figure 3-3 shows the two cylinders along the x-axis near the center if the cage and also near the inlet nozzle.

It is noted that mice select specific corners for their latrines. Latrines, being a major source of ammonia, carbon dioxide and moisture, had to be considered in the model. The four corners of the cage were assumed to be the areas of the latrines. The ammonia and CO_2 concentration from the latrines were assumed to be independent of the number of mice present in the cage. Assuming 16 ppm of ammonia to be present in the condition of steady state the mass flow rate of ammonia was back calculated. The mass flow rate used for ammonia is 4e-06 kilogram per second and mass flow rate of CO_2 1.7e-05 kilogram per second.

Air at 75°F and 50% RH was supplied to the cage through the inlet nozzles at 20, 40, 60, and 100 ACPH.

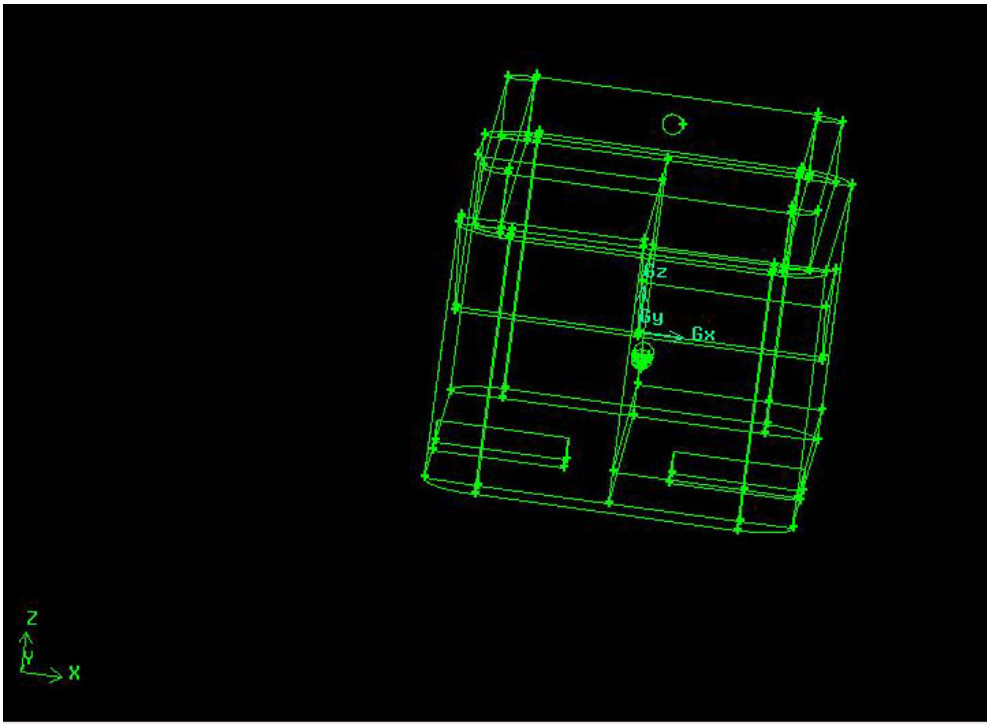

Figure 3-1. Mice positioned at the outer walls of the cage

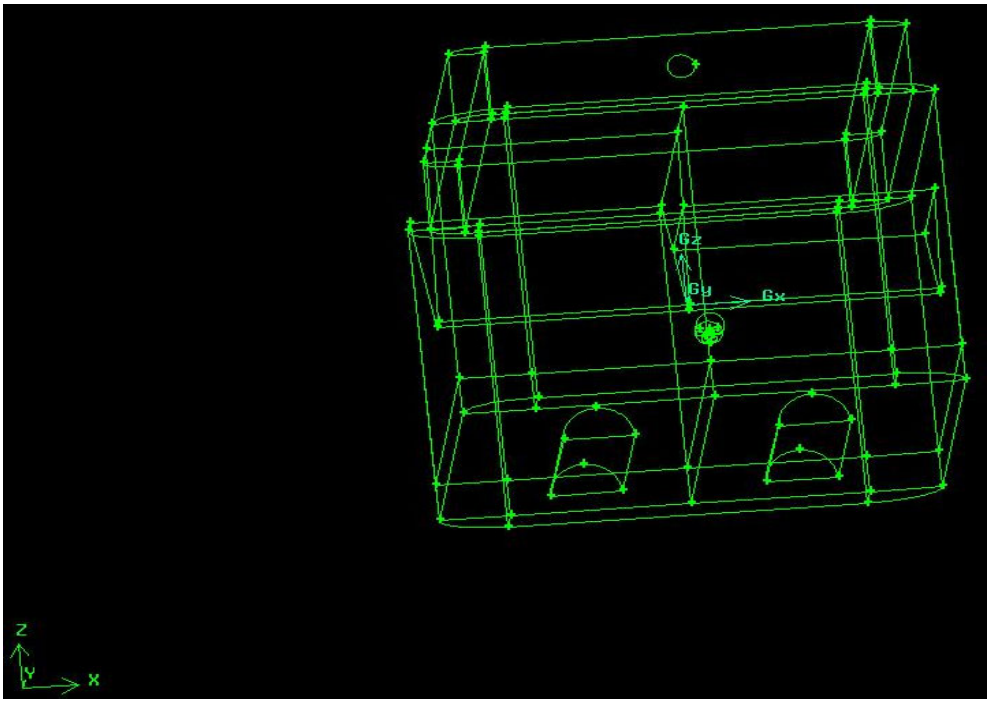

Figure 3-2. Mice positioned along the y-axis

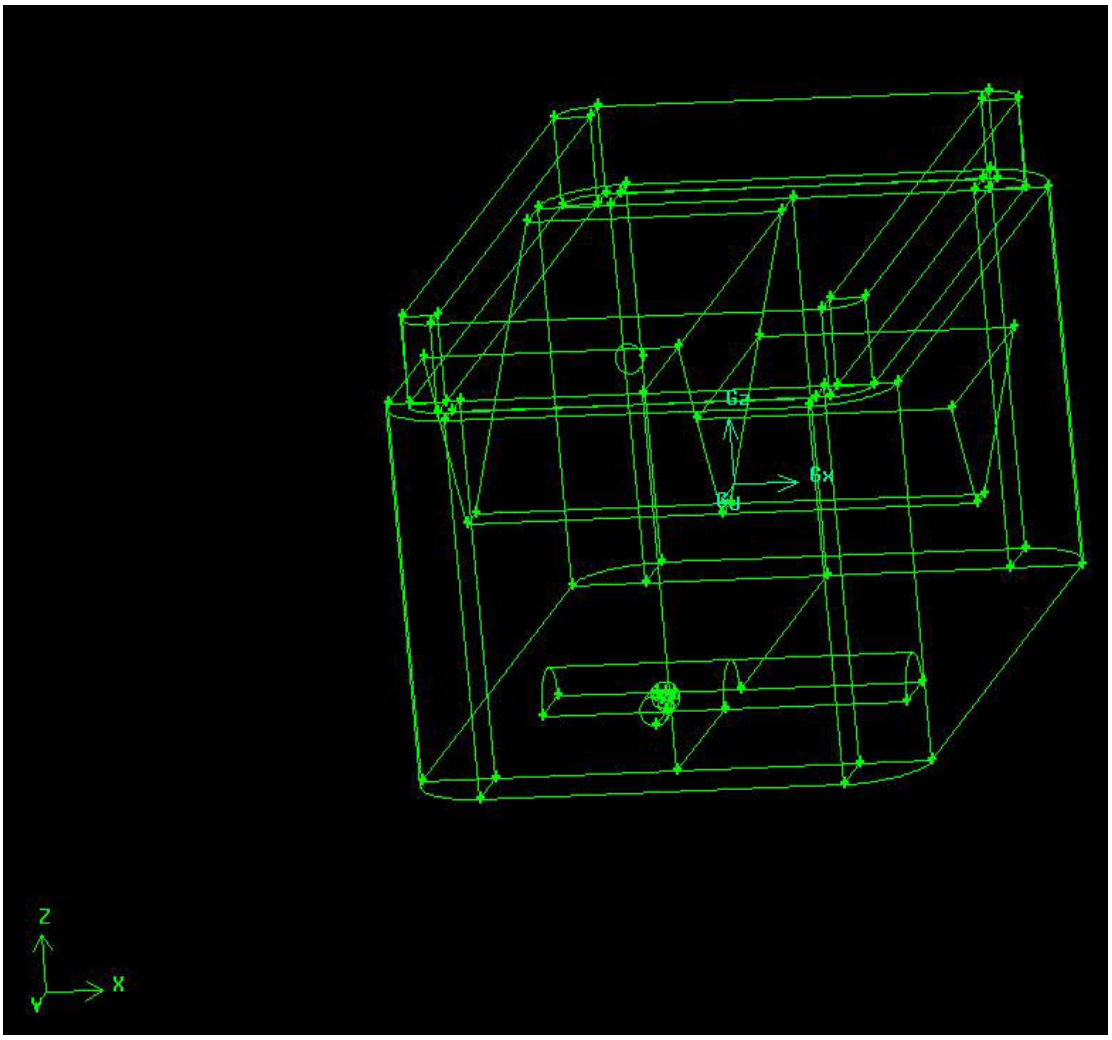

Figure 3-3. Mice positioned at the center of the cage

The geometry was then meshed in the GAMBIT software. The top part of the cage was meshed with a structured mesh of size 0.15 inches. The lower part of the cage was also meshed with a structured mesh of size 0.1 inches. The lower geometry that included the mice bodies was meshed with an unstructured mesh of size 0.1 inches. This was because the geometry was too complex to be meshed by a structured mesh. The portion of the cage with the nozzle was meshed with a size .05-inch mesh as the size of nozzle is 0.15 inch and the smaller mesh gave better results. The figures showing mesh schemes used in other cages are provided in appendix A.

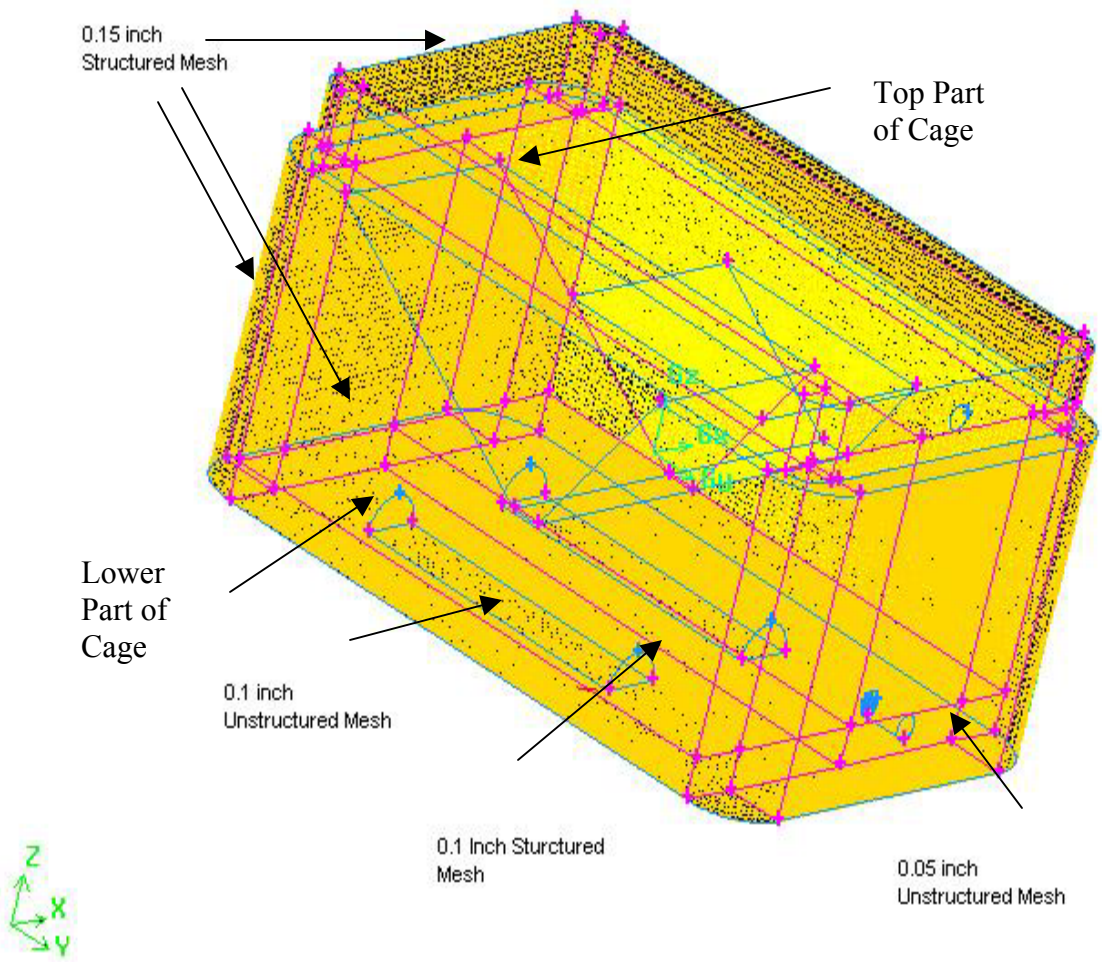

Figure 3-4. Meshing scheme used in the LM case

The geometry was then analyzed in FLUENT. First order upwind is used for this case as flow is aligned with the grid. The relaxation factors are used to control the iterations of the model. By setting a lower value the model remains more stable. The following settings were used in FLUENT.

Table 3-1. Model definitions

Model Type	**Settings**
Space	**3D**
Time	**Steady**
Viscous	**Standard k-epsilon turbulence model**
Wall treatment	**Standard Wall Functions**
Heat Transfer	**Enabled**
Solidification and Melting	**Disabled**
Radiation	**None**
Species Transport	**Non reacting**

Table 3-2. Discretization scheme

Variable	Scheme
Pressure	**Standard**
Pressure-Velocity Coupling	**Simple**
Momentum	**First Order Upwind**
Turbulence Kinetic Energy	**First Order Upwind**
Turbulence Dissipation Rate	**First Order Upwind**
CO_2	**First Order Upwind**
NH_3	**First Order Upwind**
Air	**First Order Upwind**
Energy	**First Order Upwind**
H_2O	**First Order Upwind**

Table 3-3. Variable definitions

Variable	Relaxation Factor
Pressure	**0.2**
Density	**0.5**
Body Forces	**0.5**
Momentum	**0.40000001**
Turbulence Kinetic Energy	**0.5**
Turbulence Dissipation Rate	**0.5**
Turbulent Viscosity	**0.5**
CO_2	**0.5**
NH_3	**0.5**
Air	**0.5**
Energy	**0.5**
H_2O	**0.5**

.

CHAPTER 4
RESULTS AND DISCUSSION

The purpose of this study was to study the effects of rodent activities on cage microenvironments. Computational fluid dynamic methods were used to find and plot the concentrations within the cage and also the flow profiles in the cage. The simulated mice bodies were positioned in various parts of the cage using GAMBIT software and the effect of mice positions on the microenvironment was then analyzed using the FLUENT software. Each mouse body was considered to be a source of CO_2. Three different mouse positions were analyzed in the study. In the first case two mouse bodies were positioned at the outer wall of the cage. The outer wall case was referred to with an abbreviation "OW". Figure 4-1 shows the OW case.

In the second case, two mouse bodies were positioned along the center of the cage near the inlet nozzle of the cage, referred to with an abbreviation "CC". Figure 4-2 shows the CC case. For the third case, two longer cylinders were positioned along the y-axis, referred to with an abbreviation "LM". Four mice bodies were simulated in the cage by doubling the length of the cylinders in the cage. Figure 4-3 shows the LM case.

As there is no specified acceptable CO_2 concentration for mice so assuming acceptable CO_2 concentrations for humans that is 5000 ppm as a standard. The acceptable NH_3 concentration specified by the guide for ventilated cages is 25 ppm.

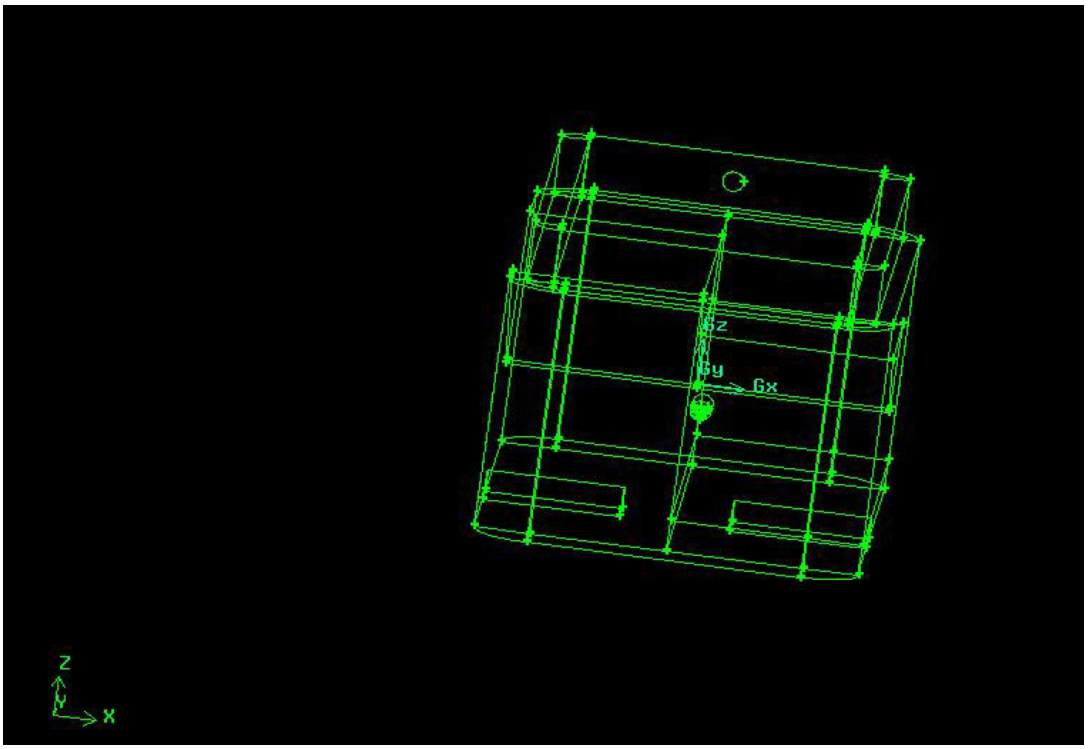

Figure 4-1. Outside wall case

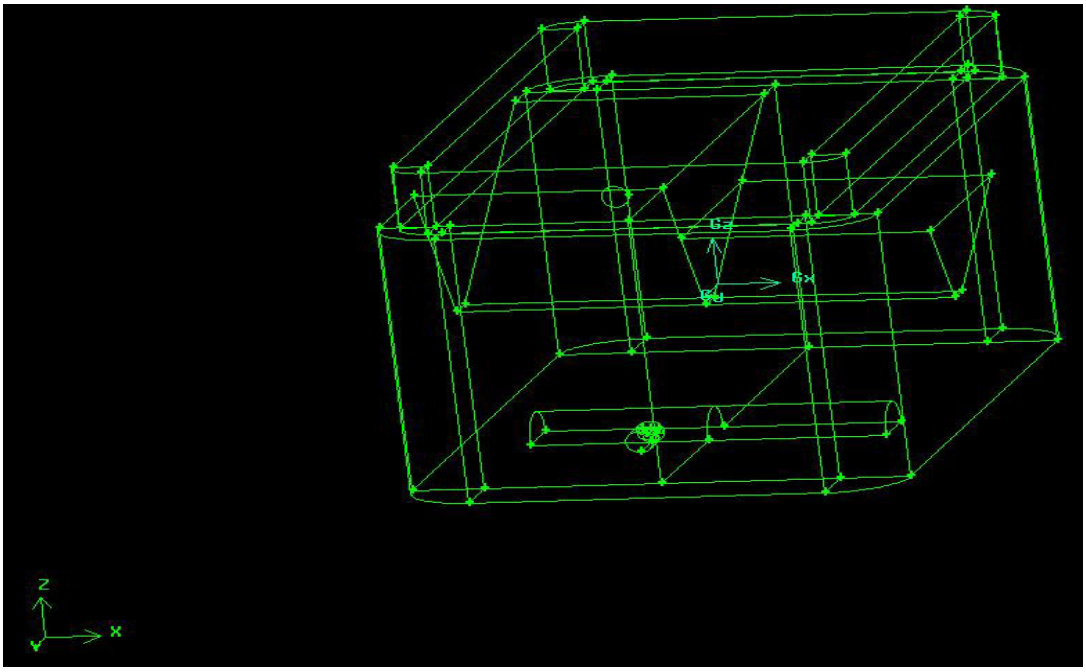

Figure 4-2. Center of cage case

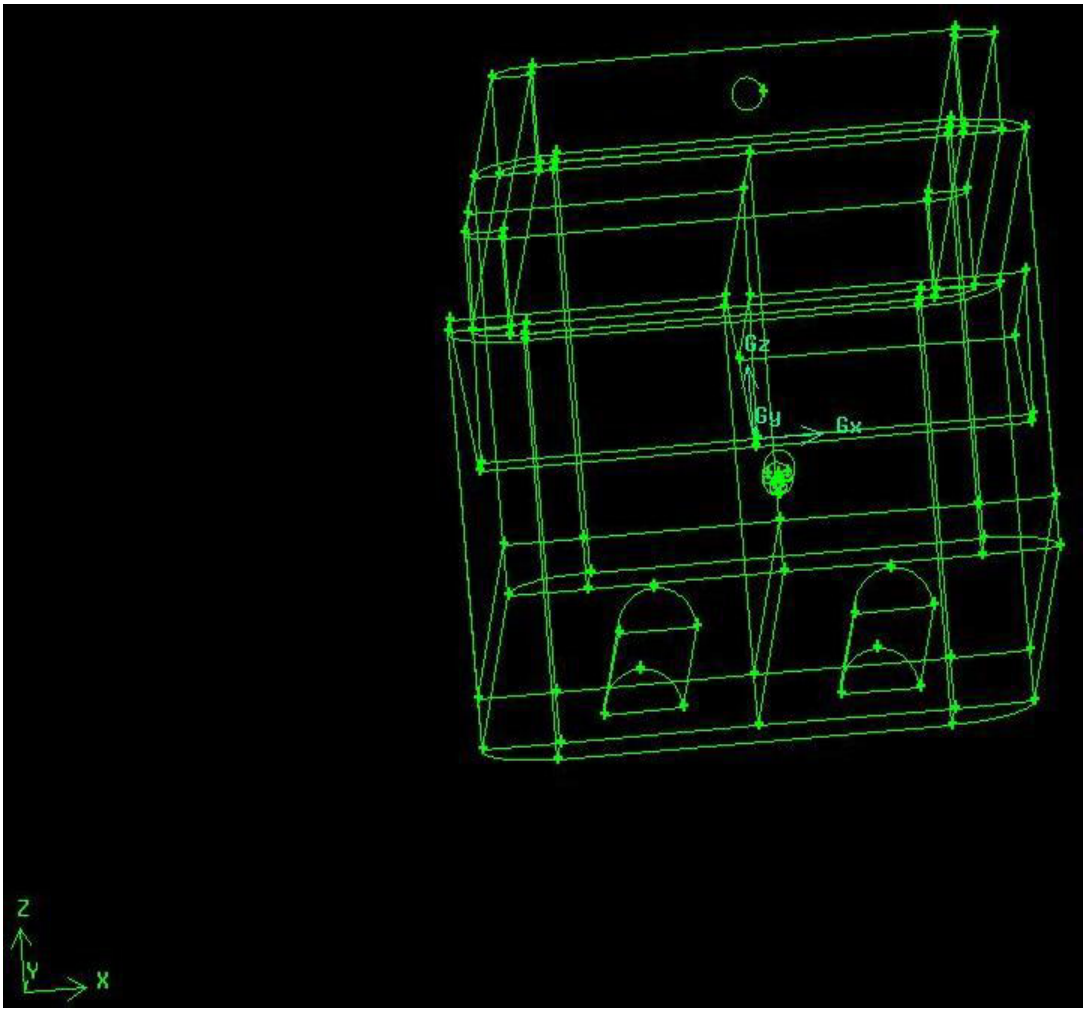

Figure 4-3. Four mice case

The CC case was analyzed for an air change rate of 100 ACPH. For 100 ACPH the velocity of inlet air was 8.57 m/s. The NH_3 mass flow rate was 4e-06 kg/s, and the CO_2 mass flow rate was 1.7e-05 kg/s. Figure 4-4 shows the air velocity profiles for this case. As expected, the profiles show that more circulation of air takes place near the nozzle of the cage. A slight bump could be seen in the velocity profile due to the presence of a mouse body at the center of the cage. The air velocity in the vicinity of the mouse was 1.02 meters per second. Assuming a comfortable air velocity of a mouse to be equal to that for a human (0.15 m/s–0.25 m/s), it can be seen that the air velocity is much higher than the acceptable level and can be concluded that the mouse would not stay at that

position for very long and move away towards the corner of the cage where the air velocity would be less. Figure 4-5 shows the contours for the CO_2 concentration in the cage at 100 ACPH. It can be seen from the figure that the CO_2 concentration near the mice bodies is less than in other areas of the cage. This is because in this case the mice are positioned near the inlet nozzle and the high air velocity forces the CO_2 to the back side of the mouse and also the air exchange rate causes the concentration to be less near the mouse body. The concentration that was most prevalent in the cage was assumed to be the average concentration of CO_2 and NH_3 in the cage.

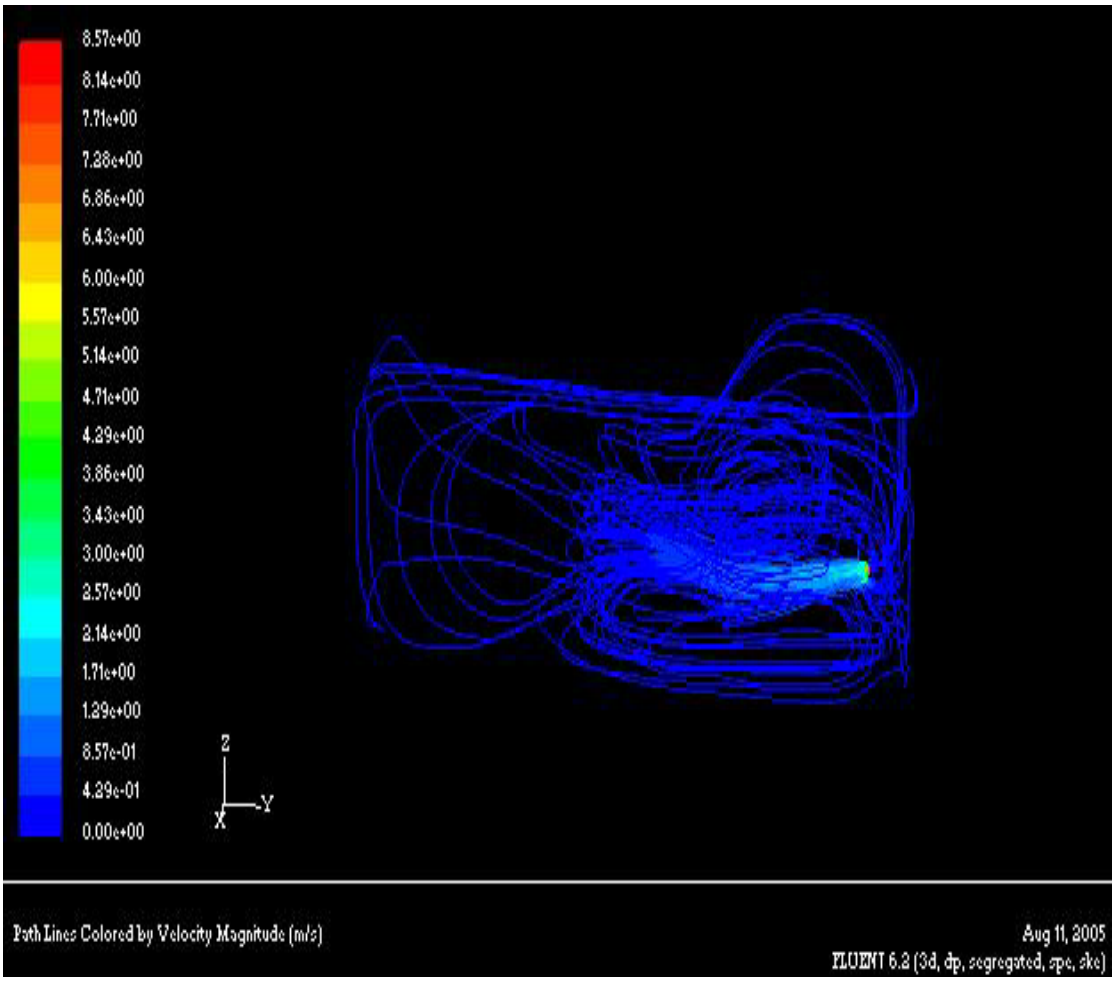

Figure 4-4. Velocity profiles for center of cage at 100 ACPH

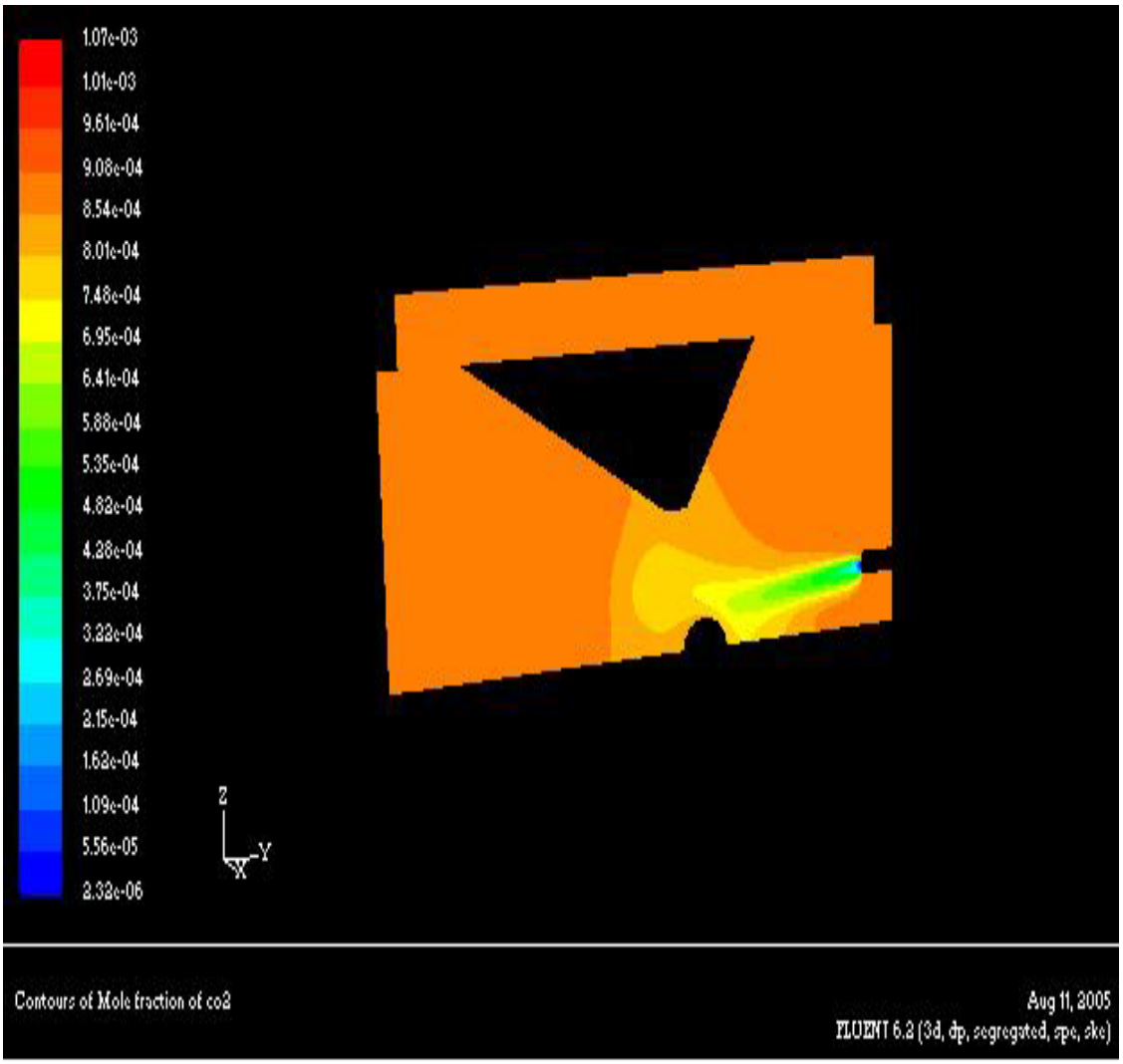

Figure 4-5. Contours of mole fraction of CO_2 for center of cage (100 ACPH)

The concentration of CO_2 in the cage was found to be 970 ppm. Figure 4-6 shows the contours for mole fractions of NH_3. The NH_3 present within the cage is 6 ppm. It can also be seen that the concentration of NH_3 near the mouse body is very low, again because the mouse body is a source of CO_2 and not ammonia, and also because the air is flowing directly on the mouse body. Figure 4-7 shows the contours of mole fraction of NH_3 viewed from the top of the mouse cage. The four corner areas defined as latrines are visible in this figure. The latrines show an NH_3 concentration of 25 ppm, which decreases as we move away from the corners and the NH_3 mixes with the air coming in the cage.

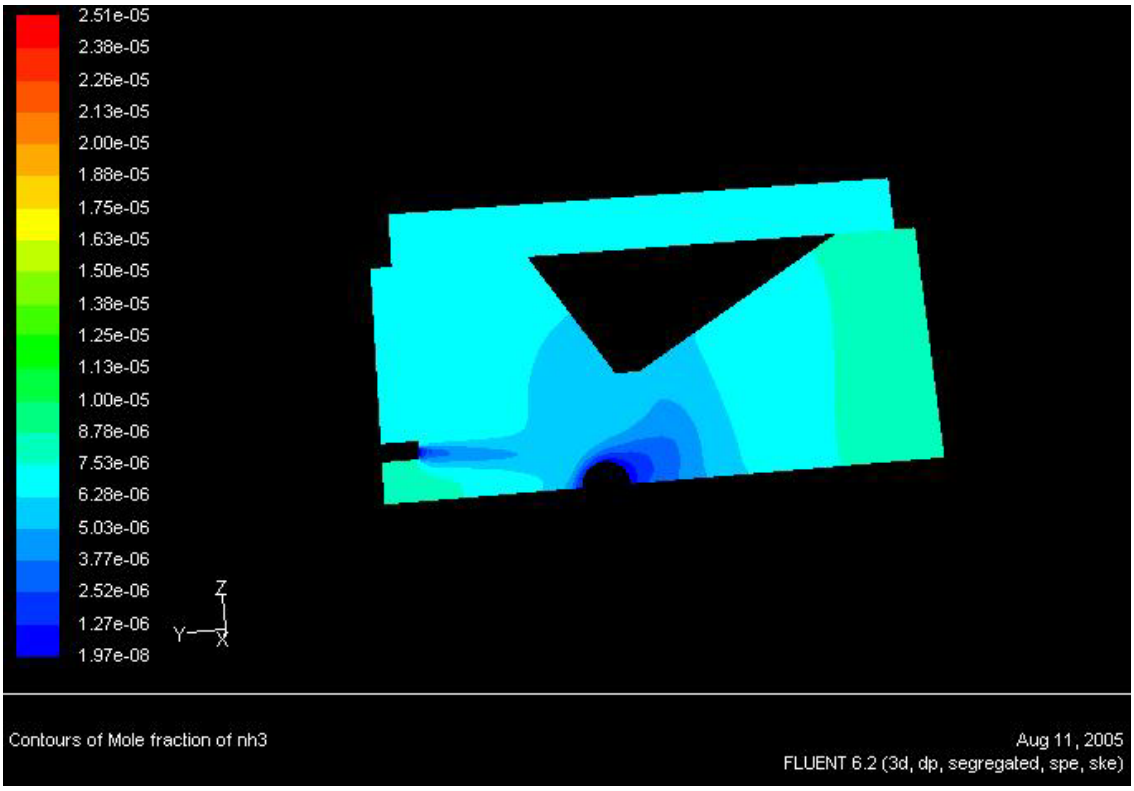

Figure 4-6. Contours of mole fraction of NH_3 for center of cage (100 ACPH)

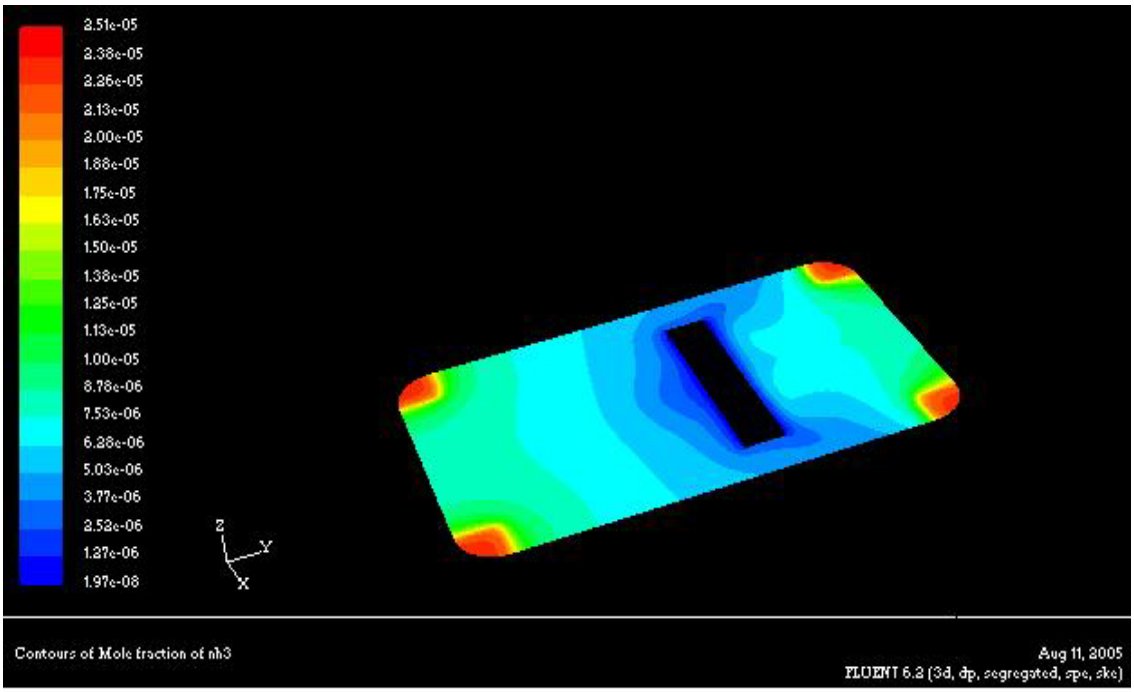

Figure 4-7. Top view of contours of mole fraction of NH_3 for center of cage (100 ACPH)

The LM case was run for 60 ACPH. For 60 ACPH the velocity of inlet air was 5.143 m/s. The NH_3 mass flow rate was 4e-06 kg/s, and the CO_2 mass flow rate was 1.7e-05 kg/s. Figure 4-8 shows the velocity profiles for the LM case at 60 ACPH. It can be seen that airflow is concentrated near the inlet nozzle of the cage. The air velocity in the vicinity of the mouse was 0.60 meters per second, which is higher than acceptable comfortable level of 0.15 m/s-0.25 m/s. Again it can be concluded that the mice would not stay at that position for very long and would move away towards the corner of the cage where the air velocity would be less. Figure 4-9 shows the contours of mole fraction of CO_2 concentrations in the cage. It can be seen from the figure that CO_2 concentrations are highest in the vicinity of the mouse body since mice are the major sources of CO_2 in the cage. The concentration is much lower near the nozzle of the cage as the fresh air is flowing into the cage. The CO_2 concentration in the cage is about 1350ppm. Figure 4-10 shows the contours of mole fraction of NH_3 in the cage. The concentration of NH_3 is less near the mouse body as the mouse is not a source of ammonia in the cage and also near the inlet as the air is flowing in to the cage. The NH3 concentration in the cage is 9 ppm.

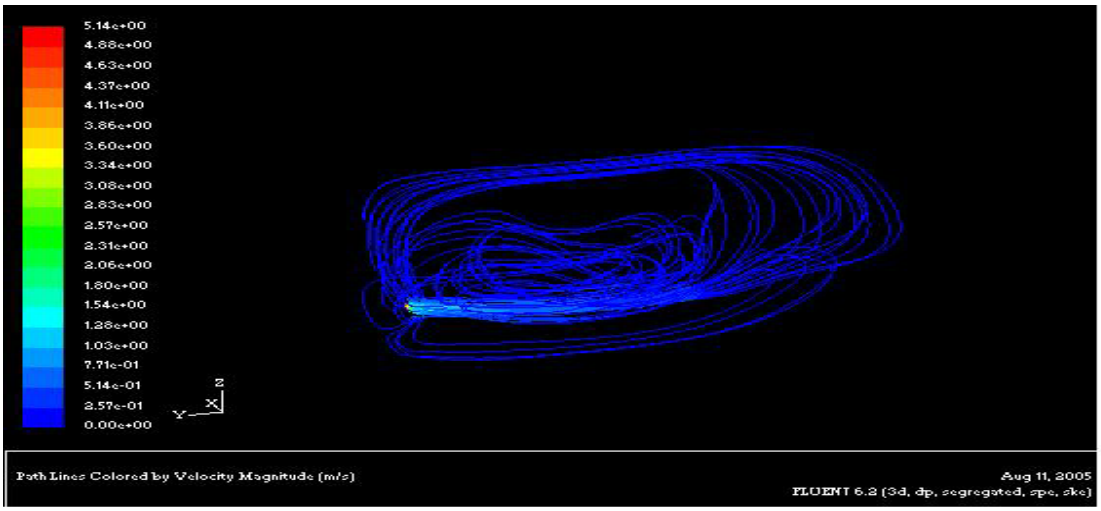

Figure 4-8. Velocity profiles for four mice at 60 ACPH

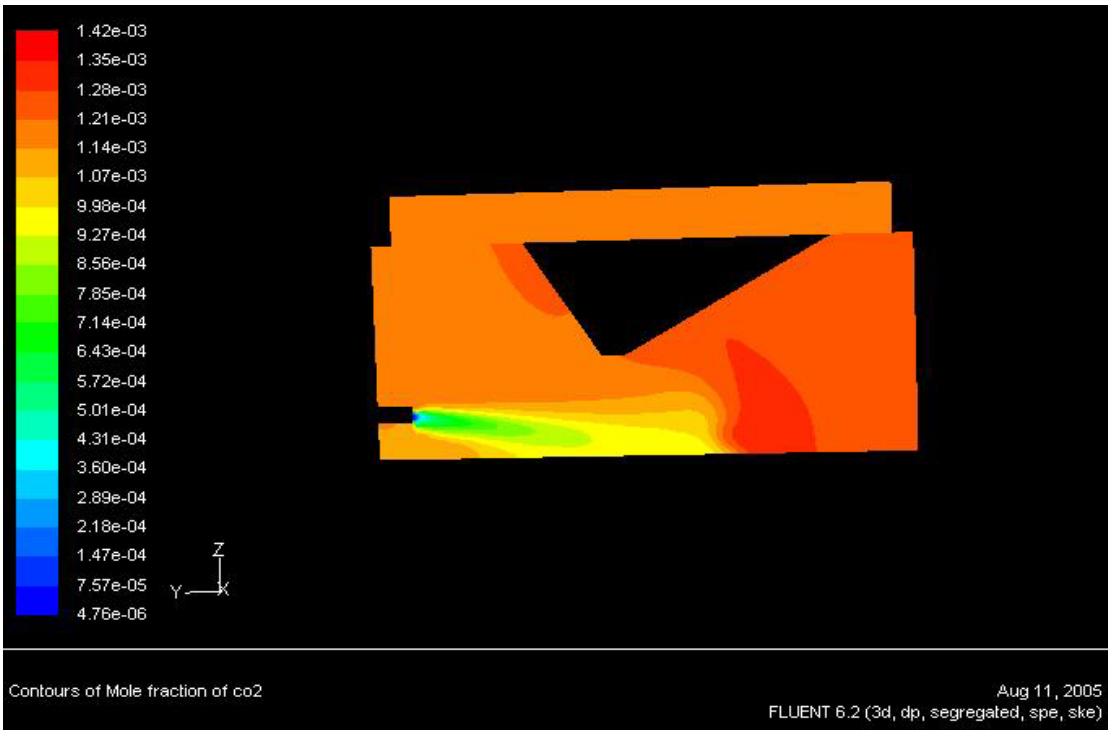

Figure 4-9. Contours of mole fraction of CO_2 for four mice (60 ACPH)

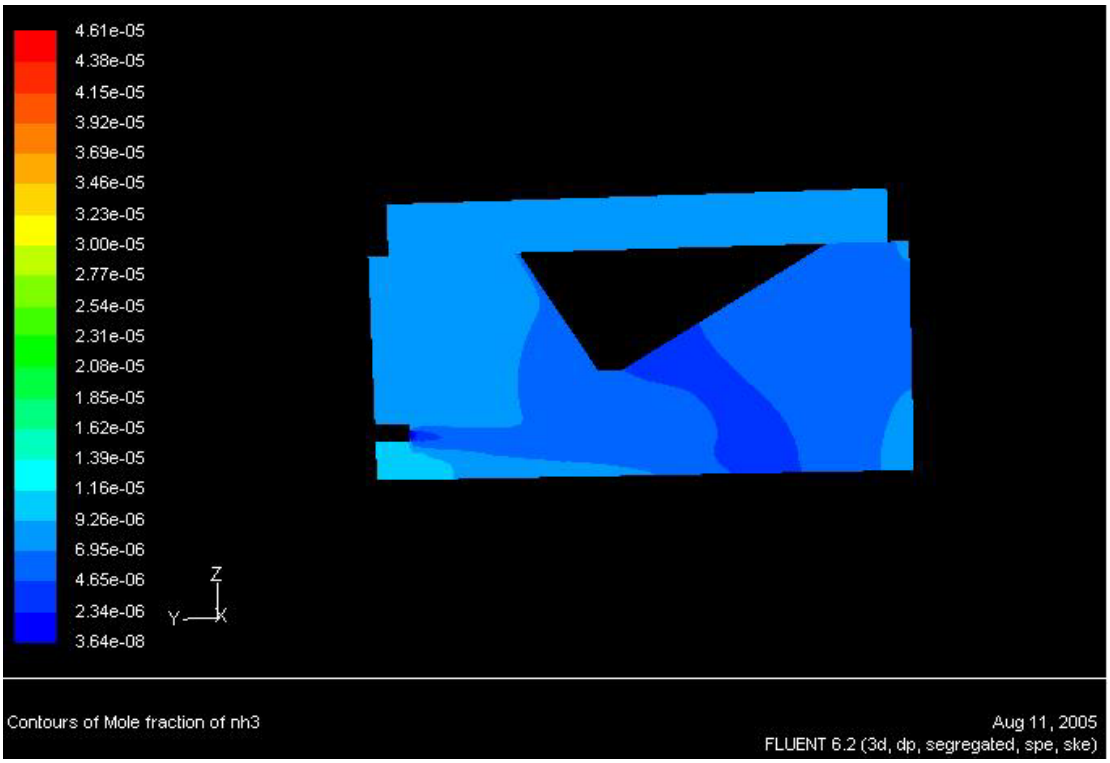

Figure 4-10. Contours of mole fraction of NH_3 for four mice (60 ACPH)

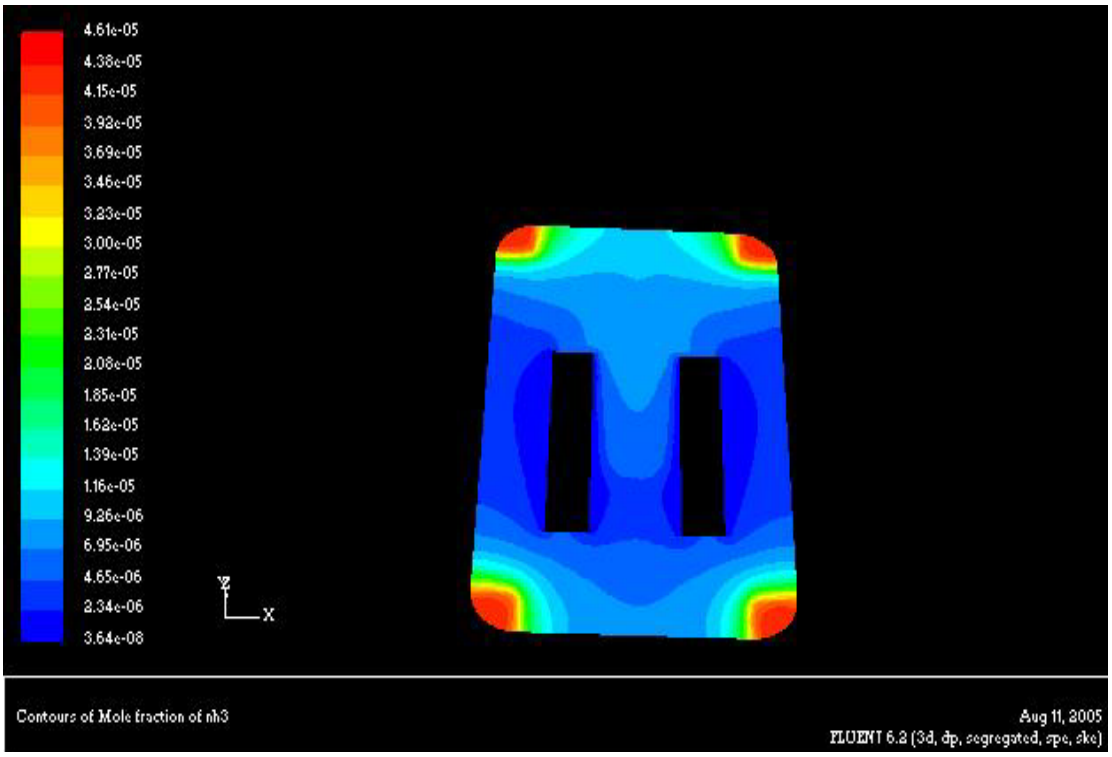

Figure 4-11. Top view of contours of mole fraction of NH3 for four mice (60 ACPH)

Figure 4-11 shows the top view of the mole fraction of NH_3 for the LM case. It can be seen that in the vicinity of the latrines ammonia concentrations are about 25 ppm, which decreases with the increase in the distance from the corners.

The OW case was run for 60 ACPH. For 60 ACPH the velocity of inlet air was 5.143 m/s. The NH_3 mass flow rate was 4e-06 kg/s, and the CO_2 mass flow rate was 1.7e-05 kg/s. Figure 4-12 shows the velocity profiles in the cage. The airflow is concentrated near the inlet to the cage. A slight bump can be seen near the outer walls of the cage away from the nozzle, which shows the presence of a mice body at that location in the cage. The air velocity in the vicinity of the mouse was 0.275 meters per second, which is slightly higher than acceptable comfortable level of 0.15 m/s-0.25 m/s. It can be concluded that the mice would not stay at that position for very long and move away towards the corner of the cage where the air velocity is less. Figure 4-13 shows the

contours of CO_2 concentration in the cage at 60 ACPH. The concentration of CO_2 is highest near the mouse body. It can also be seen that the higher CO_2 concentration is more towards the back end of the mouse body. This is because the air coming from the nozzle impinges on the front side of the mice and forces the CO_2 in that direction. The air hits the mouse body and passes above the body, not causing much effect on the CO_2 coming out from the back end of the body. The CO2 concentration in the cage is 1000 ppm. Figure 4-14 shows the mole fraction of concentration of NH_3 in the cage. The NH3 concentration within the cage is about 11 ppm. The NH_3 concentration is lowest near the mouse as it is not a source of ammonia. Figure 4-15 shows the top view of the contours of mole fraction of NH_3 concentration in the cage. The ammonia concentration is high at the corners of the cage.

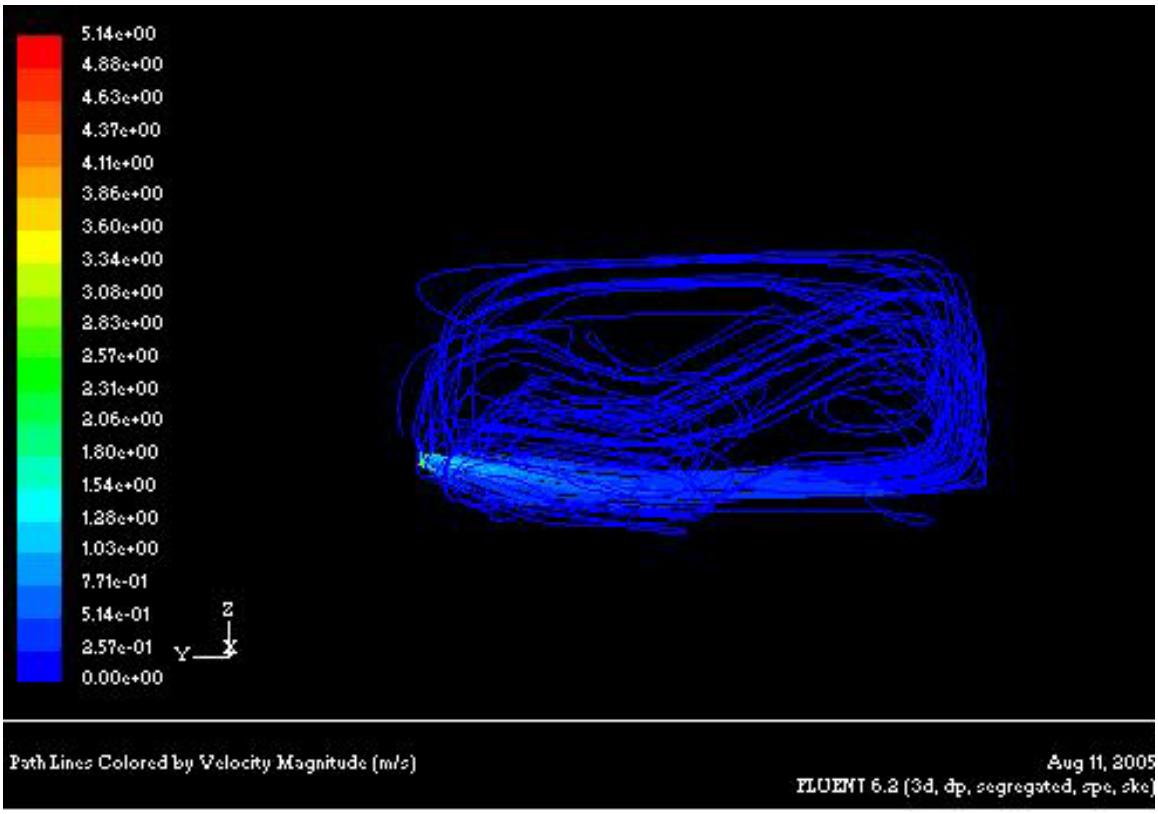

Figure 4-12. Velocity profiles for outside wall at 60 ACPH

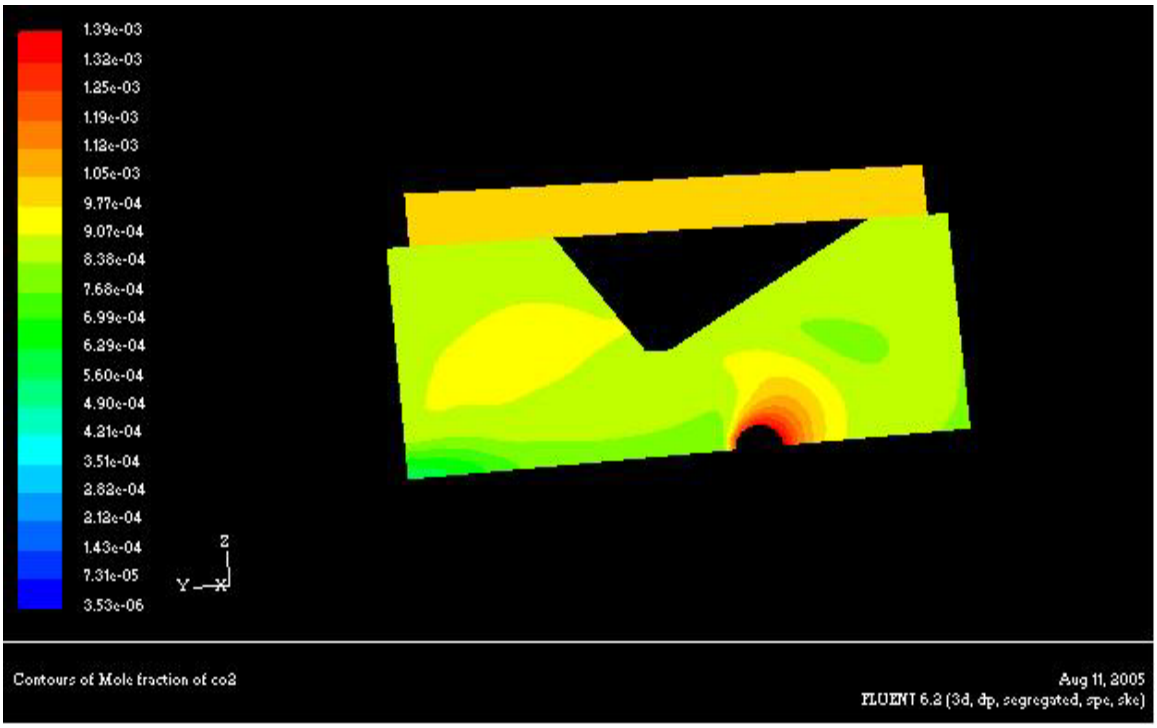

Figure 4-13. Contours of mole fraction of CO_2 for outside wall (60 ACPH)

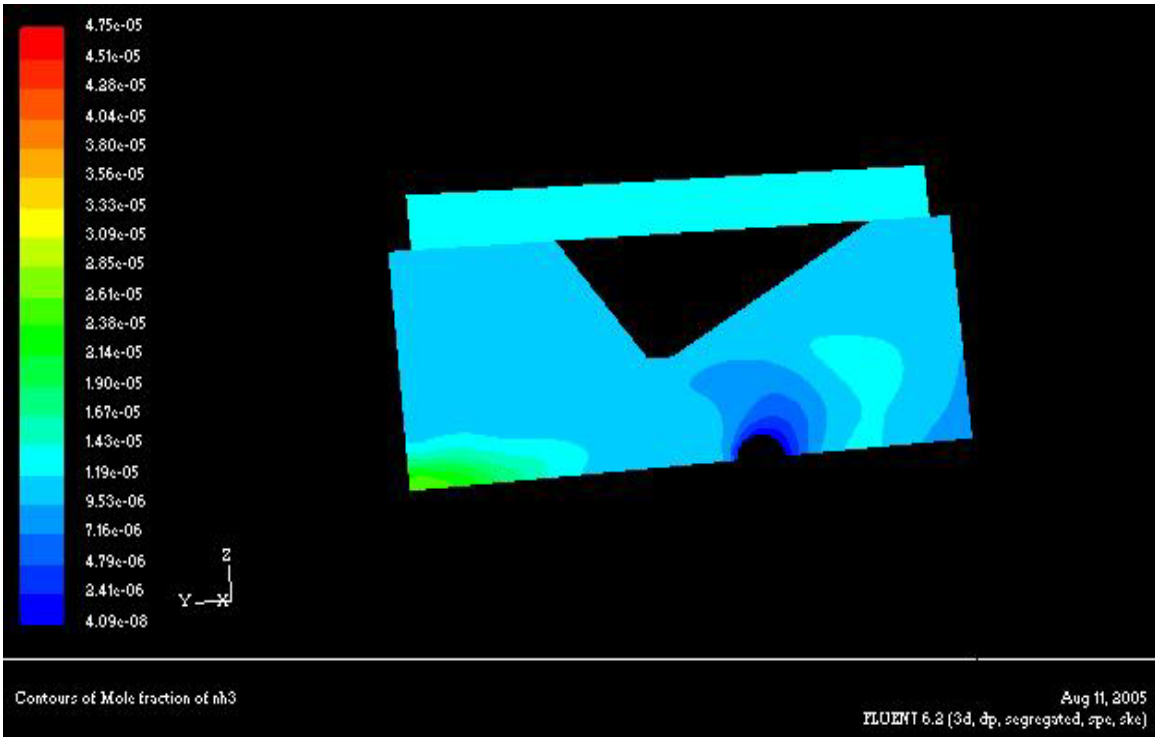

Figure 4-14. Contours of mole fraction of NH_3 for outside wall (60 ACPH)

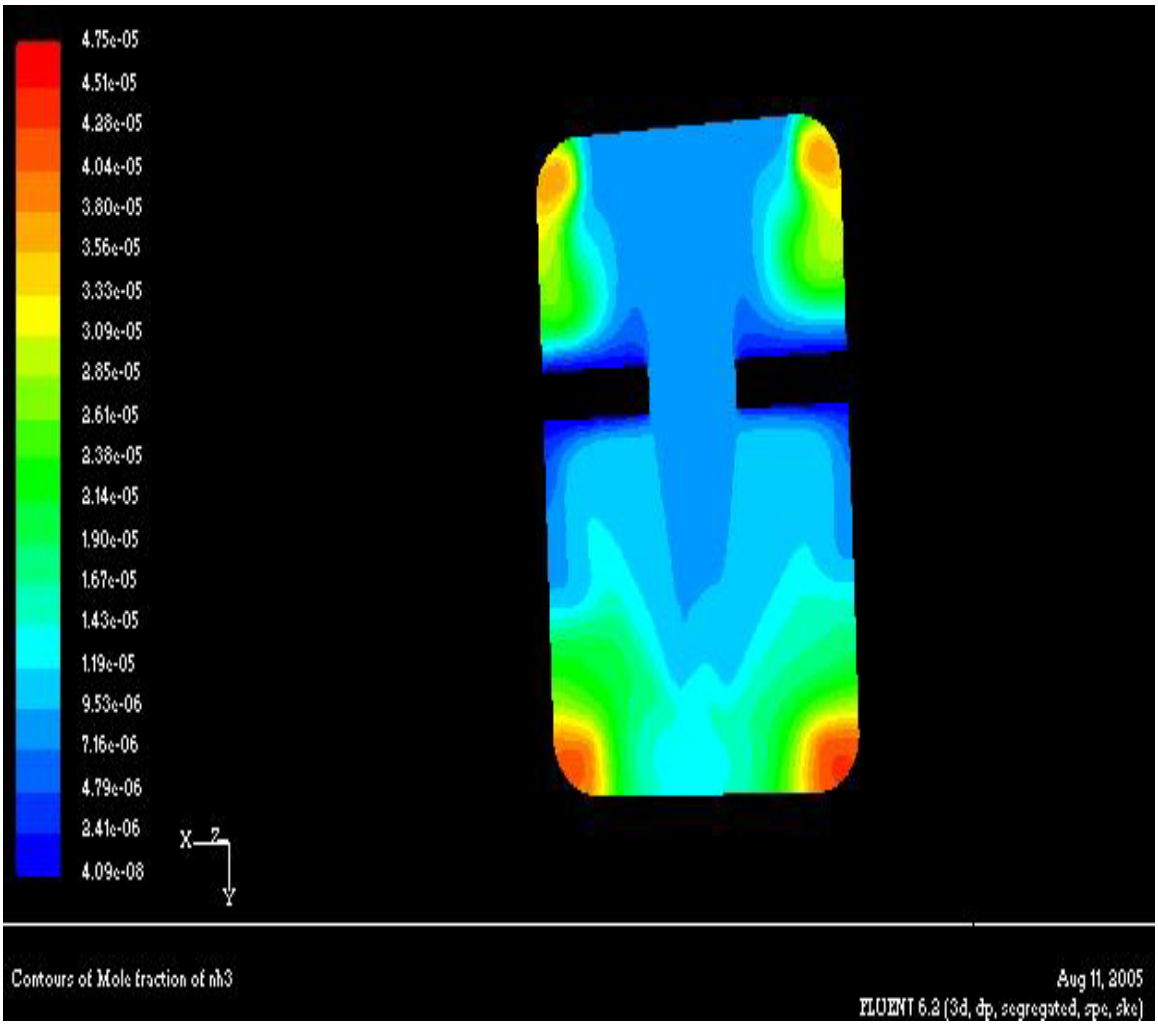

Figure 4-15. Top view of contours of mole fraction of NH_3 for outside wall (60 ACPH)

The CC case was also run at 20 ACPH. For 20 ACPH the velocity of inlet air was 1.71 m/s. The NH_3 mass flow rate was 4e-06 kg/s, and the CO_2 mass flow rate was 1.7e-05 kg/s. Figure 4-16 shows the velocity profile for this case. The velocity profile is similar to all the other cages with more airflow near the nozzle and less away from the nozzle. A slight bump can also be seen near the nozzle showing the presence of a mice body at that location in the cage. The air velocity in the vicinity of the mouse was 0.182 meters per second, which is within the acceptable comfortable level of 0.15 m/s-0.25 m/s. It can be concluded that the mouse could stay at almost any position in the cage, as the air velocity is not very high.

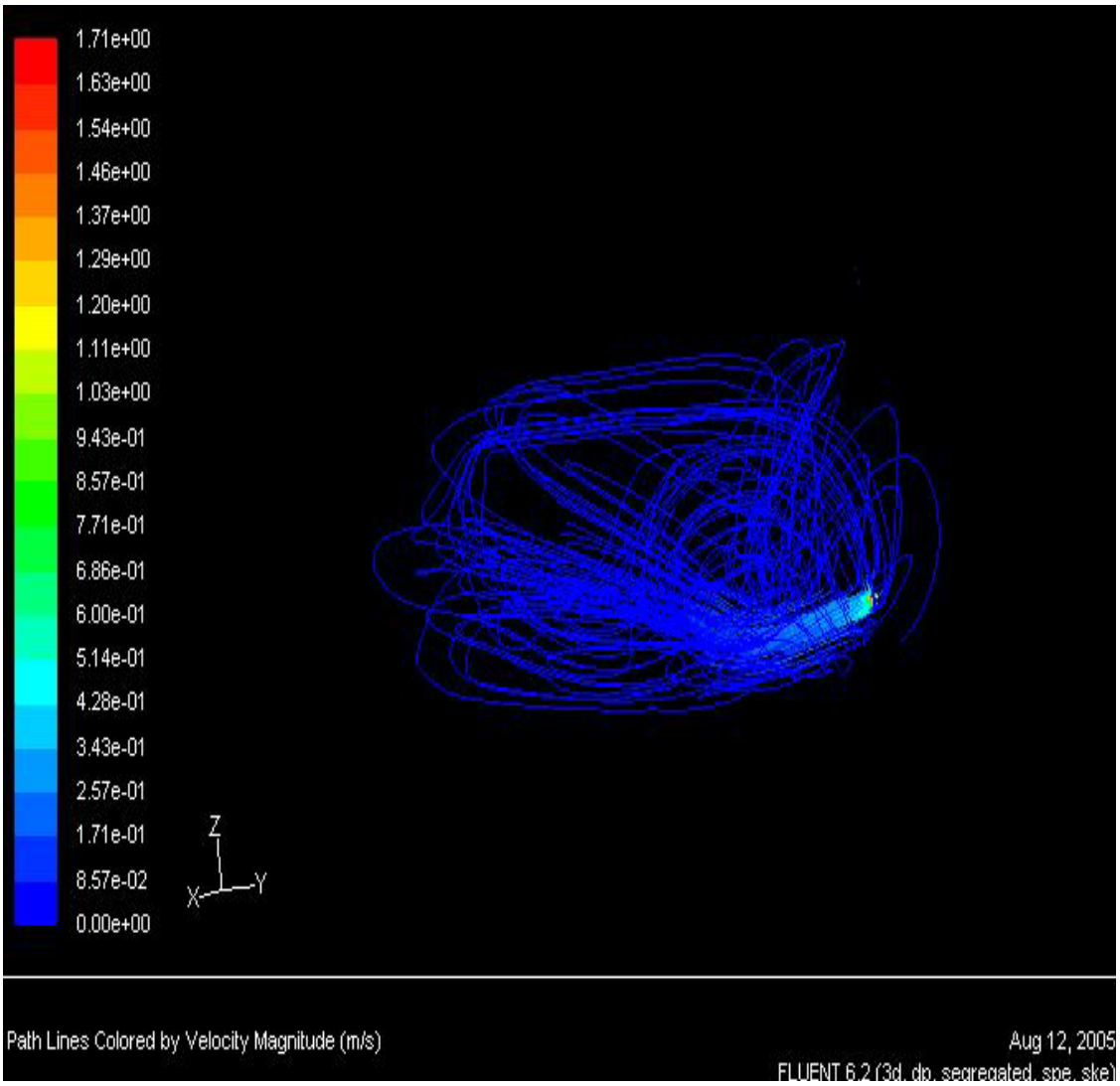

Figure 4-16. Velocity profiles for center of cage case at 20 ACPH

Figure 4-17 shows the contours of mole fraction of CO_2 concentration in the cage at 20 ACPH. It can be seen that the concentration is low at the front end of the mouse body because it is positioned very near to the inlet nozzle and the fresh air coming in from the inlet reduces the concentration of CO_2 in that area. A small area can be seen just to the back of the mouse body where a large concentration of CO_2 exists. This is because the air is not in direct contact with the mouse body in that area. The CO_2 concentration in the cage is 4300 ppm. It can be seen that CO_2 concentration is very high; this is because of a lower air change rate of 20 air changes per hour.

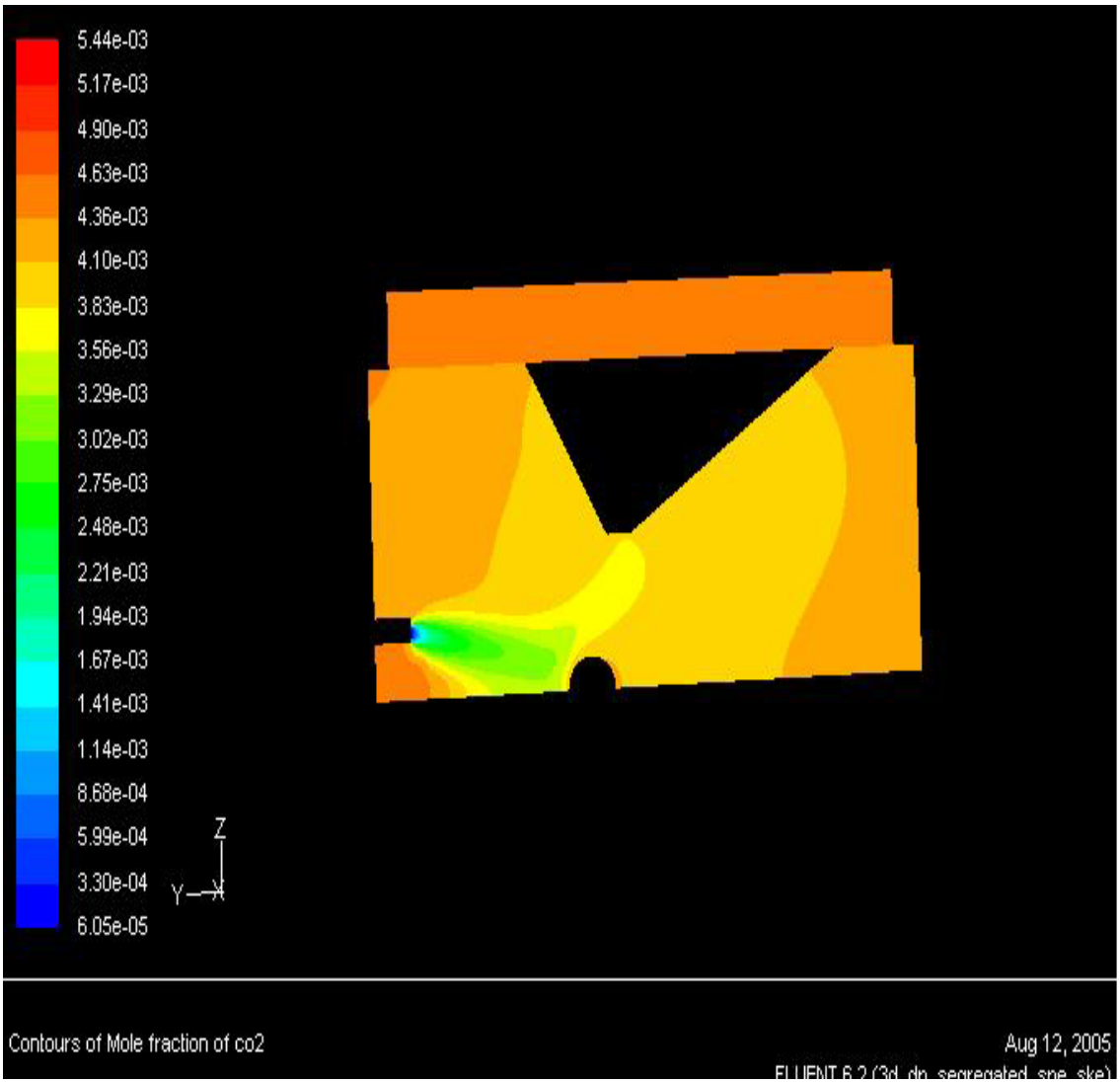

Figure 4-17. Contours of mole fraction CO_2 for center of cage (20 ACPH)

Figure 4-18 shows the contours of mole fraction of NH_3 in the CC case at 20 ACPH. The concentration of NH_3 near the mouse body is less, as the mouse body is not a source of ammonia. Figure 4-19 shows the top view of the contours of NH_3 concentration in the CC case at 20 ACPH. It can be seen that the latrines show the highest concentration of ammonia. The center of the cage experiences low concentrations of ammonia, as the airflow is high within that region. The concentration of ammonia decreases away from the corners of the cage. The NH_3 concentration in the cage is about 27 ppm. This high concentration is due to lower air change rate of 20 air changes per hour.

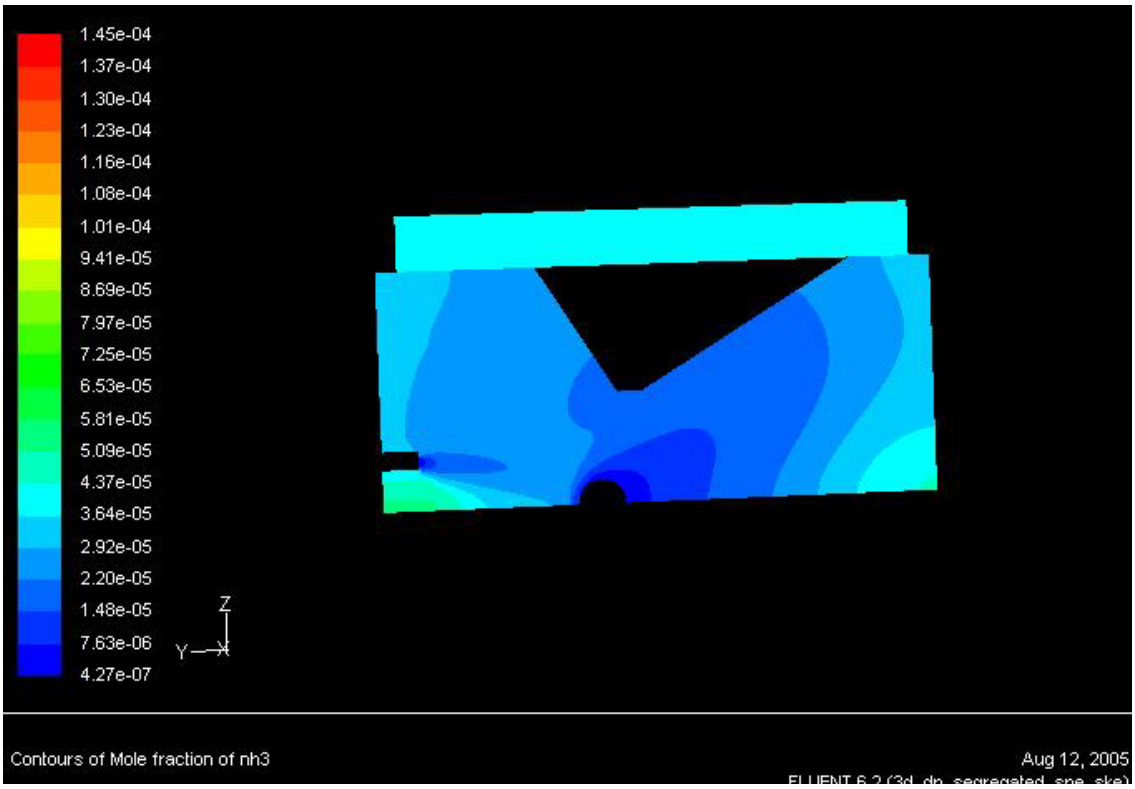

Figure 4-18. Contours of mole fraction of NH_3 for center of cage (20 ACPH)

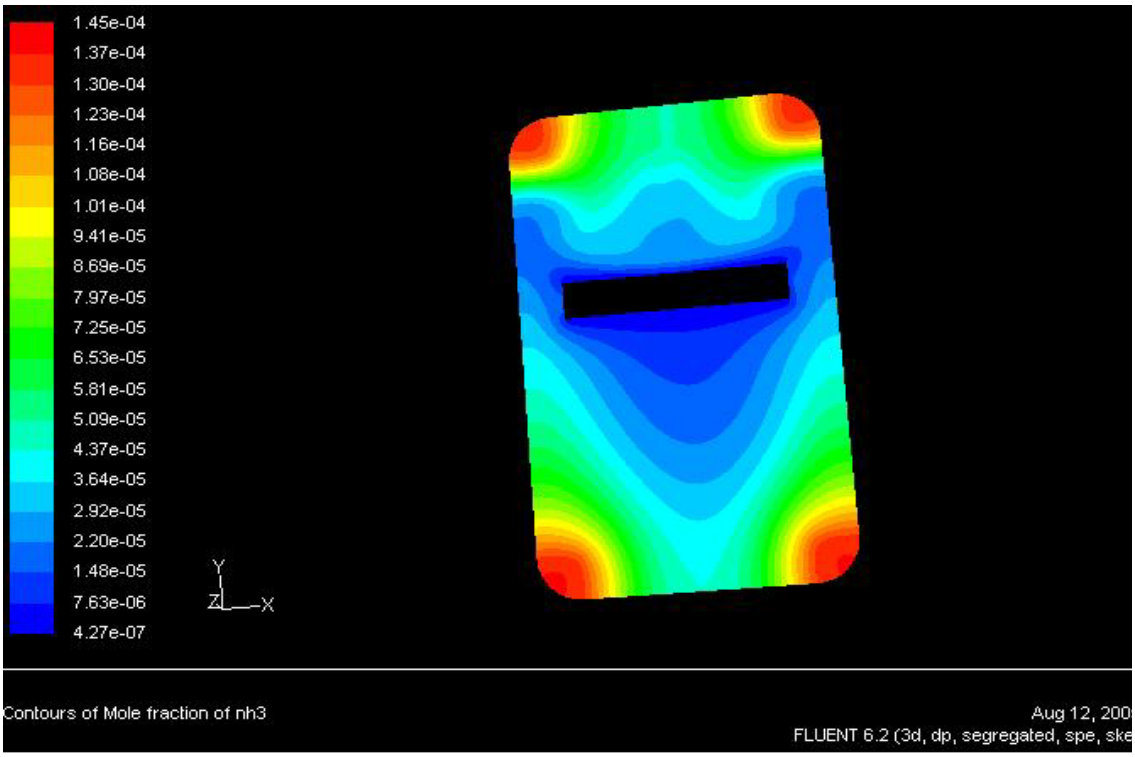

Figure 4-19. Top view of contours of mole fraction of NH_3 for center of cage (20 ACPH)

The OW case was also run for 40 ACPH. For 40 ACPH the velocity of inlet air was 3.42 m/s. The NH_3 mass flow rate was 4e-06 kg/s, and the CO_2 mass flow rate was 1.7e-05 kg/s. Figure 4-20 shows the velocity profile for OW at 40 ACPH. It can be seen that the velocity is concentrated more towards the inlet nozzle. A bump can be seen showing the presence of a mouse body in the cage. The air velocity in the vicinity of the mouse was 0.158 meters per second, which is within the acceptable comfortable level of 0.15 m/s-0.25 m/s. It can be concluded that the mouse could stay at that position and be comfortable. Figure 4-21 shows the contours of mole fraction of CO_2 concentration for OW at 40 ACPH. The concentration of CO_2 is higher near the latrines. The CO_2 concentration in the cage is 2200 ppm.

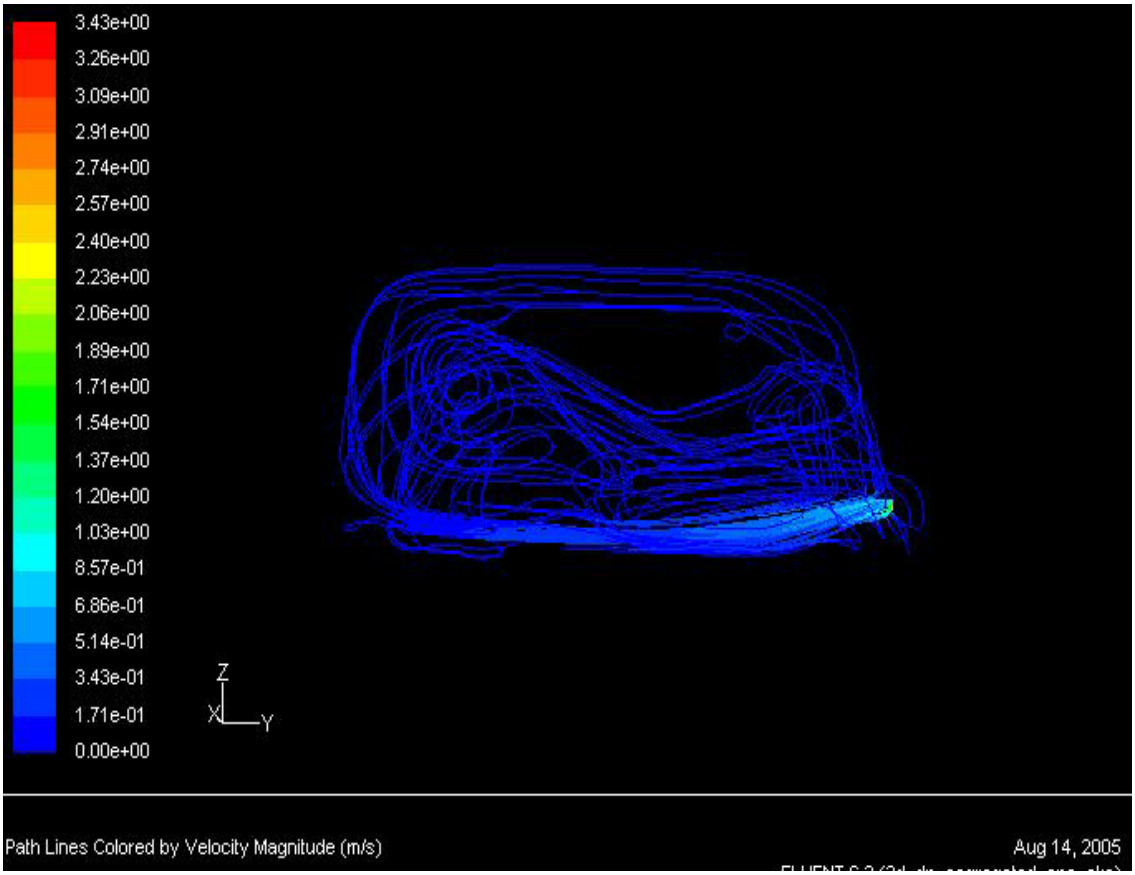

Figure 4-20. Velocity profiles for outside wall at 40 ACPH

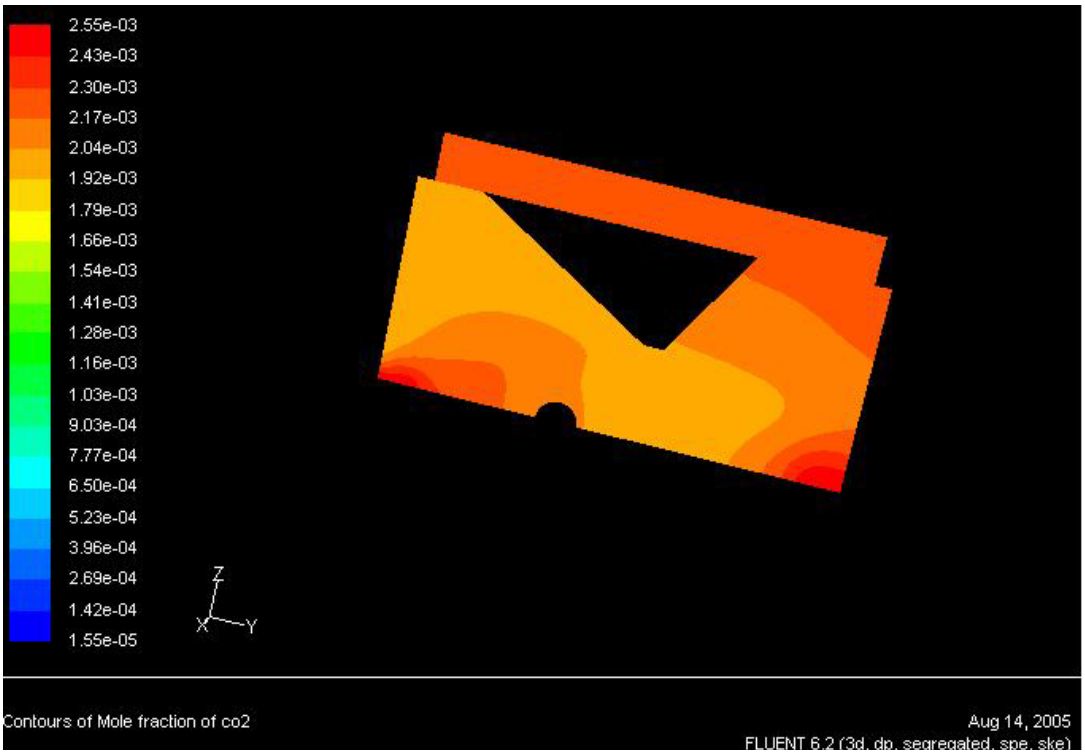

Figure 4-21. Contours of mole fraction of CO_2 for outside wall (40 ACPH)

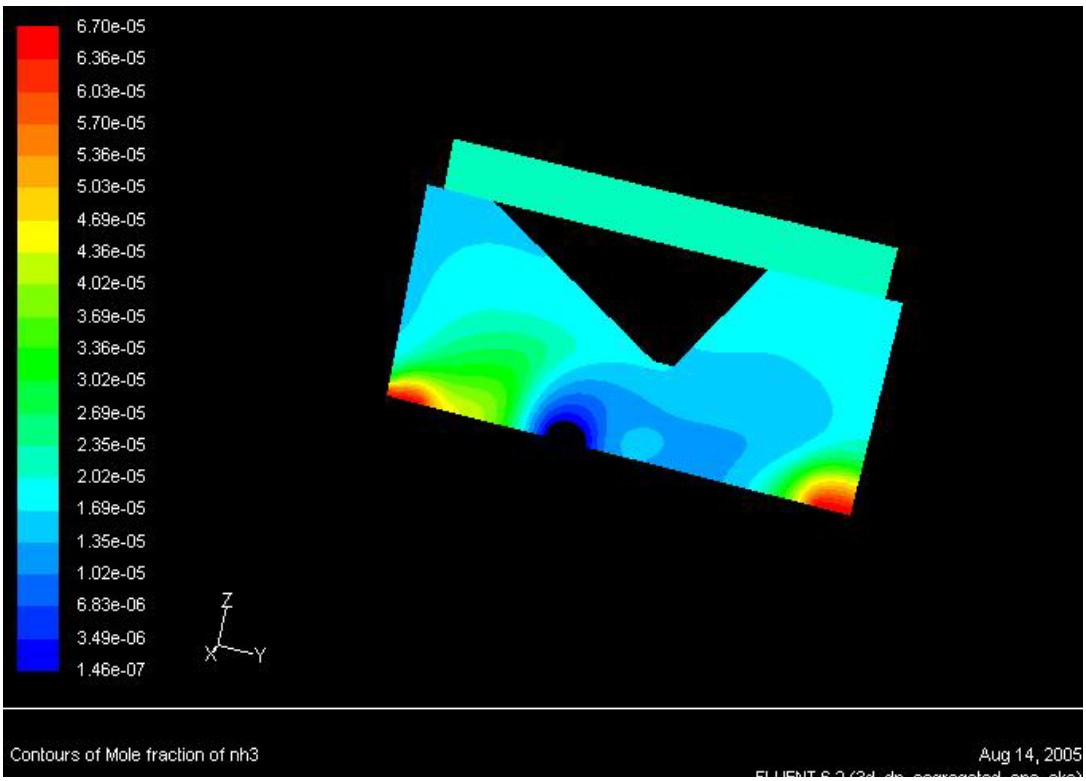

Figure 4-22. Contours of mole fraction of NH_3 for outside wall (40 ACPH)

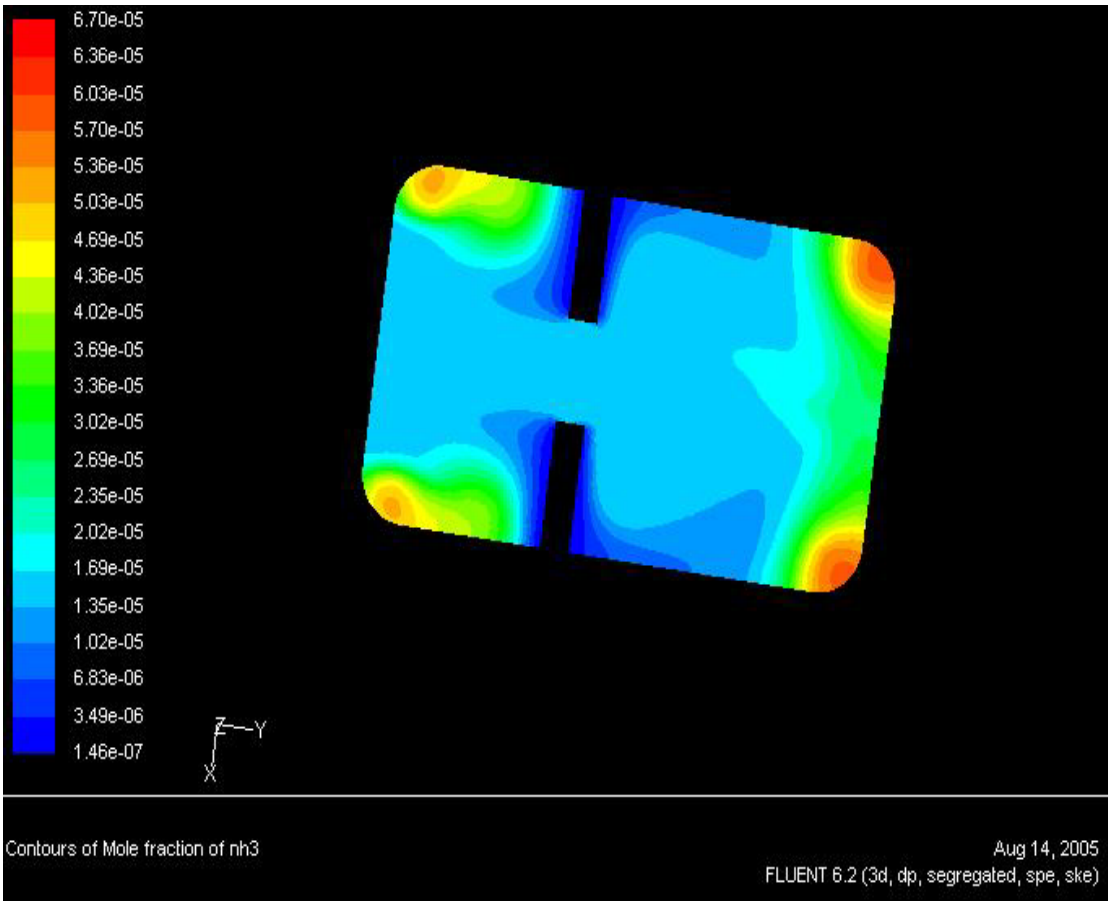

Figure 4-23. Top view of contours of mole fraction of NH_3 for outside wall (40 ACPH)

Figure 4-22 shows the contours of mole fraction of NH_3 concentration for the OW case at 40 ACPH. Figure 4-23 shows the top view of the contours of the NH_3 concentration for OW case at 40 ACPH. The ammonia concentration is higher at the corners and less near the mouse body. The NH3 concentration in the cage is 22 ppm.

Figure 4-24 shows the velocity profile for the CC case at 60 ACPH. For 60 ACPH the velocity of inlet air was 5.143 m/s. The NH_3 mass flow rate was 4e-06 kg/s, and the CO_2 mass flow rate was 1.7e-05 kg/s. As expected the velocity is concentrated near the inlet nozzle. The air velocity in the vicinity of the mouse was 0.678 meters per second, which is higher than acceptable comfortable level of 0.15 m/s-0.25 m/s. It can be concluded that the mouse would not stay at that position for very long and move away

towards the corner of the cage where the air velocity would be lesser. Figure 4-25 shows the contours of mole fraction of CO_2 concentrations for this case. The highest concentration is in the vicinity of the mouse body. The concentration of CO_2 in the cage is 1100 ppm. Figure 4-26 shows the mole fraction of NH_3 concentrations for this case. Figure 4-27 shows the top view of mole fraction of ammonia for this case. The highest concentration of ammonia is in the vicinity of the latrines. The concentration of ammonia in the cage is approximately 10 ppm.

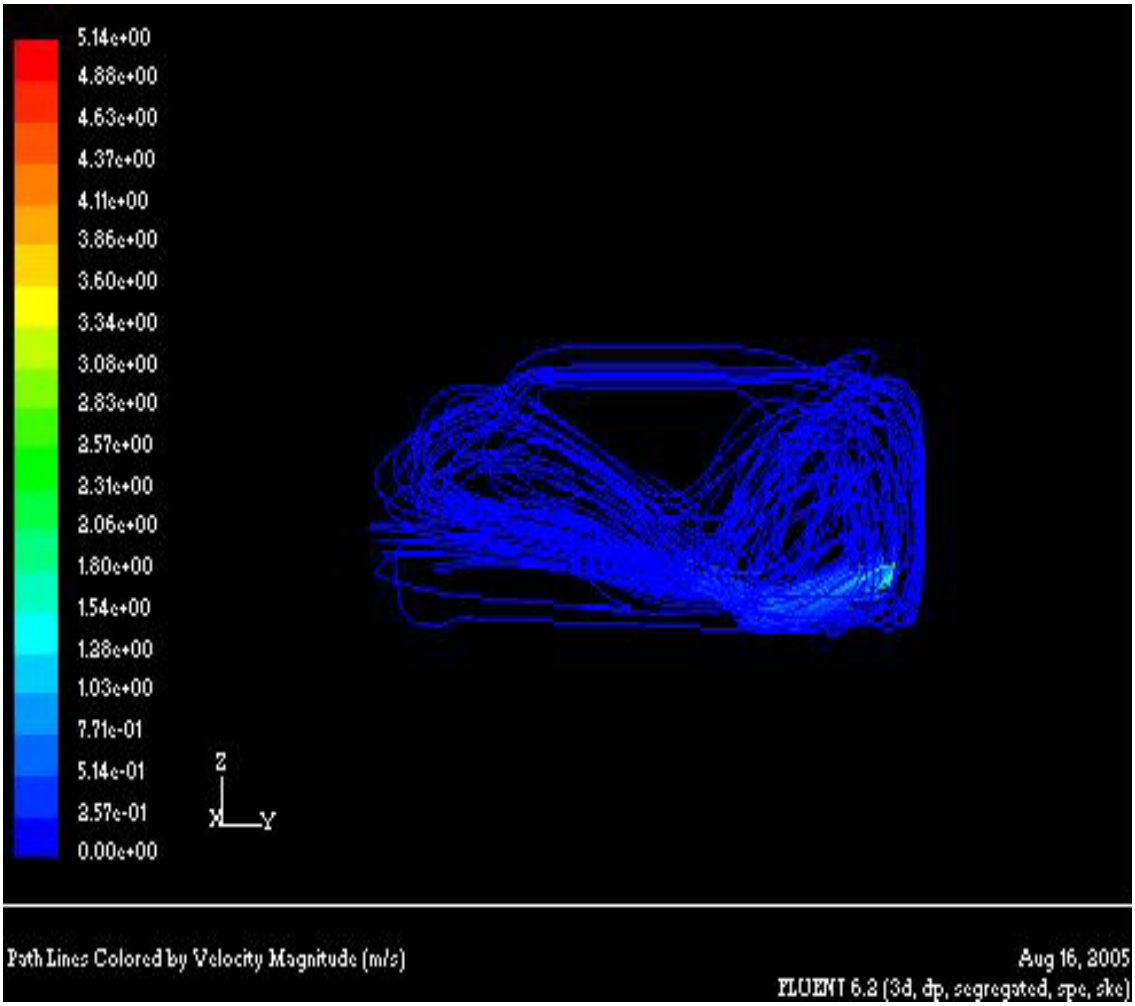

Figure 4-24. Velocity profiles for center of cage at 60 ACPH

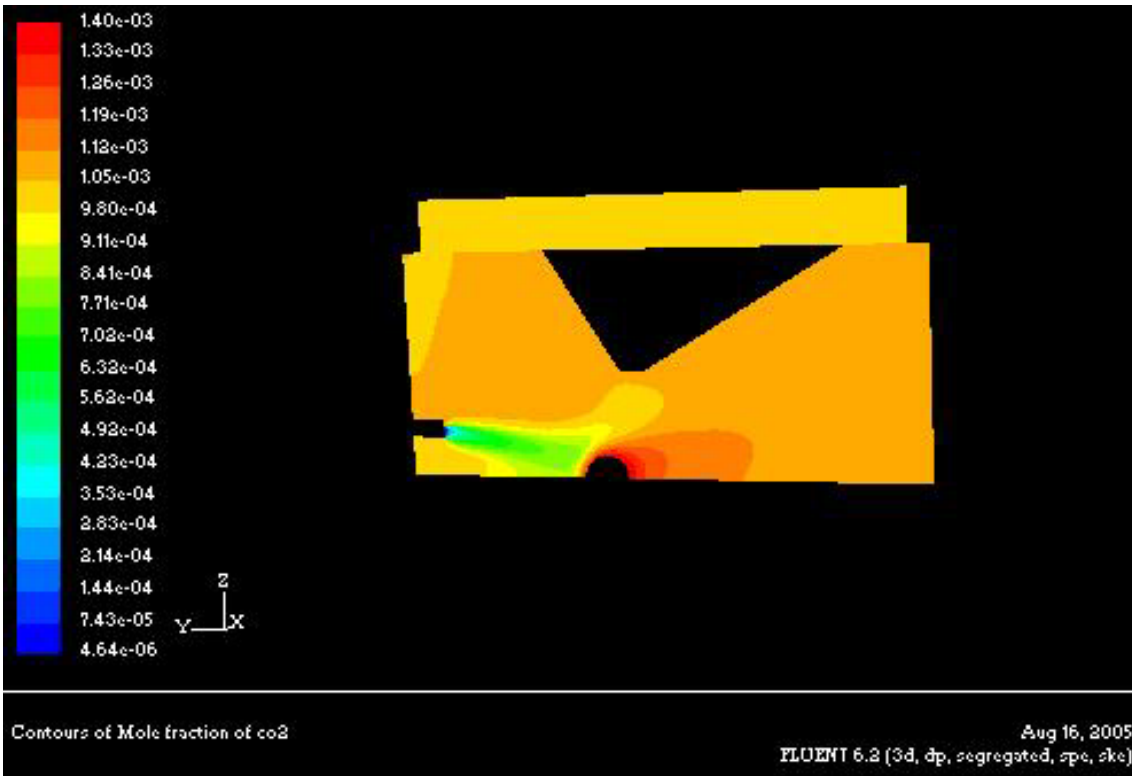

Figure 4-25. Contours of mole fraction of CO_2 for center of cage (60 ACPH)

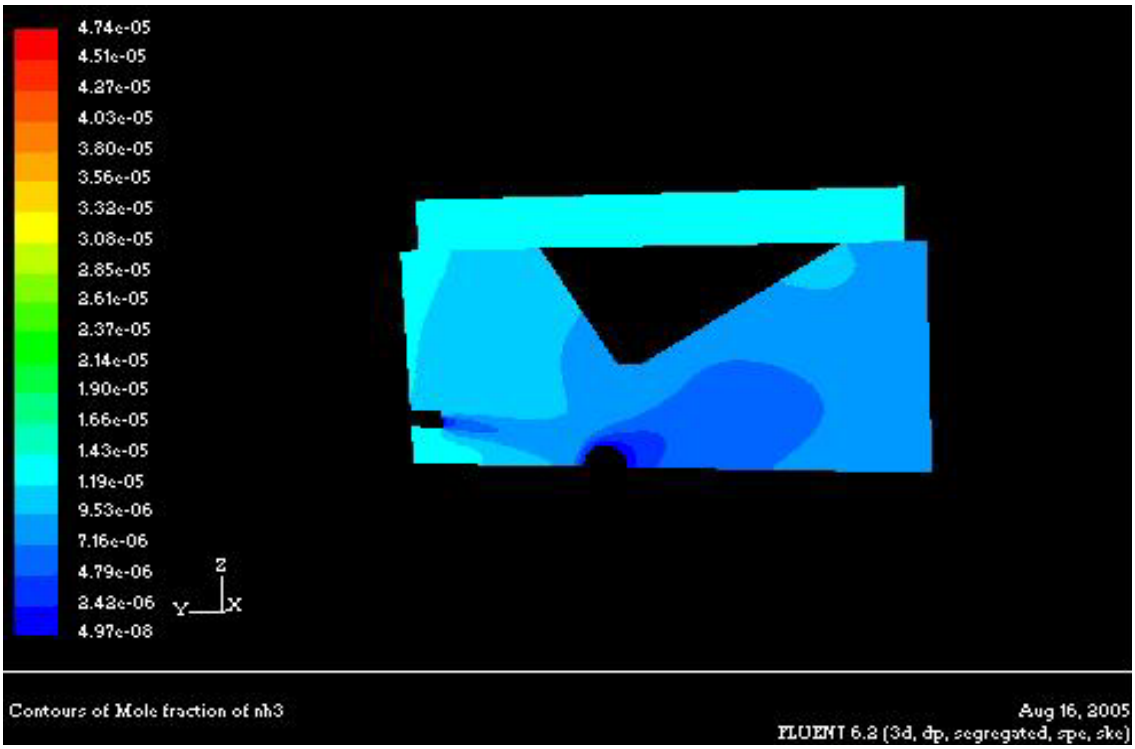

Figure 4-26. Contours of mole fraction of NH_3 for center of cage (60 ACPH)

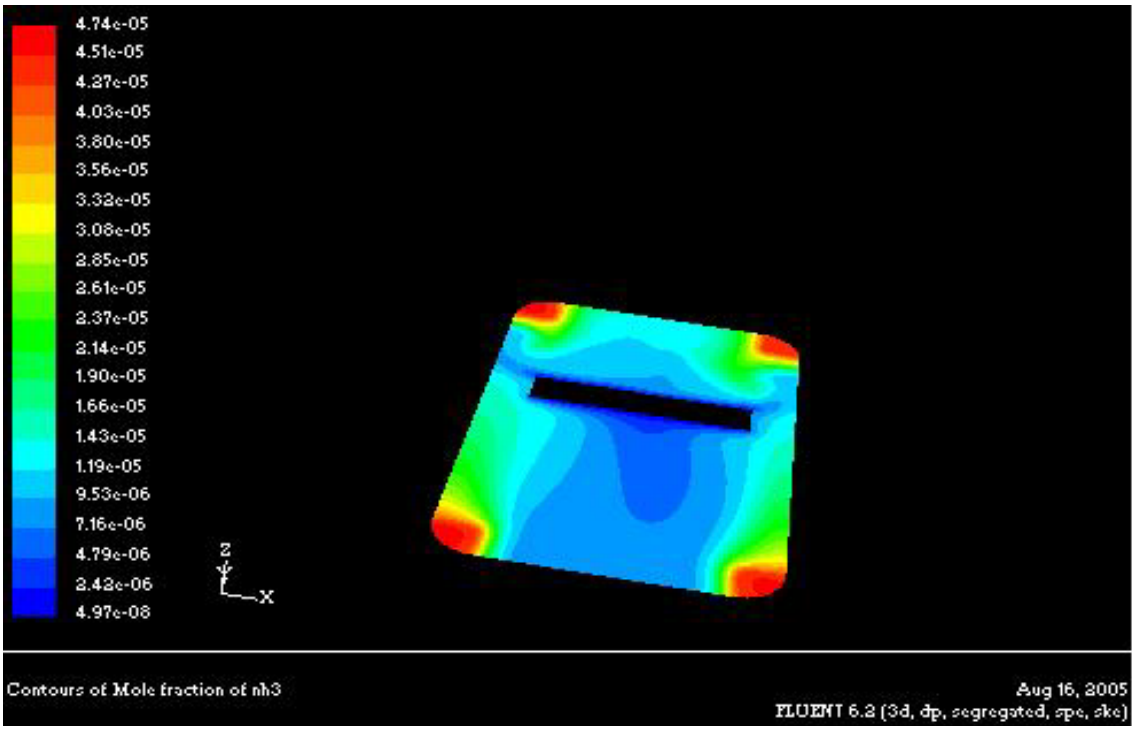

Figure 4-27. Top view of contours of mole fraction of NH_3 for center of cage (60 ACPH)

Figure 4-28 shows the velocity profiles for the CC case at 40 ACPH. For 40 ACPH the velocity of inlet air was 3.42 m/s. The NH_3 mass flow rate was 4e-06 kg/s, and the CO_2 mass flow rate was 1.7e-05 kg/s. As expected the velocity is concentrated near the inlet nozzle. The air velocity in the vicinity of the mouse was 0.376 meters per second, which is higher than acceptable comfortable level of 0.15 m/s-0.25 m/s. It can be concluded that the mouse would not stay at that position for very long and move away towards the corner of the cage where the air velocity would be lesser. Figure 4-29 shows the contours of mole fraction of CO_2 concentration at 40 ACPH. The concentration of CO_2 in the cage is 2000 ppm. Figure 4-30 shows the contours of mole fraction of NH_3 concentrations for this case. Figure 4-31 shows the top view of the contours of NH_3 concentrations for this case. The highest ammonia concentration is in the vicinity of the latrines. The concentration of ammonia in the cage is approximately 18 ppm.

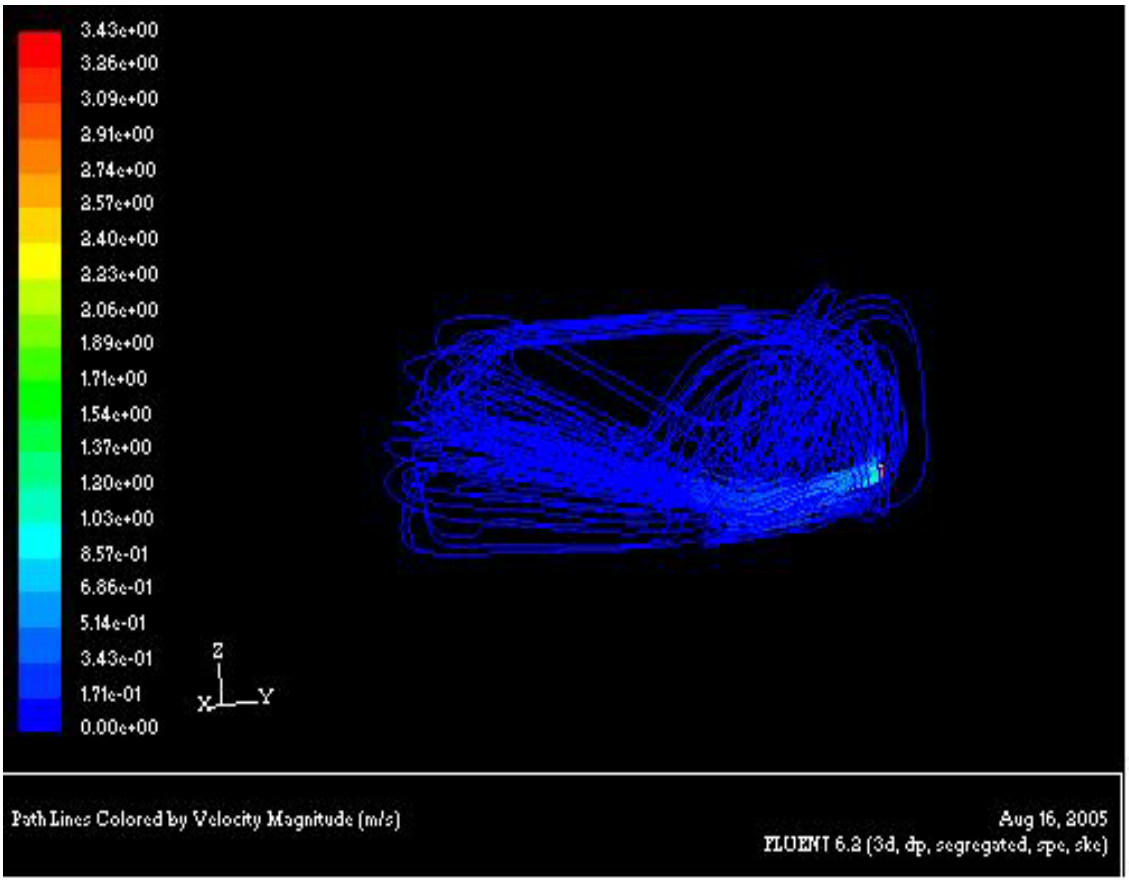

Figure 4-28. Velocity profiles for center of cage case at 40 ACPH

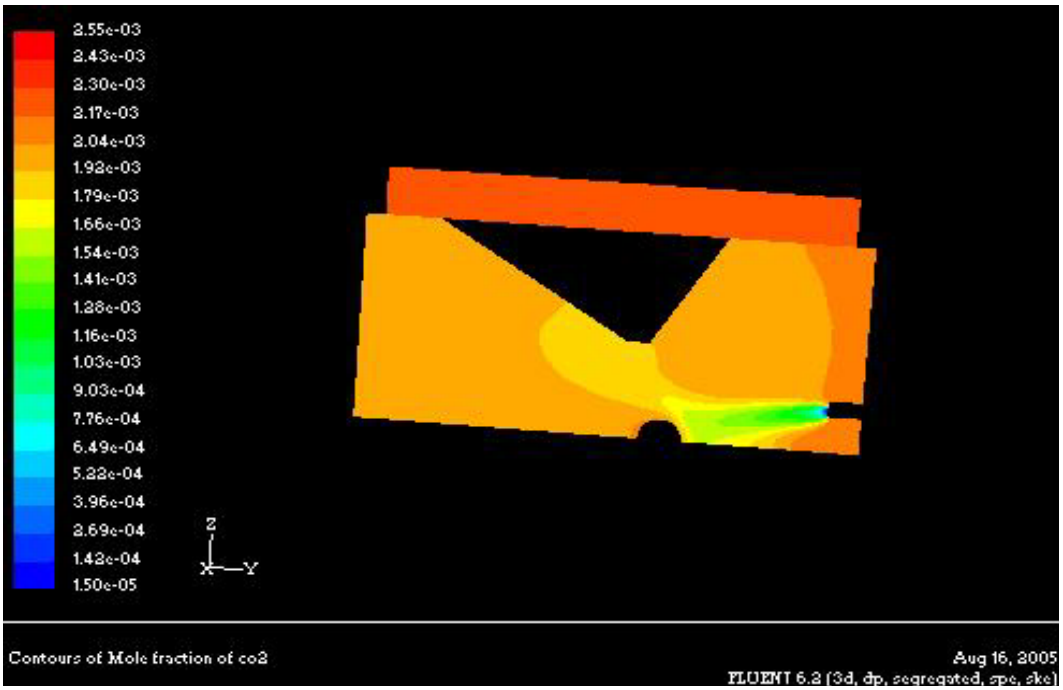

Figure 4-29. Contours of mole fraction of CO_2 for center of cage case (40 ACPH)

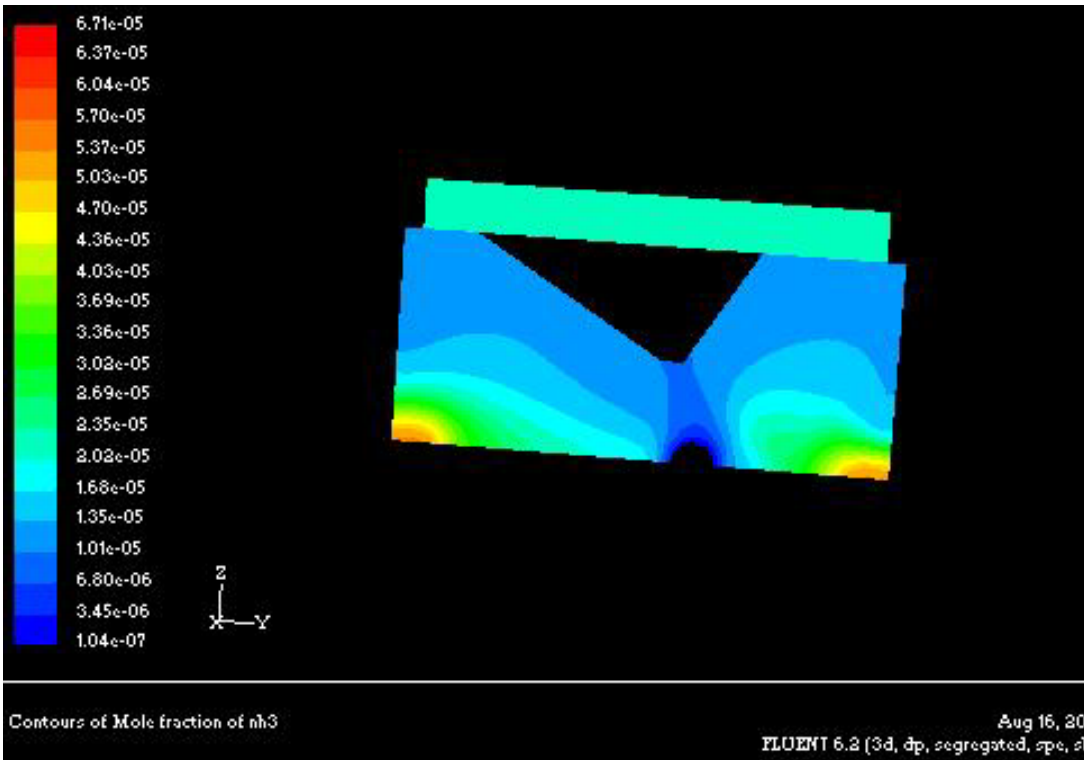

Figure 4-30. Contours of mole fraction of NH_3 for center of cage case (40 ACPH)

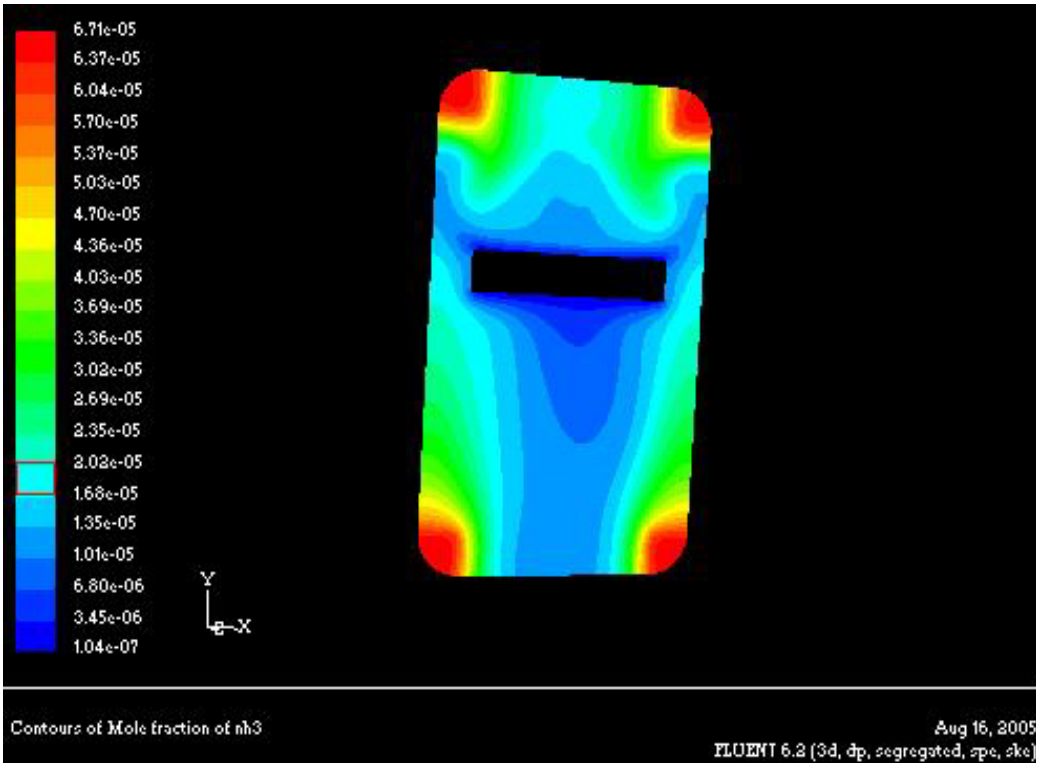

Figure 4-31. Top view of contours of mole fraction of NH_3 for center of cage case (40 ACPH)

Table 4-1 shows the CO_2 and NH_3 concentrations for all the results obtained from the CFD simulations. The concentration represented by the most prevalent color present in the cage is taken as the average concentration of the cage.

Table 4-1. Results from CFD simulations

Species	CC 100 ACPH	LM 60 ACPH	OW 60 ACPH	CC 60 ACPH	OW 40 ACPH	CC 40 ACPH	CC 20 ACPH
No. of Mice	2	4	2	2	2	2	2
CO_2	970 ppm	1350 ppm	1000 ppm	1100 ppm	2100 ppm	2000 ppm	4300 ppm
NH_3	6 ppm	9 ppm	11 ppm	10 ppm	20 ppm	18 ppm	27 ppm

As the CC case was analyzed for several levels of ACPH a comparison of ACPH effects can be made for this case. Table 4-2 shows this comparison for the CC case.

Table 4-2. CO_2 and NH_3 concentrations Vs. ACPH for center of cage case

Species	ACPH			
	100 ACPH	60 ACPH	40 ACPH	20 ACPH
Number of Mice	2	2	2	2
CO_2	970 ppm	1100 ppm	2000 ppm	4300 ppm
NH_3	6 ppm	10 ppm	18 ppm	27 ppm

Figure 4-32 shows the variation of CO_2 concentrations with increase in ACPH. It can be seen from the figure that CO_2 concentration increases with decrease in ACPH. The highest concentration of CO_2 is 4300 ppm at 20 ACPH. At 3000 ppm the ACPH comes about 30 ACPH. Figure 4-33 shows the variation of NH_3 with increase in ACPH. The highest concentration of NH_3 is 27 ppm at 20 ACPH, which is higher than the 25 ppm prescribed by the guide. An ACPH rate of 25 results in amid concentration of 28 ppm. 25-30 ACPH seems to be a logical choice to maintain acceptable levels of CO_2 and NH_3 in the cage.

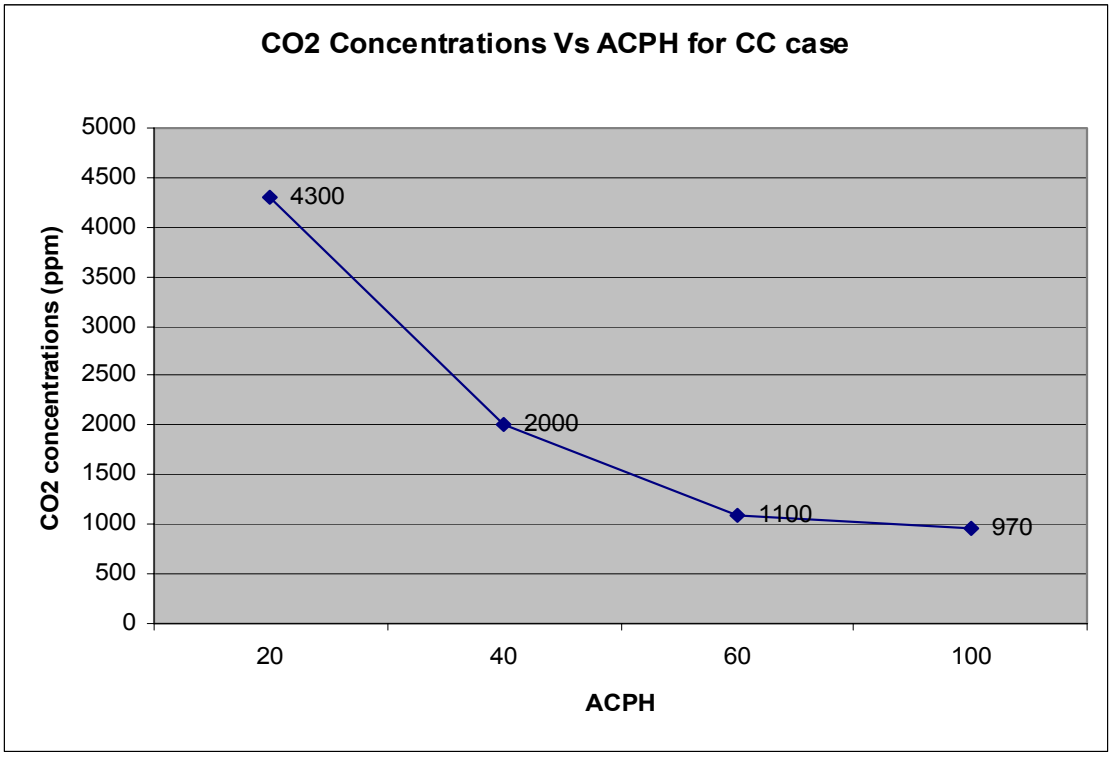

Figure 4-32. CO_2 concentrations Vs. ACPH

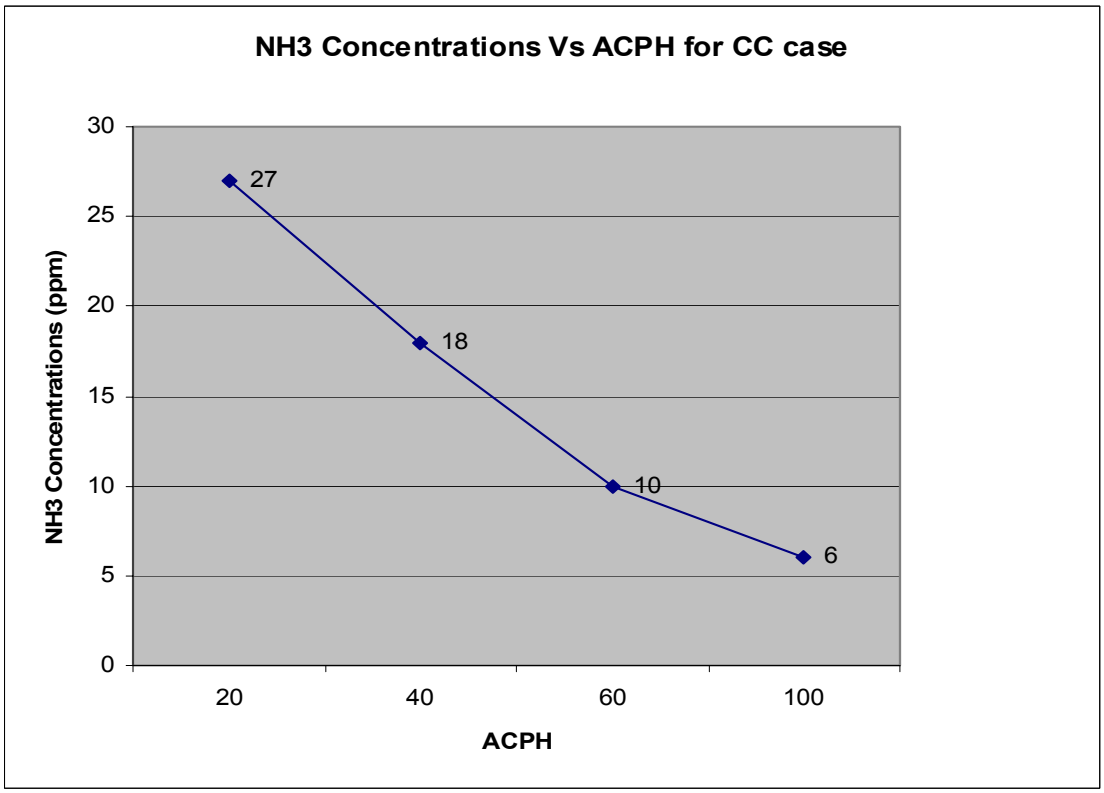

Figure 4-33. NH_3 concentrations Vs. ACPH

Three cases were run for 60 ACPH, CC, LM and OW. As four mice are considered for the LM case, the CO_2 concentrations cannot be compared. Since it was assumed that ammonia concentrations are independent of the number of mice bodies, the ammonia concentration for all the three cases at 60 ACPH can be compared. Table 4-3 shows the comparison of NH_3 concentrations for three cases at 60 ACPH. It can be seen from the table that concentrations are very similar.

Table 4-3. Comparison of NH_3 concentrations for different cases at 60 ACPH

	60 ACPH		
Species	**CC**	**OW**	**LM**
NH_3	**10 ppm**	**11 ppm**	**9 ppm**

The CO_2 concentrations for CC and OW can be compared for 60 ACPH. The CO_2 concentration for CC at 60 ACPH is 1000 ppm and 1100 ppm for OW at 60 ACPH. The CO_2 concentrations are almost equal.

Pandey (2005) carried out similar analysis on Allentown cages for five mice but without considering mice bodies in the geometry. As the ammonia in the cage is independent of the number of mice in the cage, the results for ammonia for the current study can be compared with the results of the analysis carried out by Pandey. Table 4-4 shows the comparison of results at 100 ACPH. Table 4-5 shows the comparison of results at 60 ACPH. The results show a good agreement with results reported by Pandey

Table 4-4. Comparisons of NH_3 concentrations against results reported by Pandey (2005) at 100 ACPH

Species	**Center of Cage (100 ACPH)**	**Pandey (2005) Corner Bottom (100 ACPH)**
NH_3	**6 ppm**	**6.5 ppm**

Table 4-5. Comparisons of NH_3 concentrations against results reported by Pandey (2005) at 60 ACPH

Species	Center of Cage (60 ACPH)	Four Mice (60 ACPH)	Outside Wall (60 ACPH)	Pandey (2005) Corner Bottom (60 ACPH)
NH_3	**10 ppm**	**9 ppm**	**11 ppm**	**13 ppm**

As the flow rate of air decreases from 100 to 60 to 40 to 20 ACPH the ventilation from power consumed is less and savings are more. The savings by using lower air change rates as compared to 100 ACPH are shown below. The calculations are for savings and power consumed are provided in Appendix C. P_1 is the power of fan at 100 ACPH.

Savings for 60 ACPH is 79% which comes out to S_1= \$549.4P_1 per year

Savings for 40 ACPH is 93.7% which comes out to S_2= \$656.6P1 per year

Savings for 30 ACPH is 97.3% which comes out to S_4= \$681.9P_1 per year

Savings for 20 ACPH is 99.3% which comes out to S_3= \$695.9P_1 per year

At 30 ACPH the savings are 97.3% of money used at 100 ACPH.

The mass flow rate for CO_2 used in the study can also be verified by the calculations shown in Appendix D. It can be seen that at 20 and 40 ACPH the percent error is very less 3% and 6% respectively. The error for 100 ACPH is 18%, this is due to the fact that most prevalent concentration was assumed as the CO_2 leaving the cage is lower, and there are areas in the cage where the concentration of CO_2 is much higher than the prevalent concentration. At 60 ACPH the error is highest 38%, this is again due the prevalent CO_2 is very less and there are areas near the mice and latrines where CO_2 concentration is much higher than prevalent concentration.

CHAPTER 5
SUMMARY AND CONCLUSIONS

The purpose of this study was to perform a computational fluid dynamic analysis to study the effect of rodent activity on ventilated cages. The air velocity profiles and concentrations of ammonia, carbon dioxide were developed for each cage configuration. The concentrations were calculated at 20, 40, 60, and 100 ACPH. Stationary mice bodies were simulated in the cage. Different positions were analyzed for the mice bodies. An Allentown rodent cage PC 7115RT was used for the study.

Three different mice positions were considered for the study. The concentration that was most prevalent in the cage was assumed to be the average concentration of CO_2 and NH_3 in the cage. Two mice were positioned at the outer wall of the cage, away from the inlet nozzle, referred to with an abbreviation “OW”. This case was analyzed for 40, and 60 ACPH. The results CO_2 concentration was 1000 ppm for 60 ACPH and 2100 ppm for 40 ACPH. The NH_3 concentration was 11 ppm for 60 ACPH and 20 ppm for 40 ACPH.

For the second case two mice bodies were positioned near the center of the cage and close to the inlet nozzle, referred to with an abbreviation “CC”. This case was run for 20, 40, 60, and 100 ACPH. The resulting CO_2 and NH_3 concentrations were 970 ppm and 6 ppm respectively for 100 ACPH, 4300 ppm and 27 ppm respectively for 20 ACPH, 1100 ppm and 10 ppm respectively for 60 ACPH, and 200 ppm and 18 ppm respectively for 40 ACPH.

Two mice bodies were positioned near the center of the cage along y-axis of the cage, referred to with an abbreviation “LM”. The lengths of the cylinders were doubled to simulate four mice. This case was analyzed for 60 ACPH. The average CO_2 and NH_3 concentrations were 1350 ppm and 9 ppm respectively at 60 ACPH.

The following conclusions are based on the results obtained from the simulations

1. The ammonia concentrations for all the models at 100 and 60 ACPH agreed with the results reported by Pandey (2005) for ammonia.
2. As the ventilation rate was decreased from 100 ACPH to 20 ACPH, the average concentration of carbon dioxide increased from 970 ppm to 4300 ppm, and the average ammonia concentrations increased from 6 ppm to 27 ppm in the cage.
3. The concentration of carbon dioxide also increased with an increase in the number of mice as expected.
4. The size of the cylinder would also have an effect on the CO_2 concentrations in the cage. The bigger the mouse more CO_2 it produces.
5. The concentrations of ammonia and carbon dioxide were much less in the vicinity of the inlet nozzle due to the fresh air introduced by the nozzle.
6. The area of the mouse body that comes in direct contact with the air indicates a lower concentration of CO_2 than the area, which is not in contact with the direct airflow.
7. In the CC case for 100 ACPH, the mice body is placed near the inlet nozzle and shows a lower concentration of CO_2 near the mice body. The air hits the mouse body with a volumetric flow rate of 1.27e-07 m^3/s, and the CO_2 concentration in that area is 695 ppm, which increases to 850 ppm moving away from that area. In the LM case for 60 ACPH, in the area where the flow hits directly, the CO_2 concentration is 700

ppm and increases to 1450 ppm moving away from the nozzle. In the OW case, for 60 ACPH the CO_2 concentration at the area of direct contact with the air is 838 ppm, which is higher than the other two cases as the mouse body is further away from the nozzle. The CO_2 concentration on the rest of the mouse body is 1390 ppm and decreases with the increase in distance from the body.

8. It can be seen that by introducing mice bodies in the cage and by positioning mice at different locations, affects the overall performance of the cage ventilation system. It can be seen that the mouse position has an effect on the concentration of CO_2 in that area. An increase was also seen in the concentration of CO_2 for the same air change rates when the numbers of mice were increased in the cage.
9. At 100, and 60 ACPH the air velocity was much higher in the cage than the assumed acceptable levels. At 40 ACPH the air velocity was higher near the inlet nozzle but was within the acceptable level away from the nozzle. At 20 ACPH the air velocity level was within the comfortable level throughout the cage.
10. As the flow rate of air decreases from 100 ACPH the power consumed by the fan also decreases, and the savings increase. The savings compared to 100 ACPH are
    a. 79% for 60 ACPH
    b. 93.7% for 40 ACPH
    c. 97.3% for 30 ACPH
    d. 99.3% for 20 ACPH.

With further CFD studies it may be possible to produce a design that could effectively ventilate rodent cages in the 20-30 ACPH range, which could result in significant energy savings over current practices.

CHAPTER 6
RECOMMENDATIONS

1. A model to analyze the urea and water reactions in the cage should be investigated. This model can simulate ammonia as it is produced due to composition of urea in real cages.
2. Improve the model for the mouse geometry. The mouse body can be simulated as a full cylinder for better airflow analysis in the cage. Other locations for mouse and latrines can also be analyzed.
3. The mouse body can also be simulated to be a source of heat and water vapor in the cage. This should be added to the model.
4. As it was seen that NH_3 concentrations exceeded the acceptable level of 25ppm for 20 ACPH, simulations should be run for other ACPH to optimize around the acceptable NH_3 concentrations.
5. Redesign the inlet nozzle and model the effects with CFD. Ammonia and carbon dioxide concentrations should be analyzed for two inlet nozzles opposite to each other and air being injected at a lower ACPH. By using a lower air change rate the savings also increase. The savings are within the range of 90-99% of power being consumed at 100 ACPH.
6. Conduct experiments to validate the CFD model. Both live and simulated mice should be used for the study.

APPENDIX A
MESH CAGE PROFILES

This appendix includes the plot showing the type of mesh used in the cage. Figure A-1 shows the type of mesh used in the CC cage. The top and sides of the cage are meshed with 0.15 inch structured mesh. The inside volumes are meshed with 0.1 inch structured mesh. The nozzle area is meshed with an unstructured mesh of 0.05 inch, this is because the nozzle size is very small.

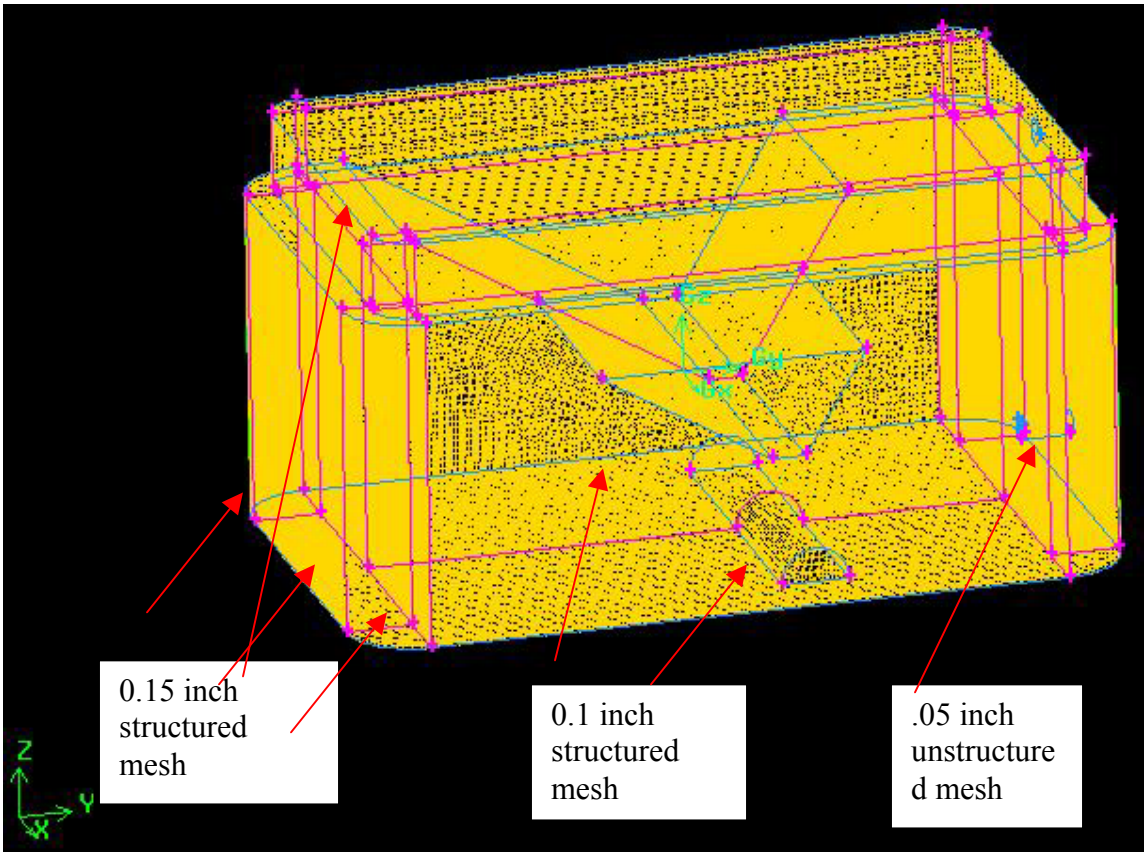

Figure A-1. Mesh used for CC case

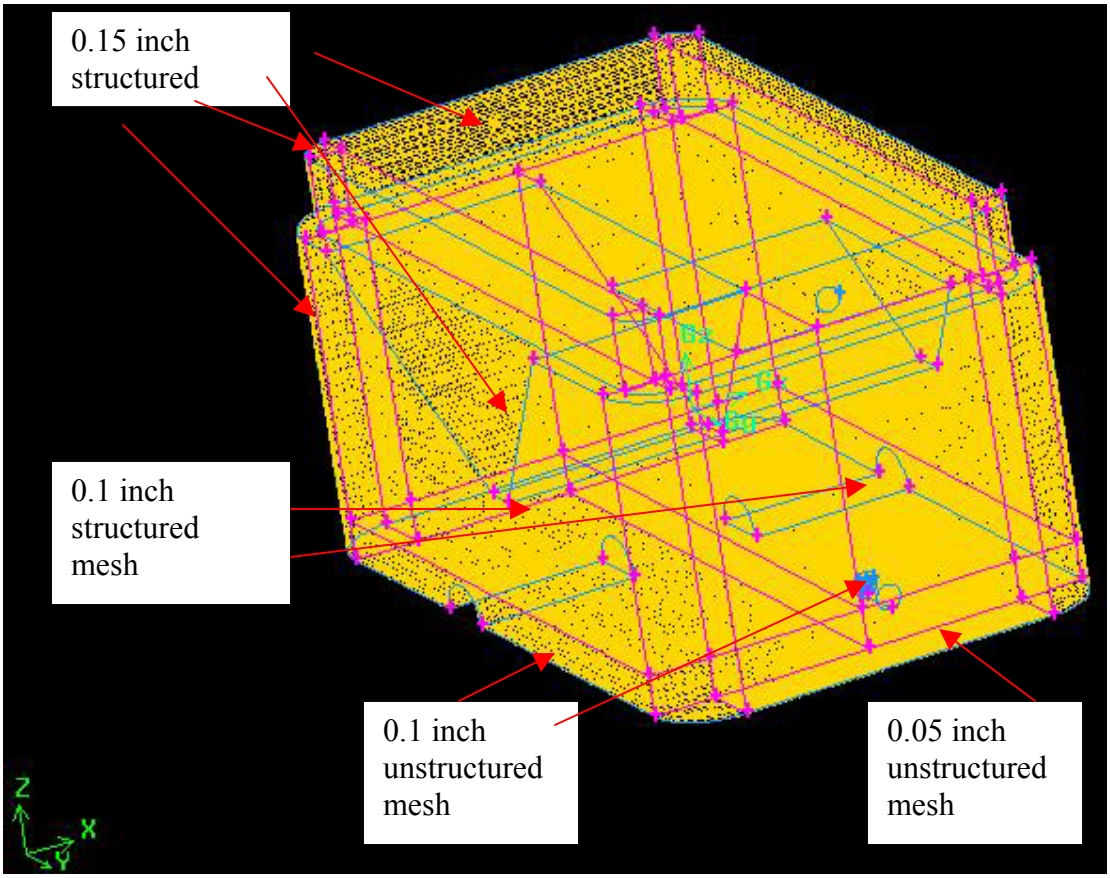

Figure A-2. Mesh used for OW case

Figure A-2 shows the mesh used for OW cage. The top and sides are meshed with a structured mesh on size 0.15 inches. The inside volumes is divided into two parts as it was not possible to mesh the whole volume with a structured mess. The upper part of the volume is meshed with 0.1 inch structured mesh. The lower part is meshed with 0.1 inch unstructured mesh. The part with nozzle is meshed with 0.05 inch unstructured mesh as the size of nozzle is very small.

APPENDIX B
CONTOURS OF DIFFERENT SPECIES

This appendix includes the plots of contours of carbon dioxide and ammonia for CC case at 100 ACPH, and LM and OW cases for 60 ACPH

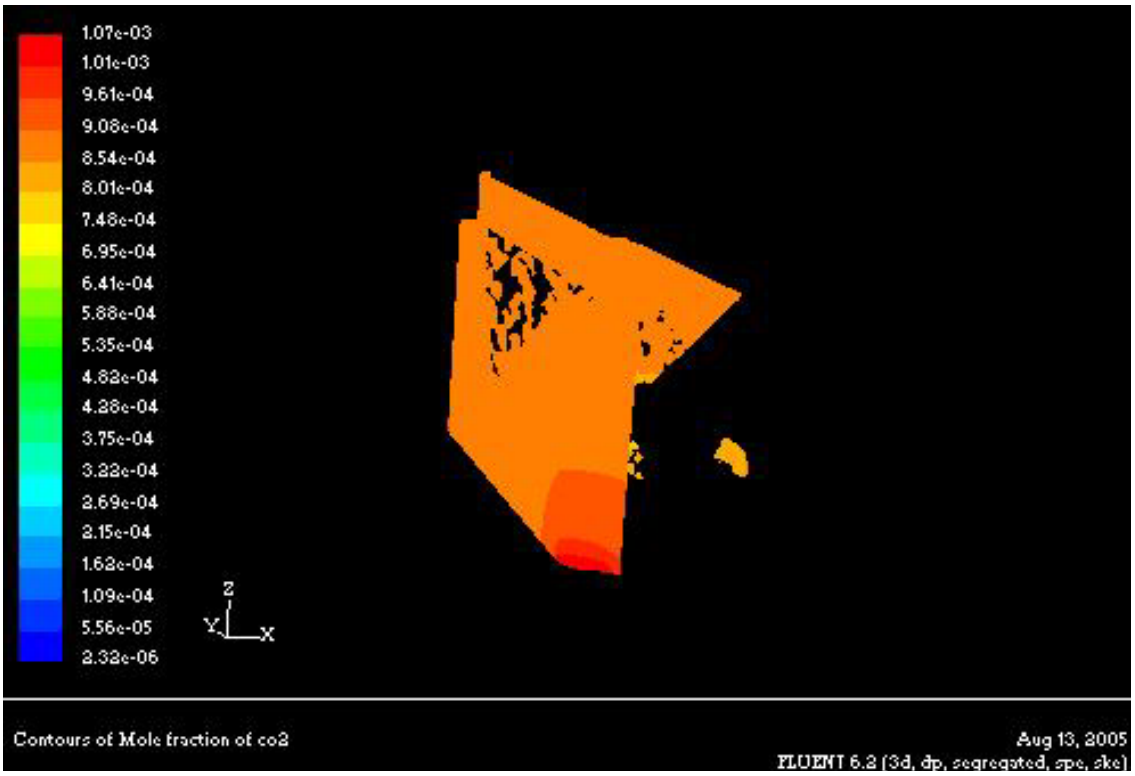

Figure B-1. Contours of CO_2 for CC in X-Y-Z plane (100 ACPH)

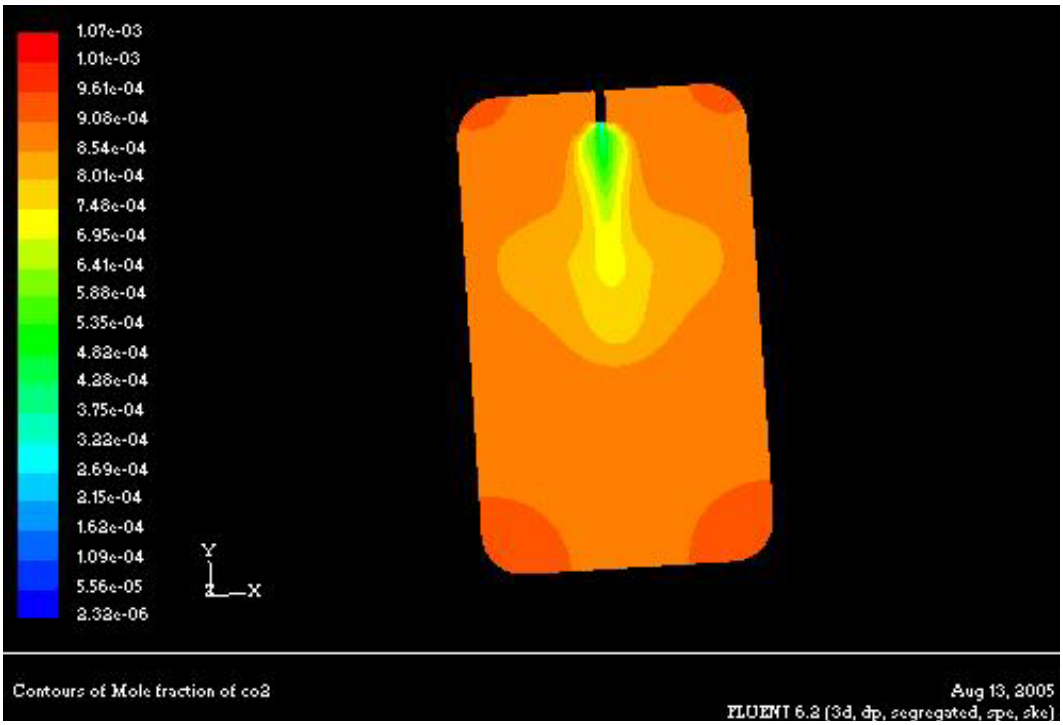

Figure B-2. Contours of CO_2 for CC in X-Y plane (100 ACPH)

Figure B-3. Contours of CO_2 for CC in Z-X plane (100 ACPH)

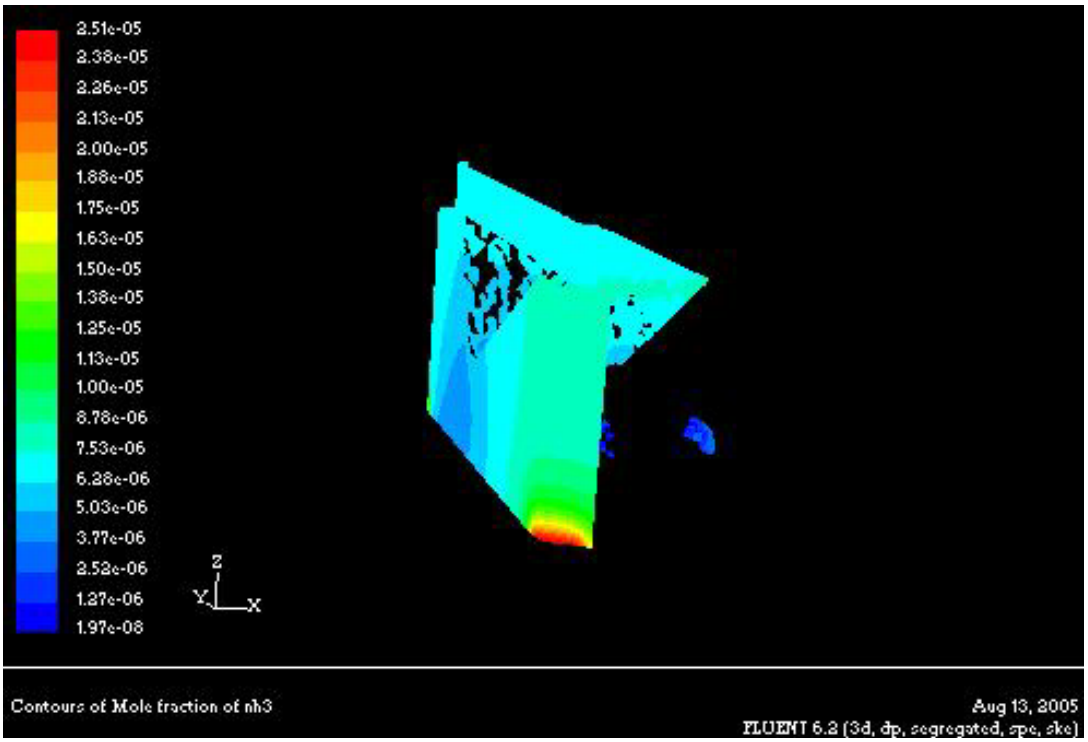

Figure B-4. Contours of NH_3 for CC in X-Y-Z plane (100 ACPH)

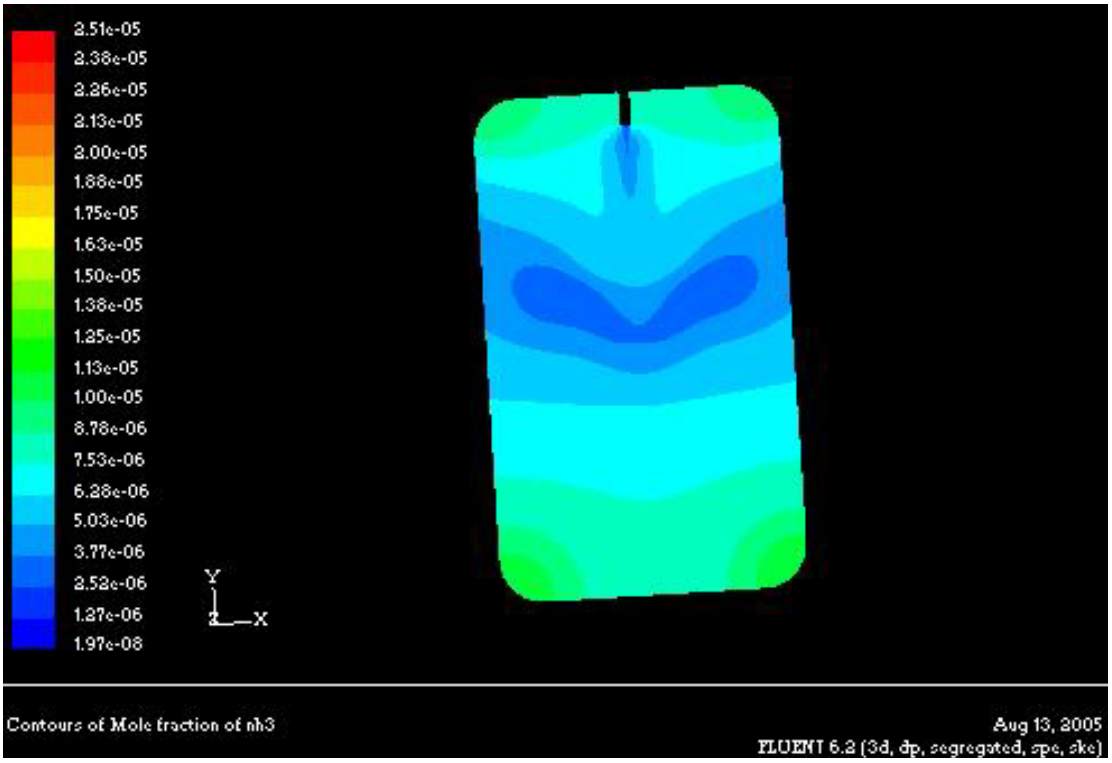

Figure B-5. Contours of NH_3 for CC in X-Y plane (100 ACPH)

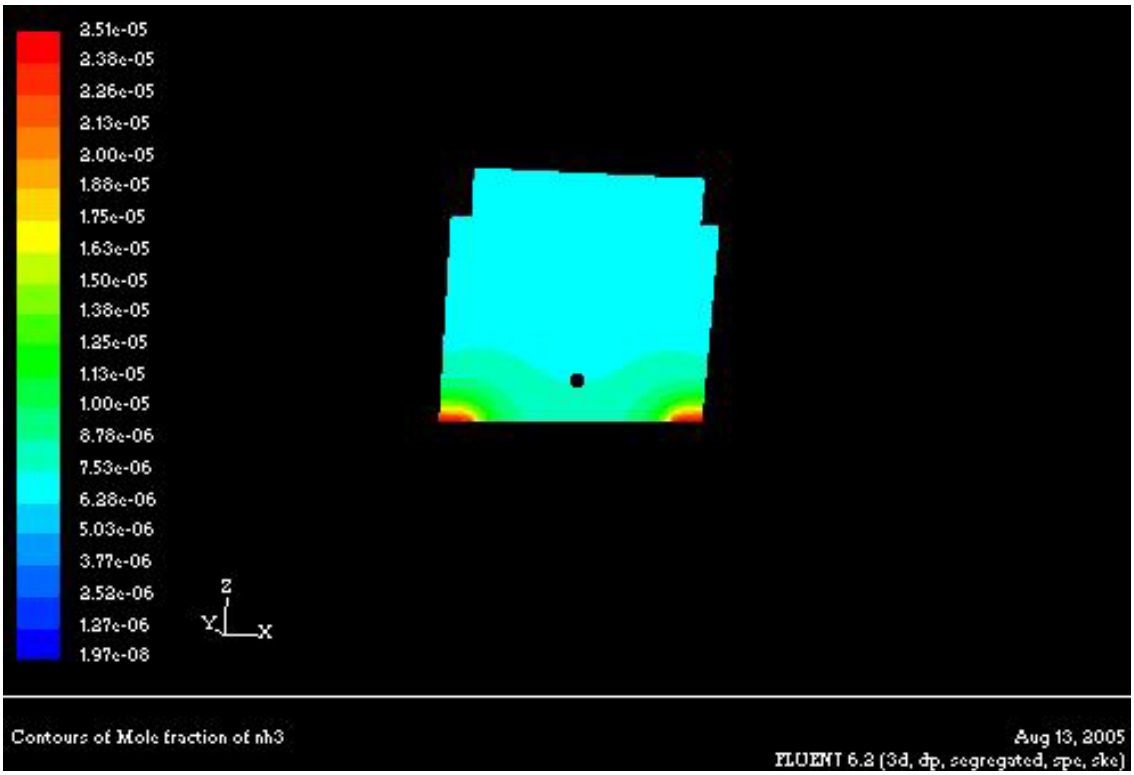

Figure B-6. Contours of NH_3 for CC in Z-X plane (100 ACPH)

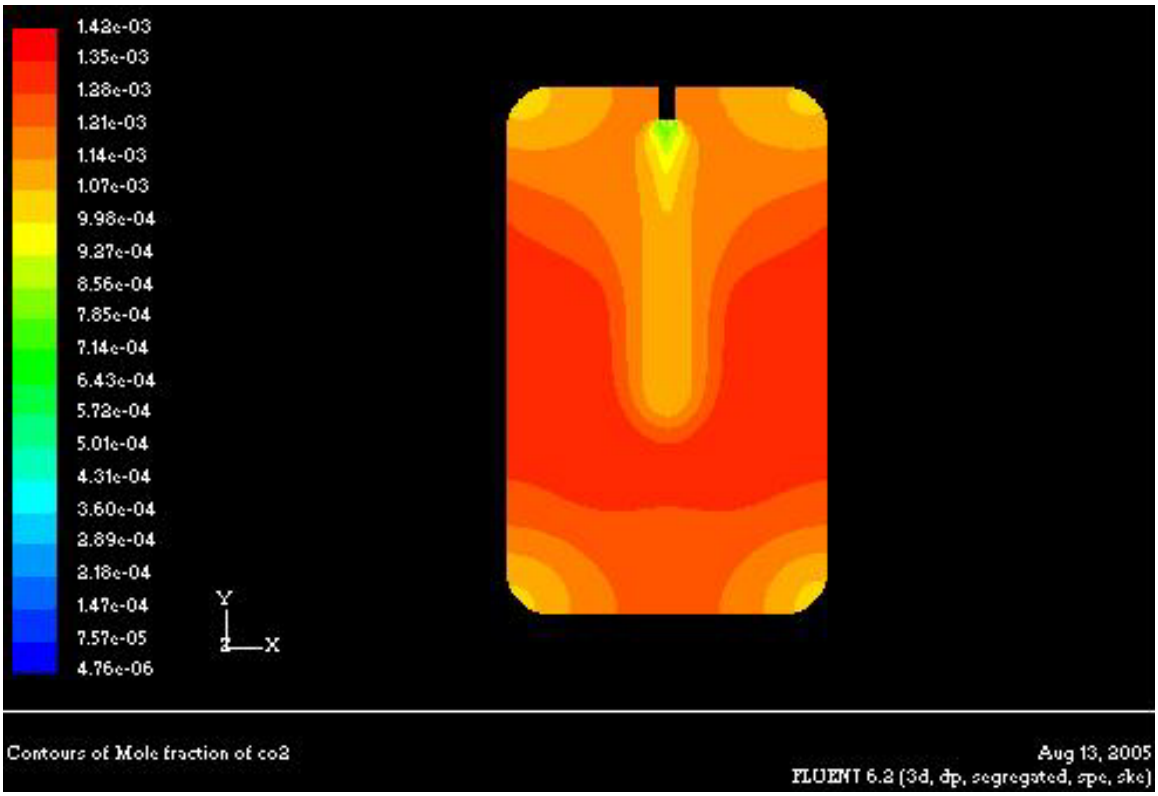

Figure B-7. Contours of CO_2 for LM in X-Y plane (60 ACPH)

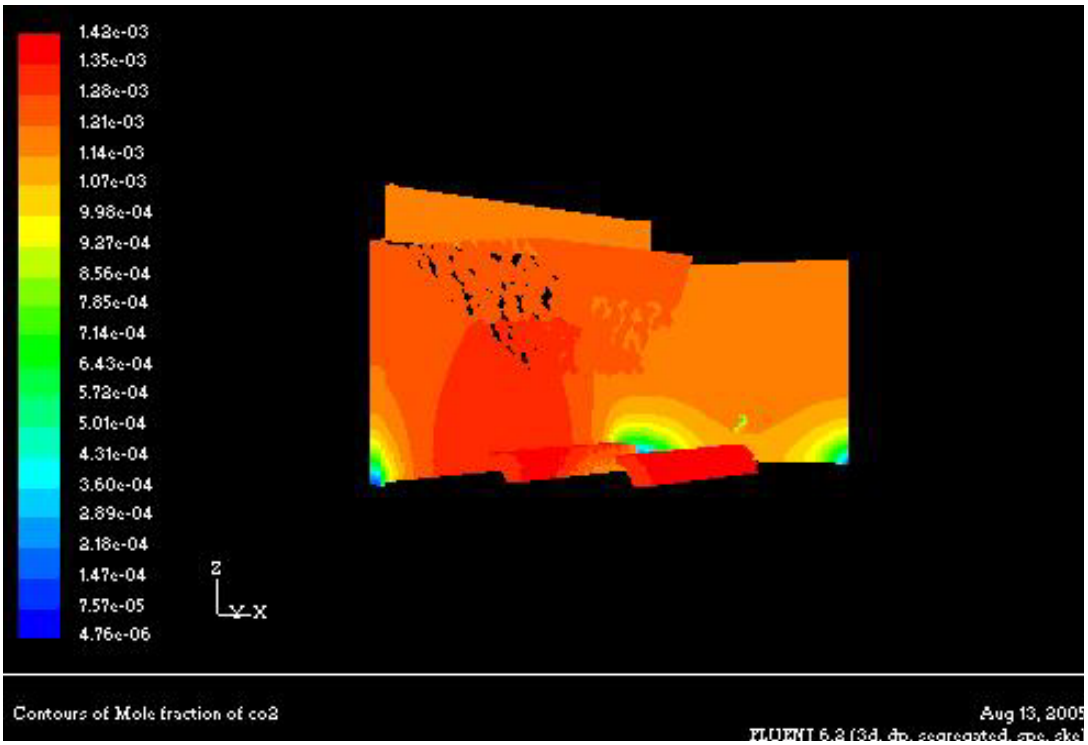

Figure B-8. Contours of CO_2 for LM in X-Y-Z plane (60 ACPH)

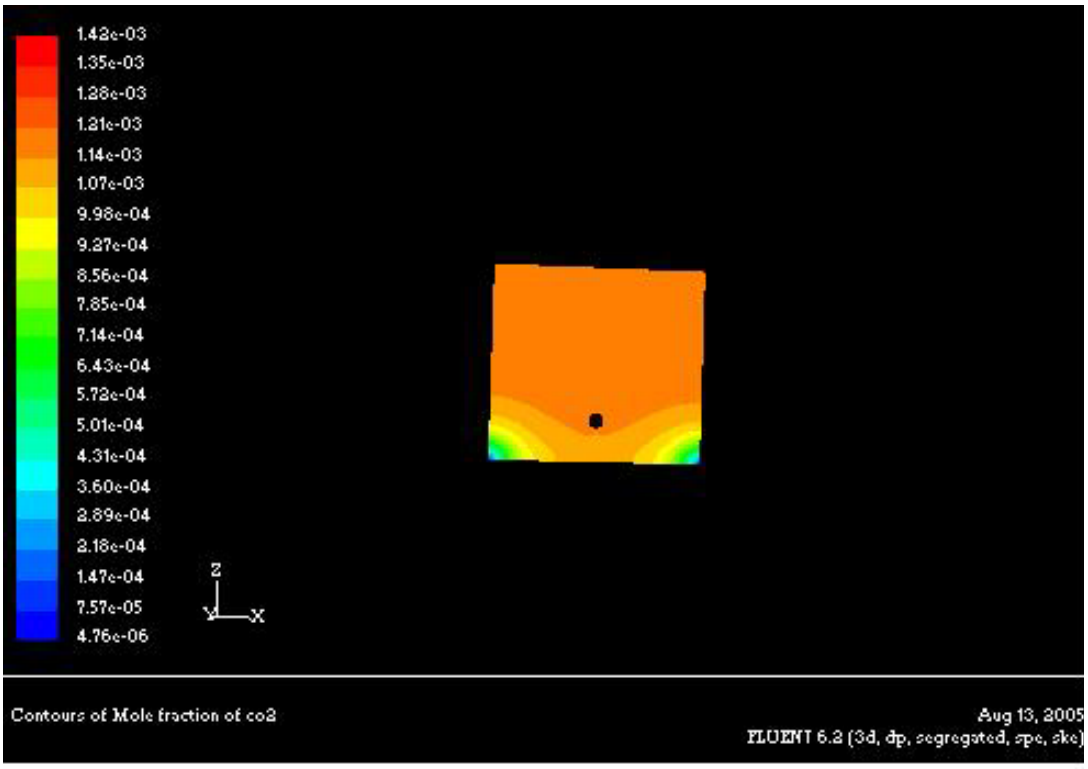

Figure B-9. Contours of CO_2 for LM in Z-X plane (60 ACPH)

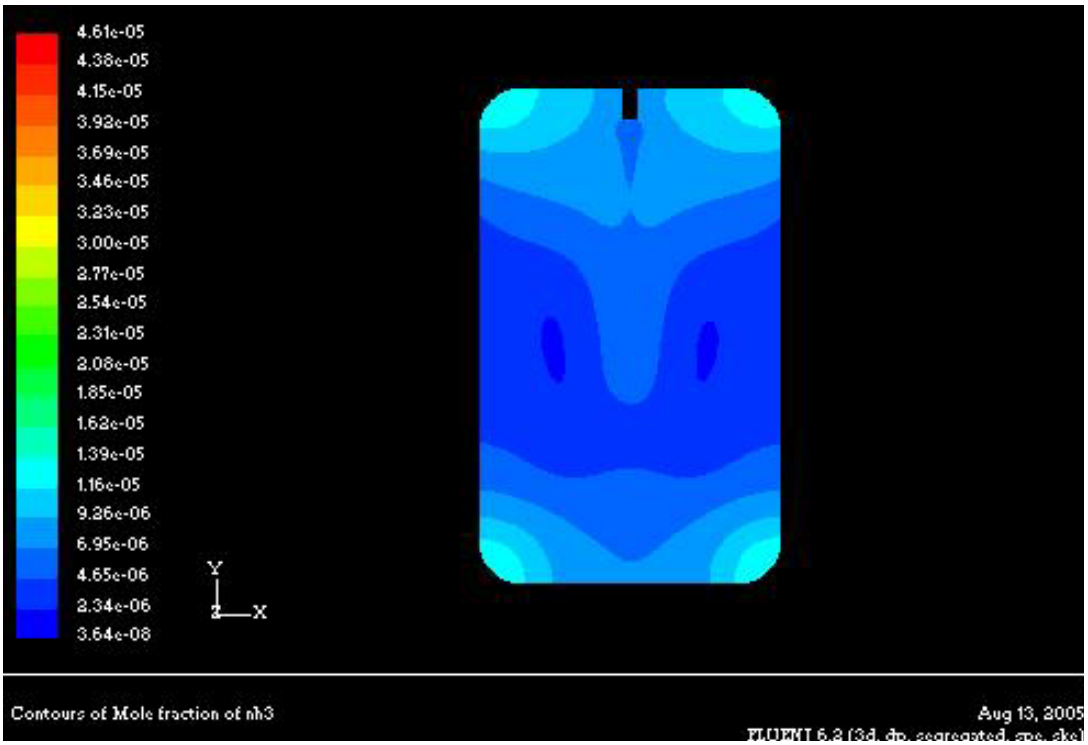

Figure B-10. Contours of NH_3 for LM in X-Y plane (60 ACPH)

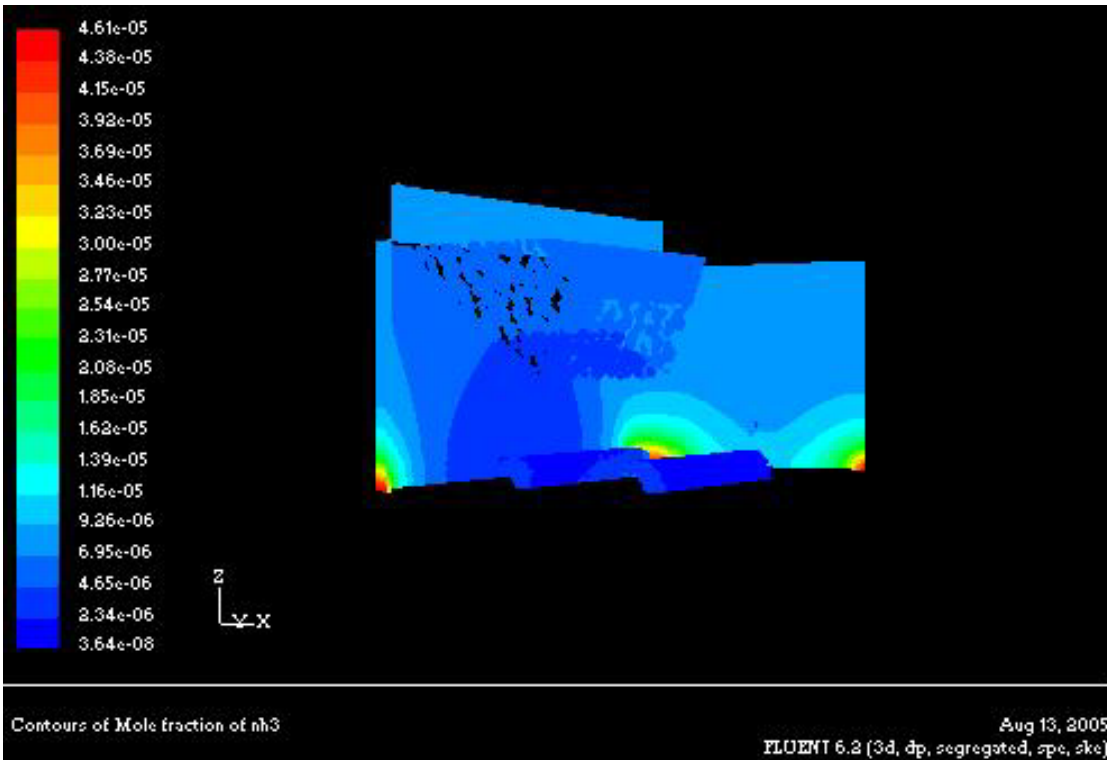

Figure B-11. Contours of NH_3 for LM in X-Y-Z plane (60 ACPH)

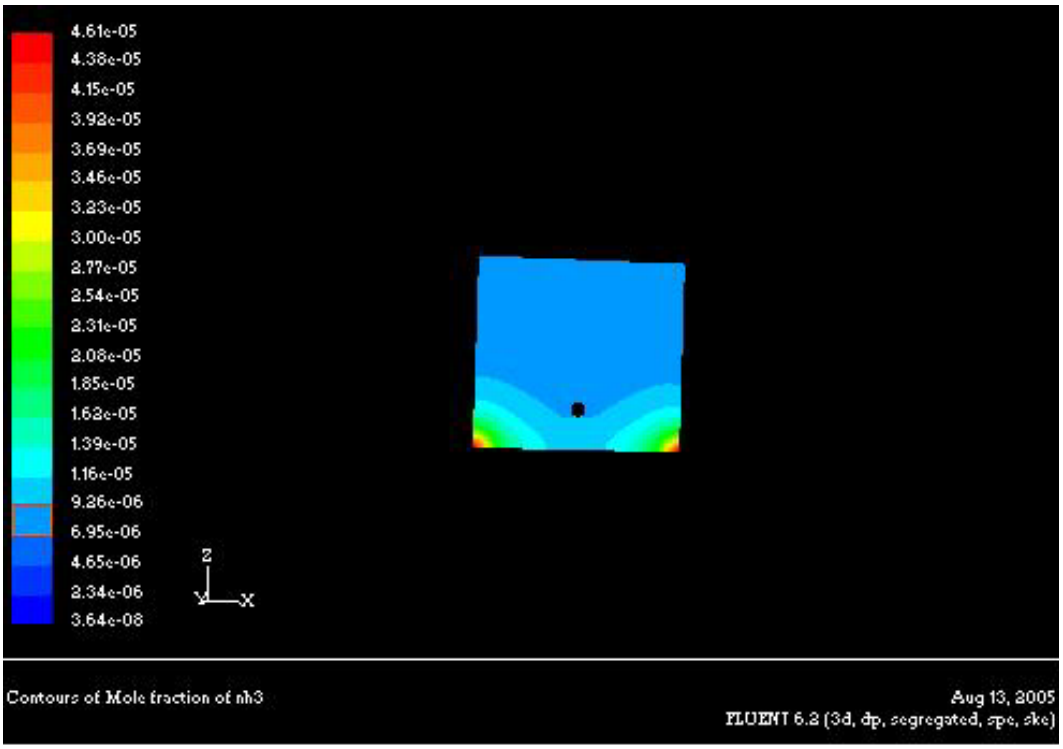

Figure B-12. Contours of NH_3 for LM in Z-X plane (60 ACPH)

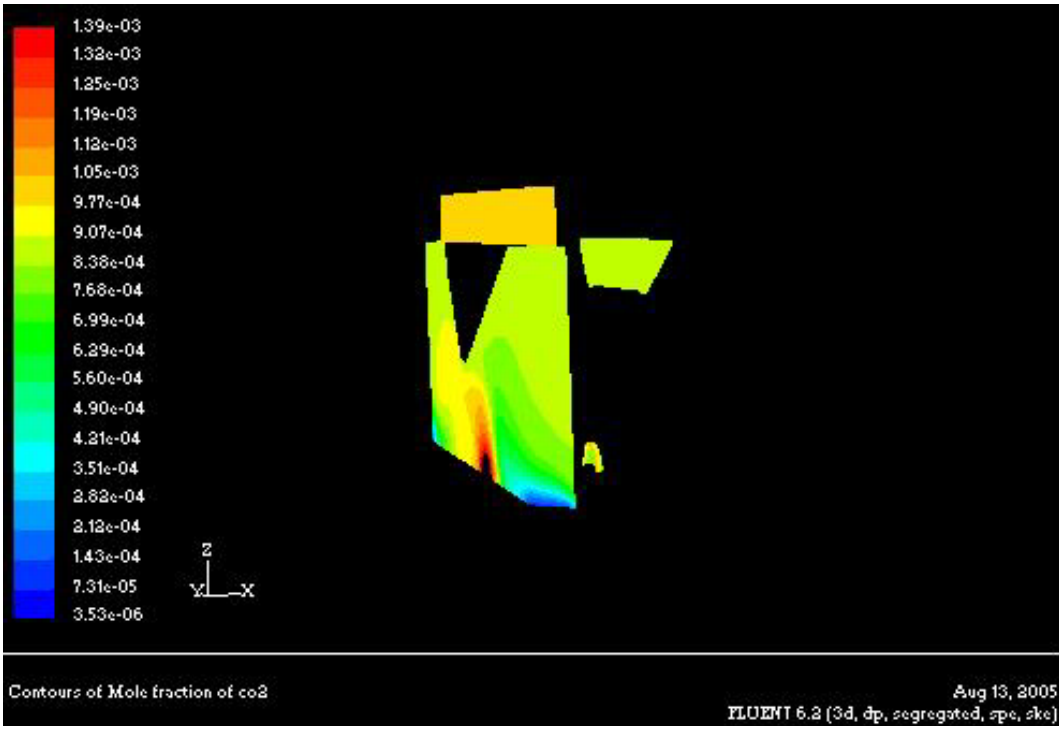

Figure B-13. Contours of CO_2 for OW in X-Y-Z plane (60 ACPH)

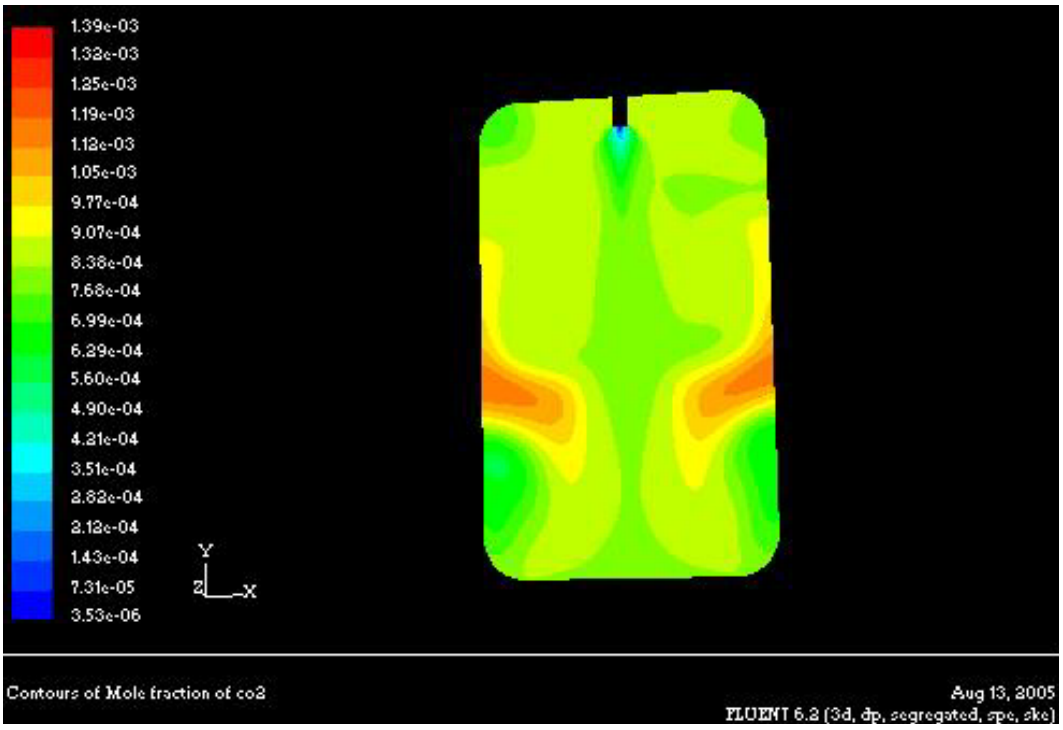

Figure B-14. Contours of CO_2 for OW in X-Y plane (60 ACPH)

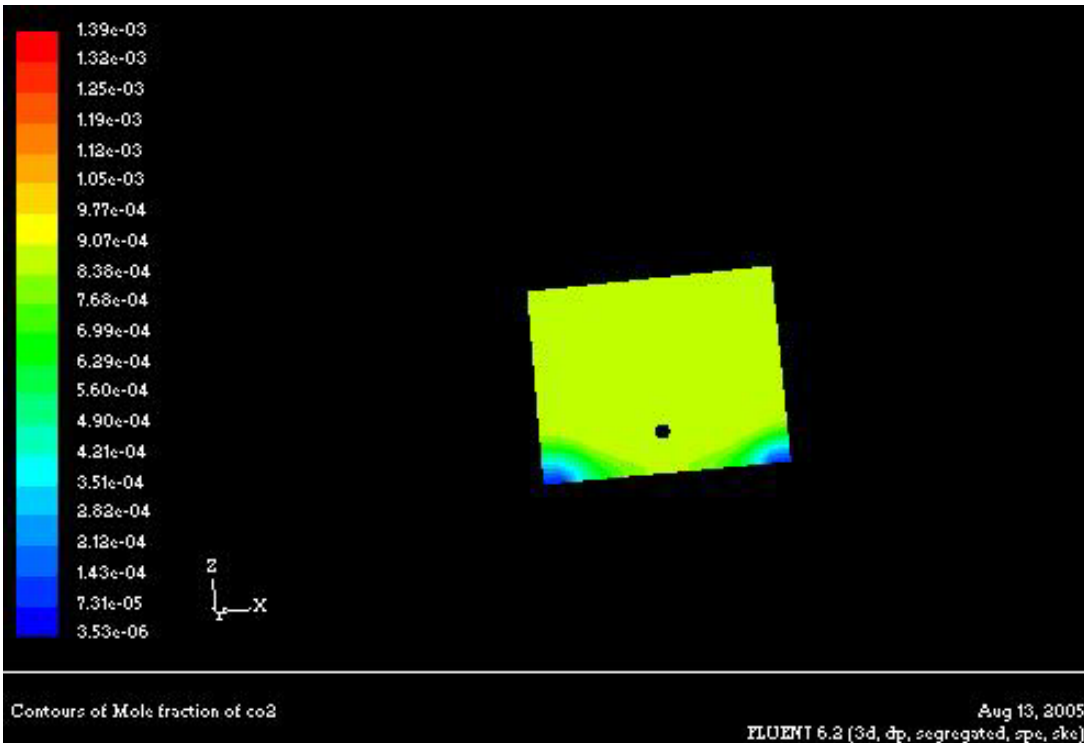

Figure B-15. Contours of CO_2 for OW in Z-X plane (60 ACPH)

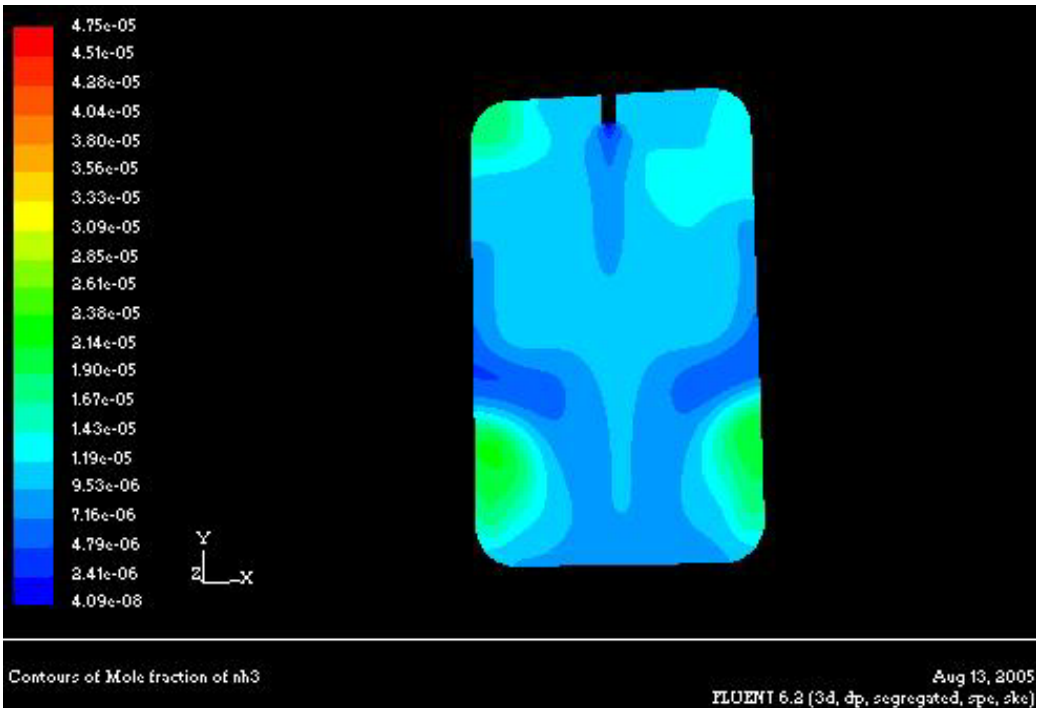

Figure B-16. Contours of NH_3 for OW in X-Y plane (60 ACPH)

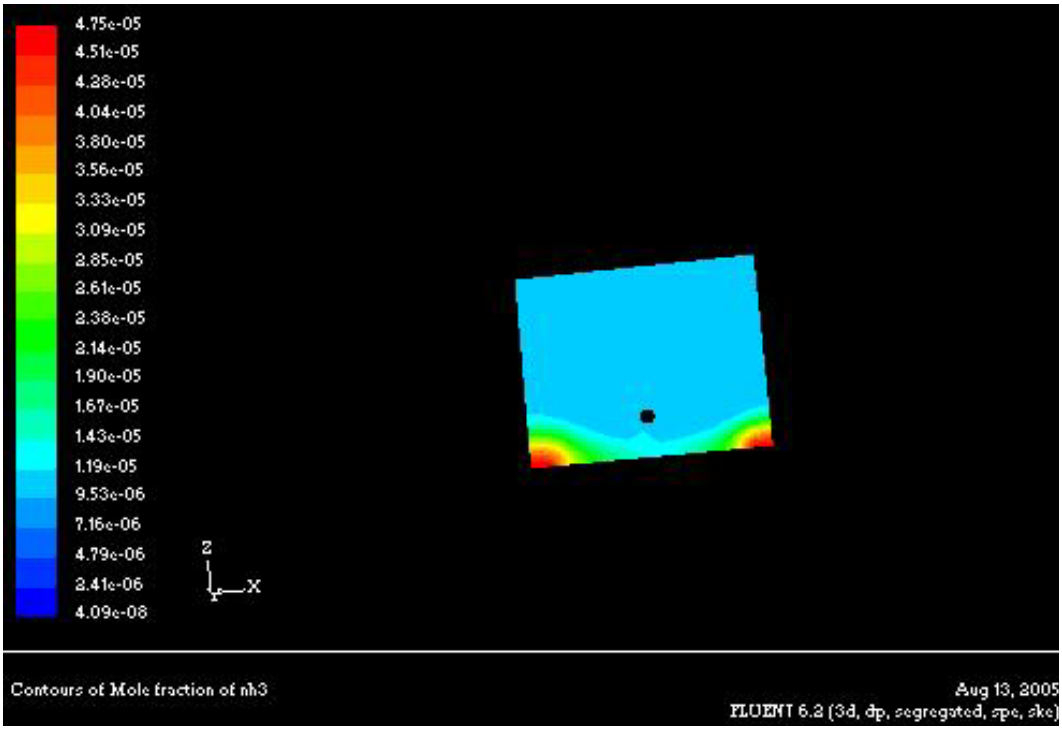

Figure B-17. Contours of NH_3 for OW in Z-X plane (60 ACPH)

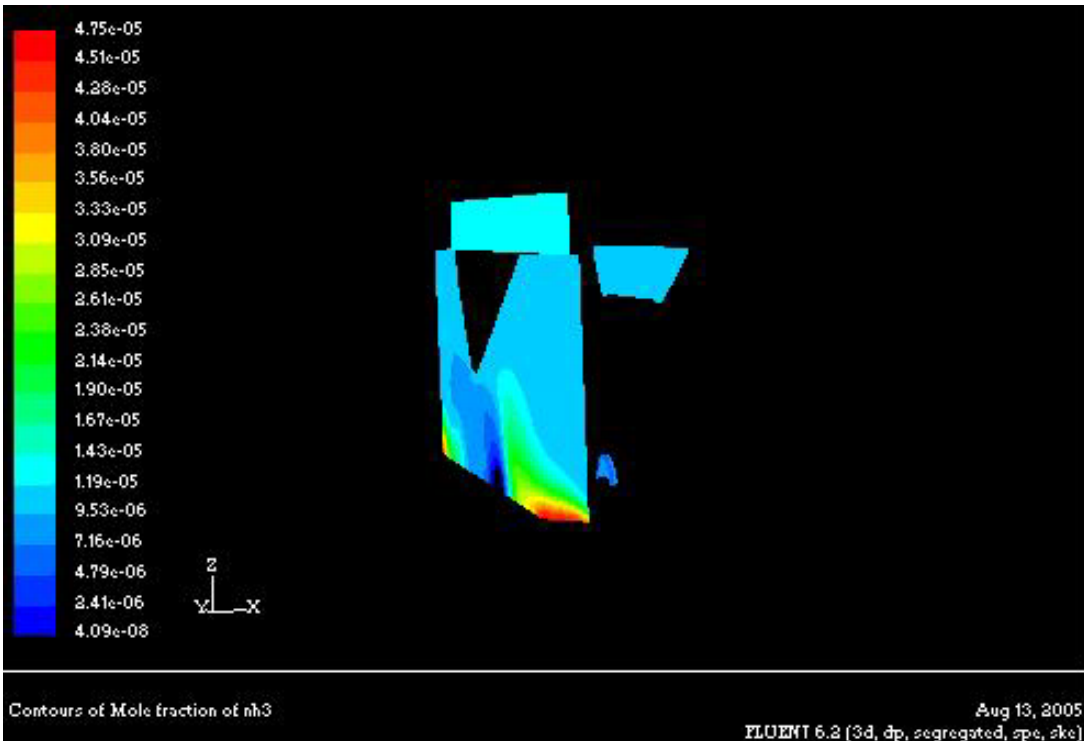

Figure B-18. Contours of NH_3 for OW in X-Y-Z plane (60 ACPH)

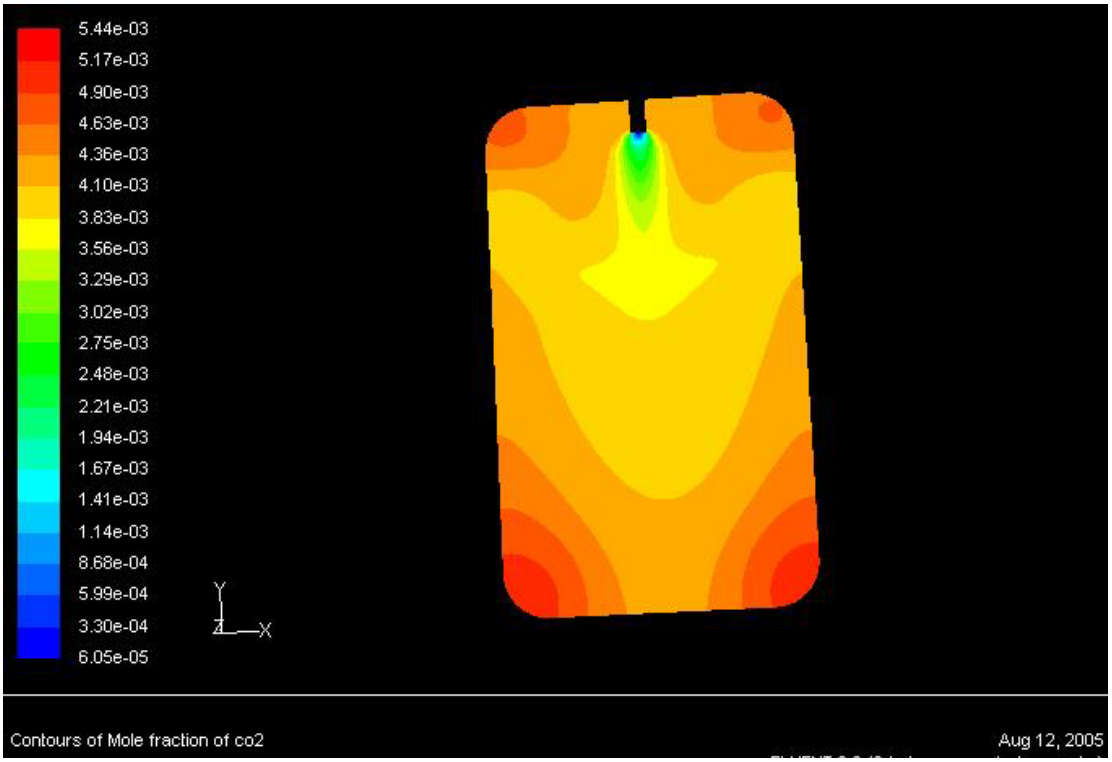

Figure B-19. Contours of CO_2 for CC in X-Y plane (20 ACPH)

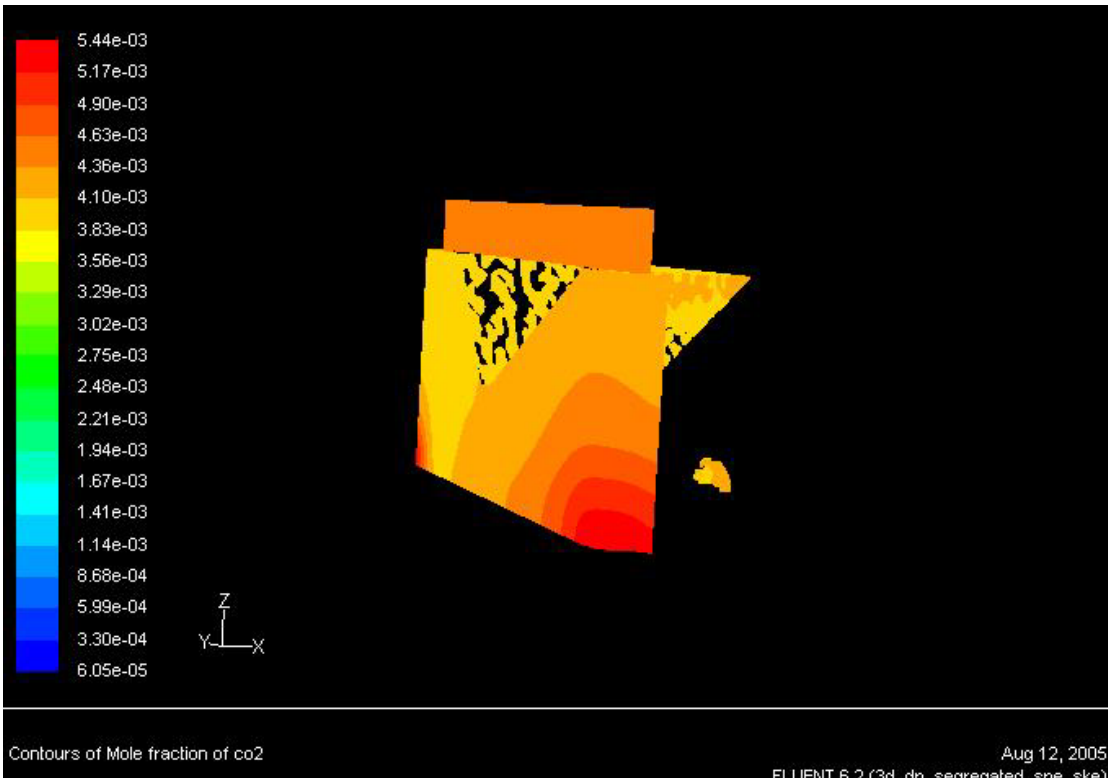

Figure B-20. Contours of CO_2 for CC in X-Y-Z plane (20 ACPH)

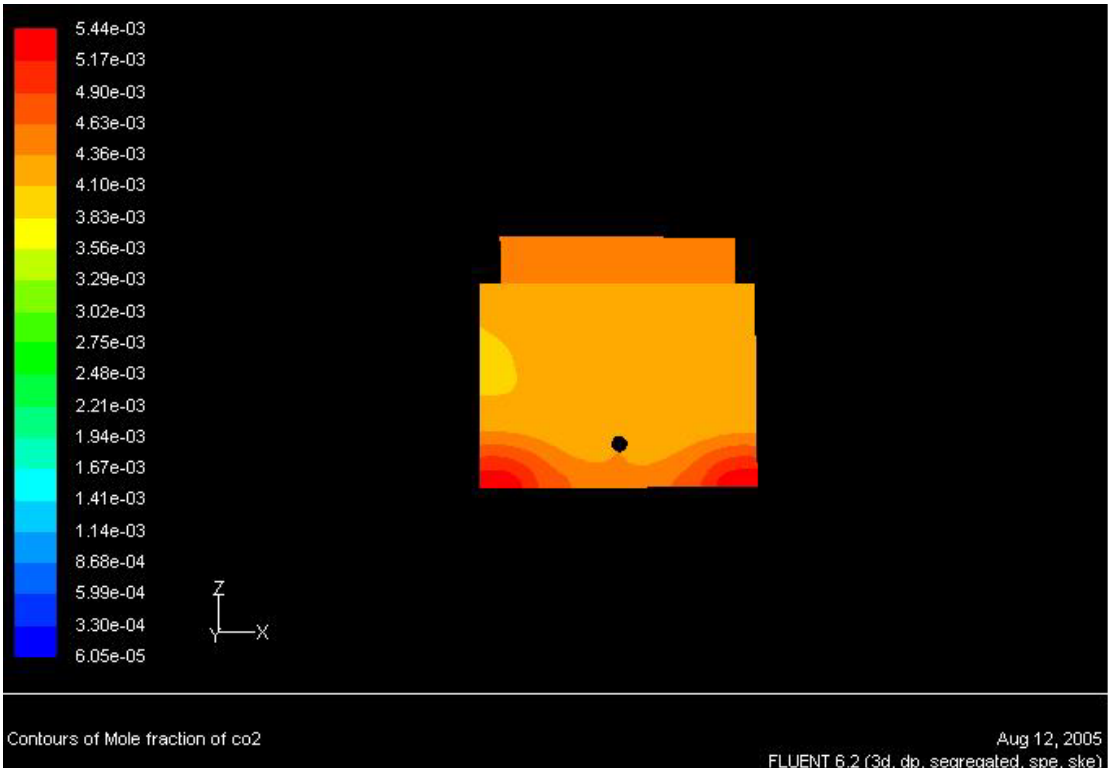

Figure B-21. Contours of CO_2 for CC in Z-X plane (20 ACPH)

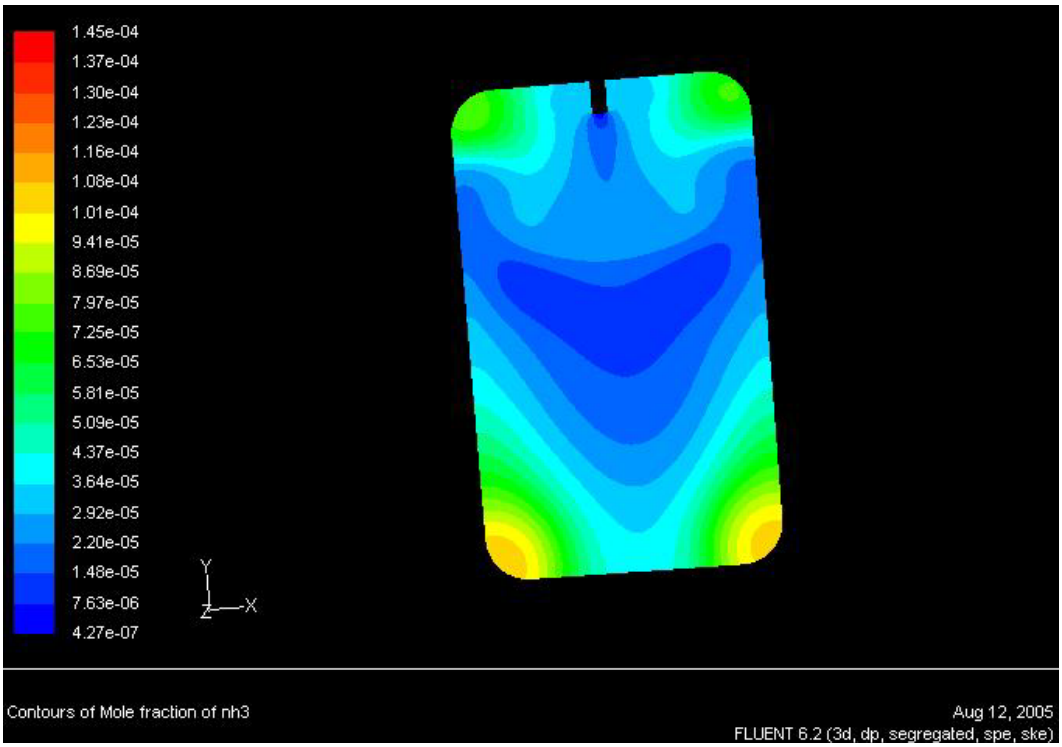

Figure B-22. Contours of NH_3 for CC in X-Y plane (20 ACPH)

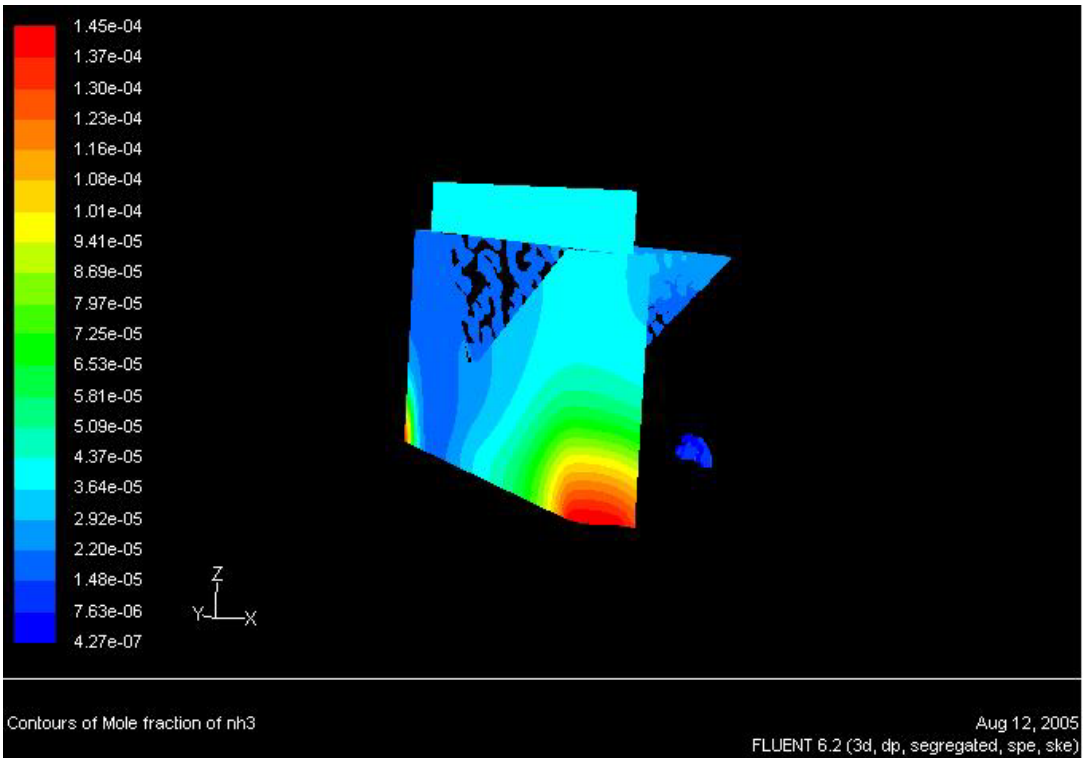

Figure B-23. Contours of NH_3 for CC in X-Y-Z plane (20 ACPH)

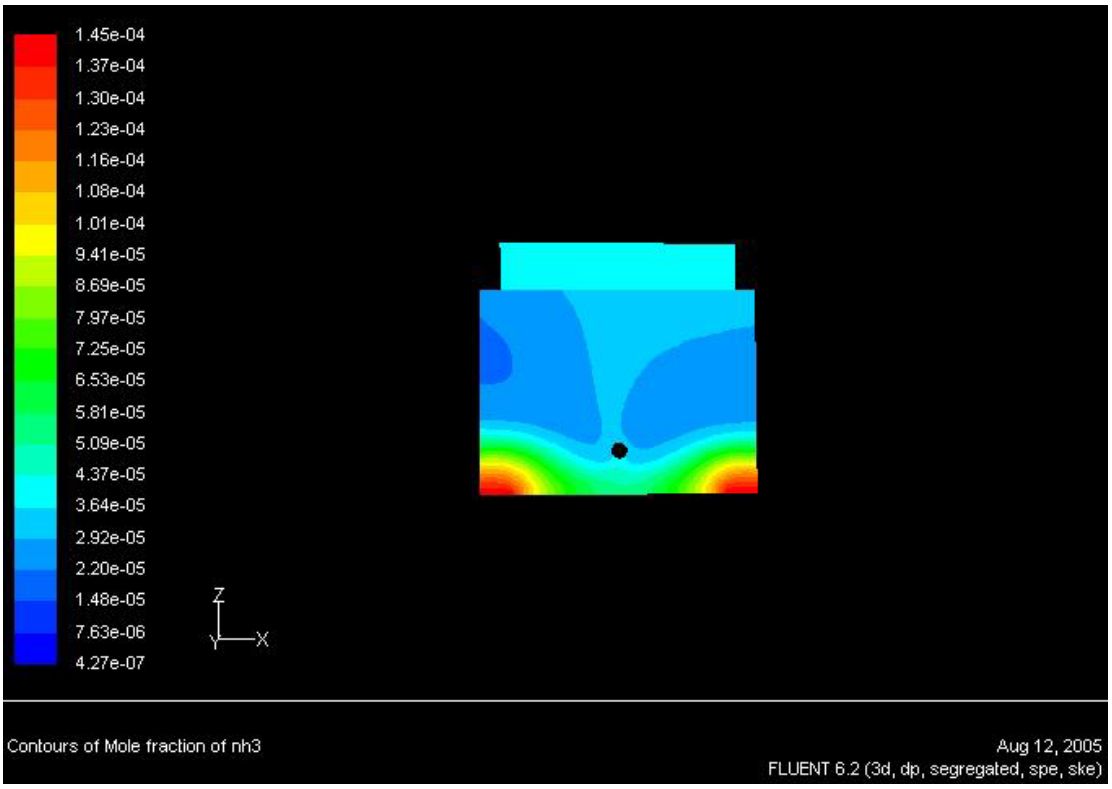

Figure B-24. Contours of NH_3 for CC in Z-X plane (20 ACPH)

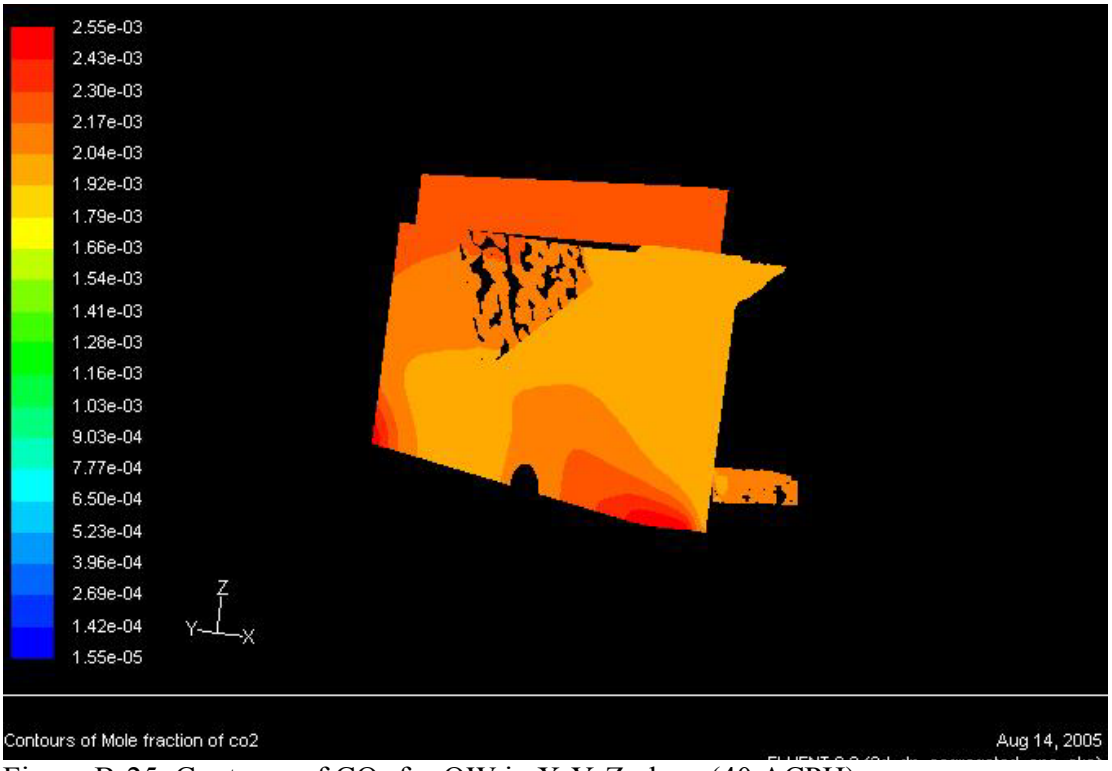

Figure B-25. Contours of CO_2 for OW in X-Y-Z plane (40 ACPH)

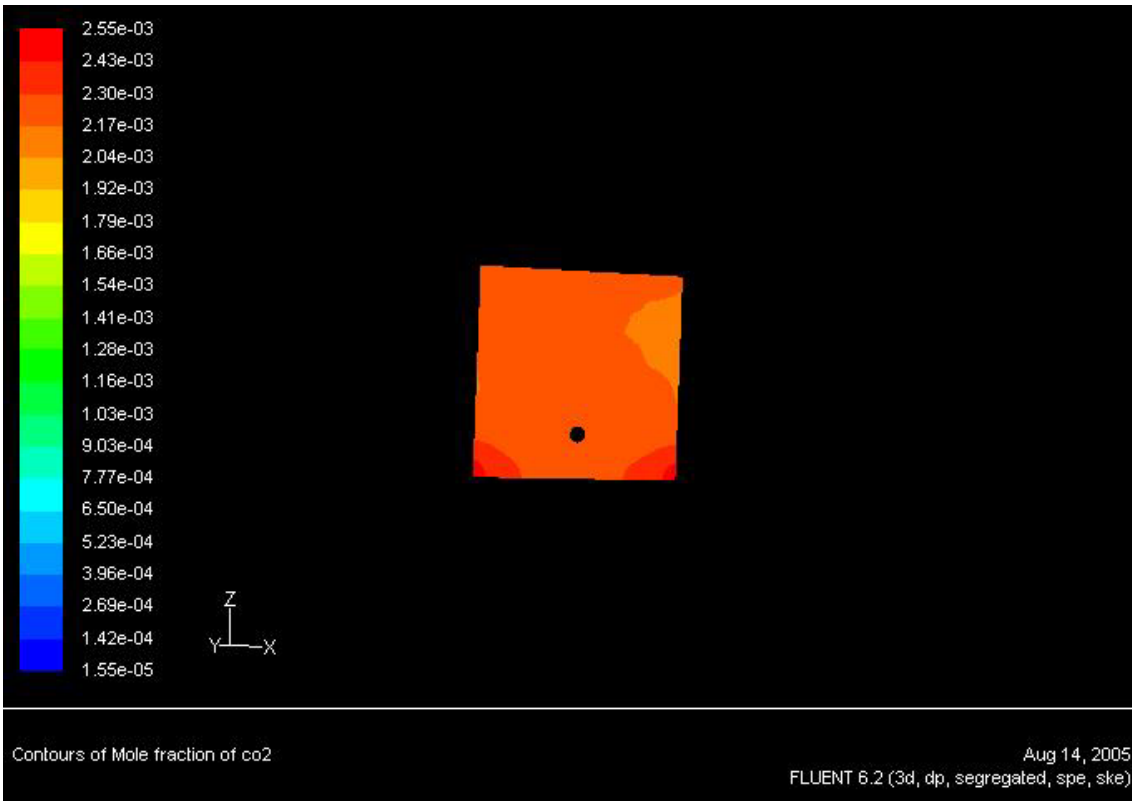

Figure B-26. Contours of CO_2 for OW in Z-X plane (40 ACPH)

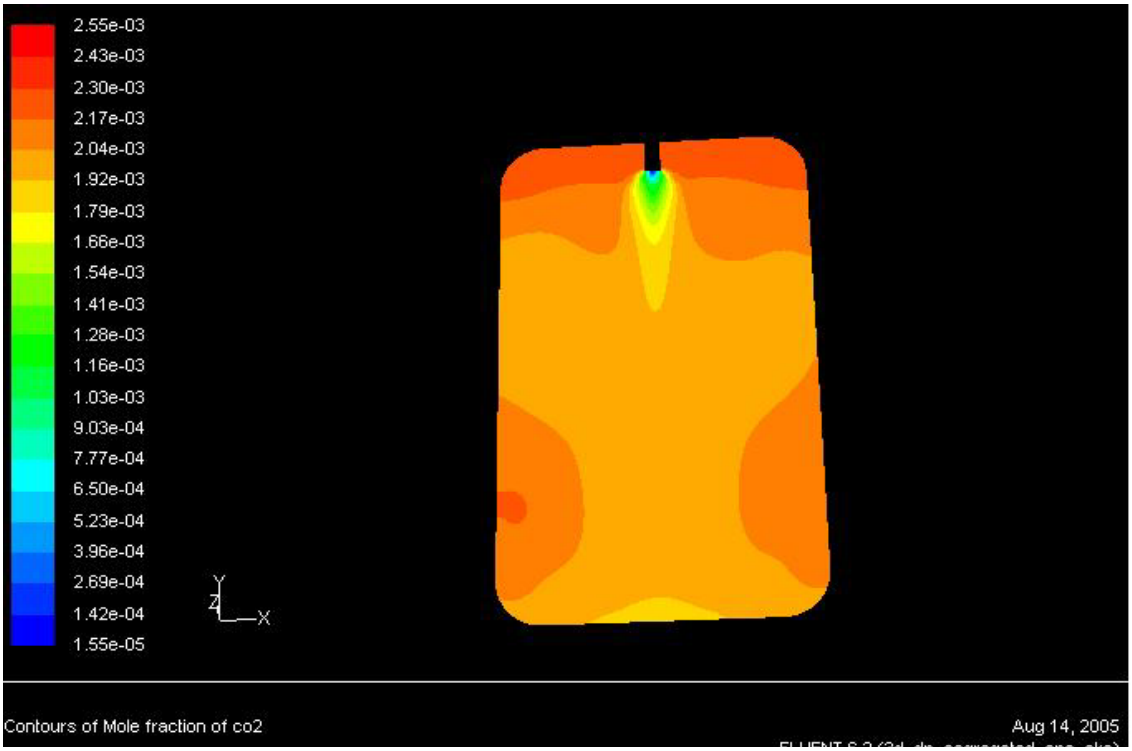

Figure B-27. Contours of CO_2 for OW in X-Y plane (40 ACPH)

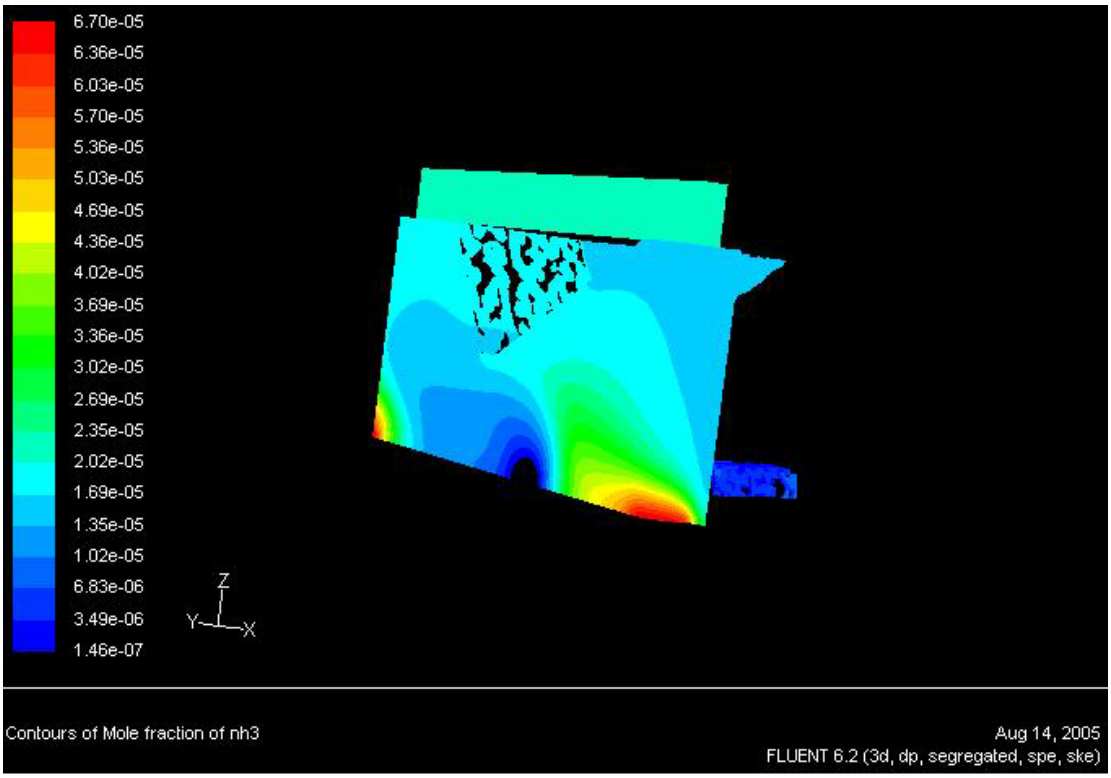

Figure B-28. Contours of NH_3 for OW in X-Y-Z plane (40 ACPH)

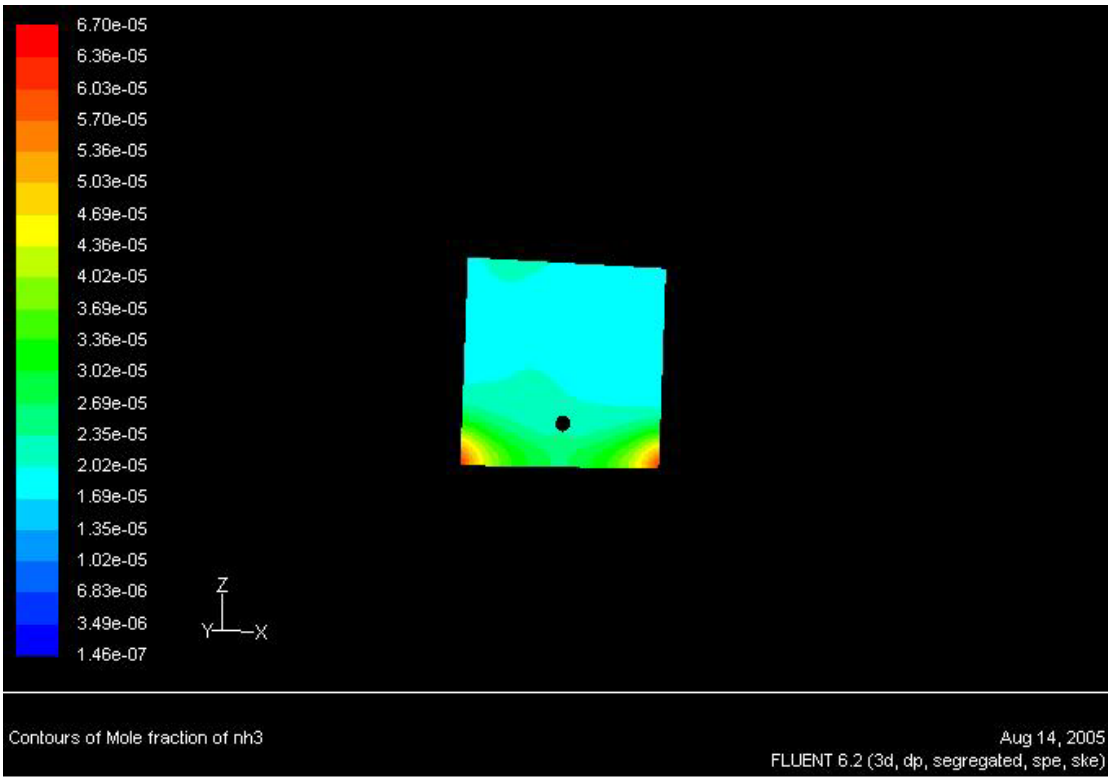

Figure B-29. Contours of NH_3 for OW in Z-X plane (40 ACPH)

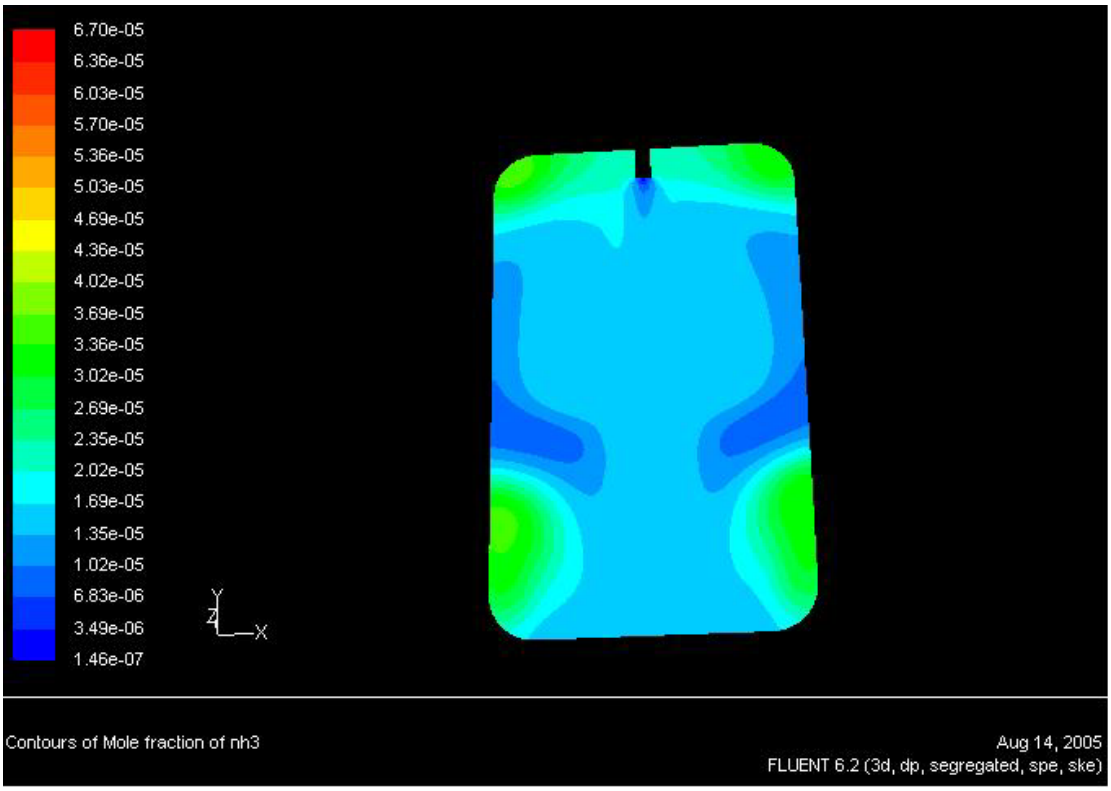

Figure B-30. Contours of NH_3 for OW in X-Y plane (40 ACPH)

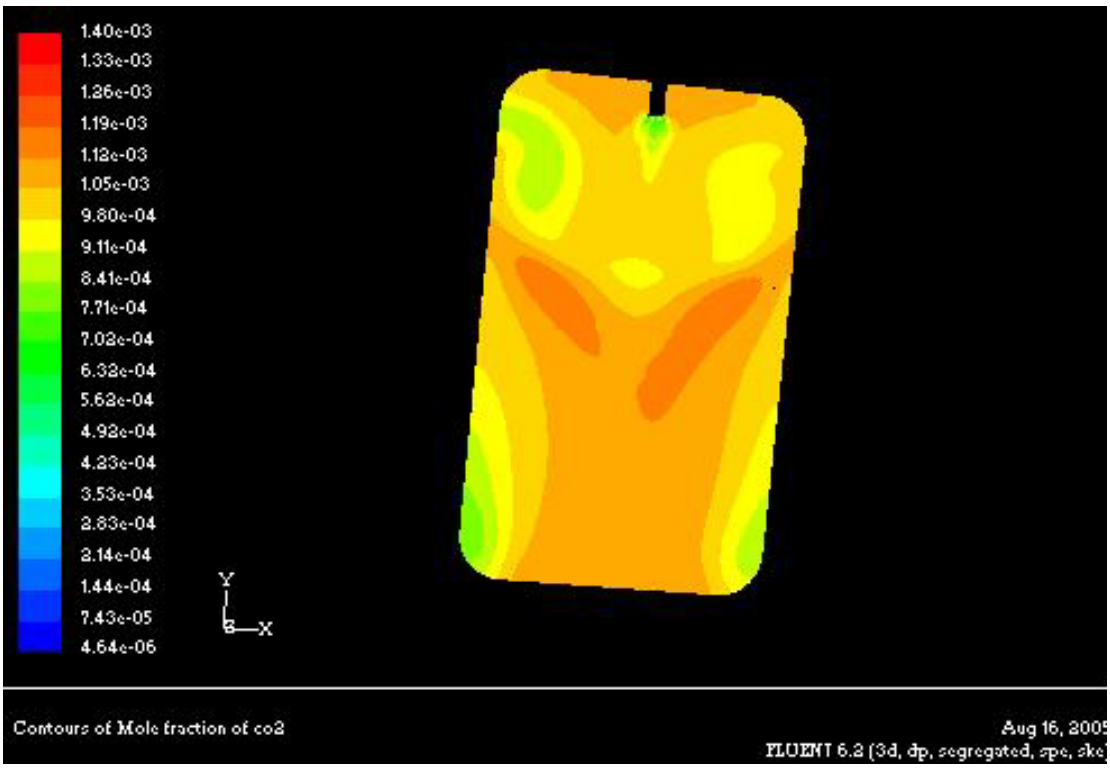

Figure B-31. Contours of CO_2 for CC in X-Y plane (60 ACPH)

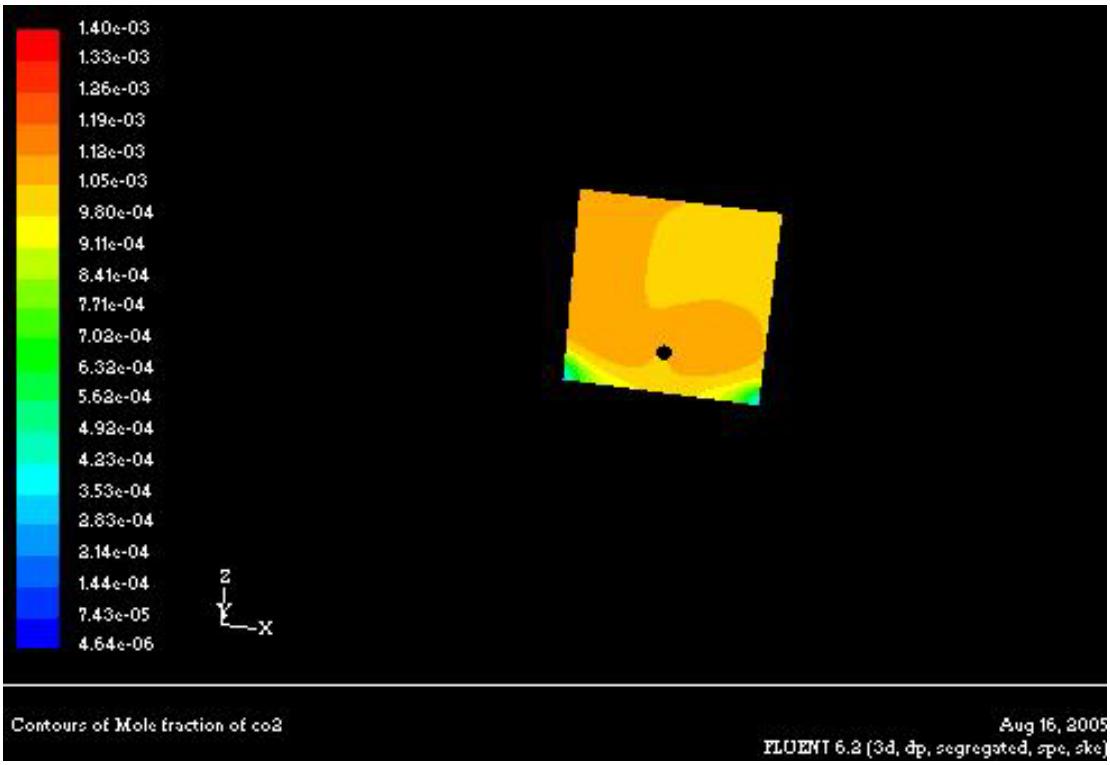

Figure B-32. Contours of CO_2 for CC in Z-X plane (60 ACPH)

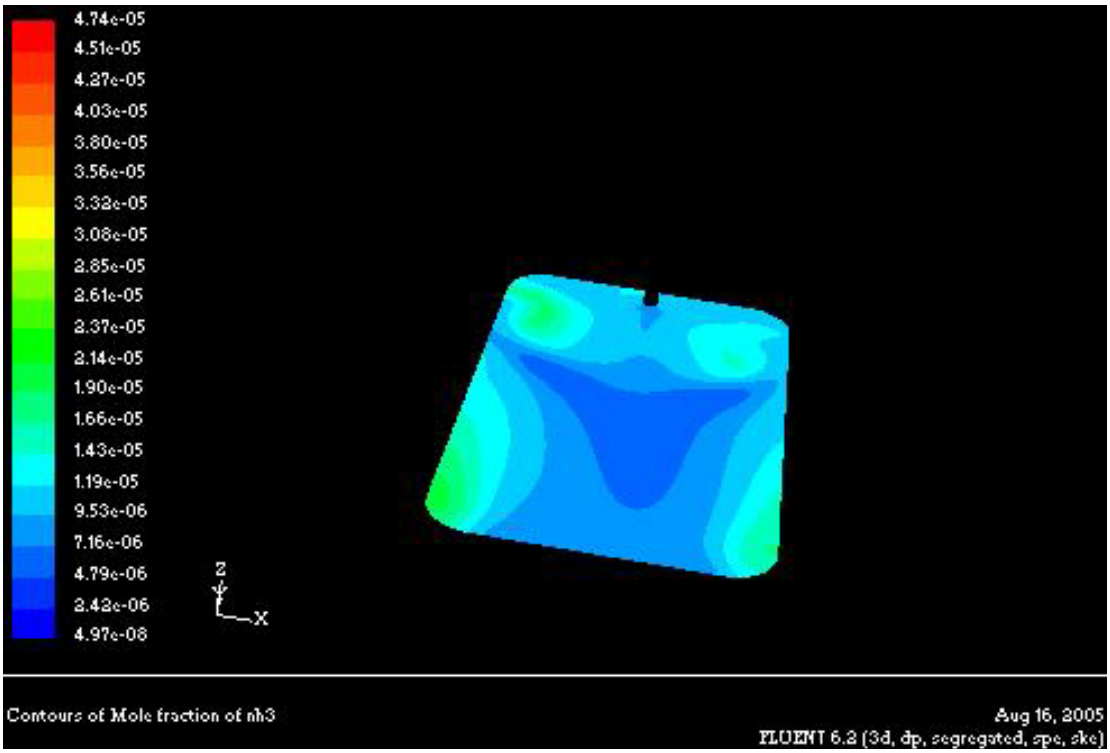

Figure B-33. Contours of NH_3 for CC in X-Y plane (60 ACPH)

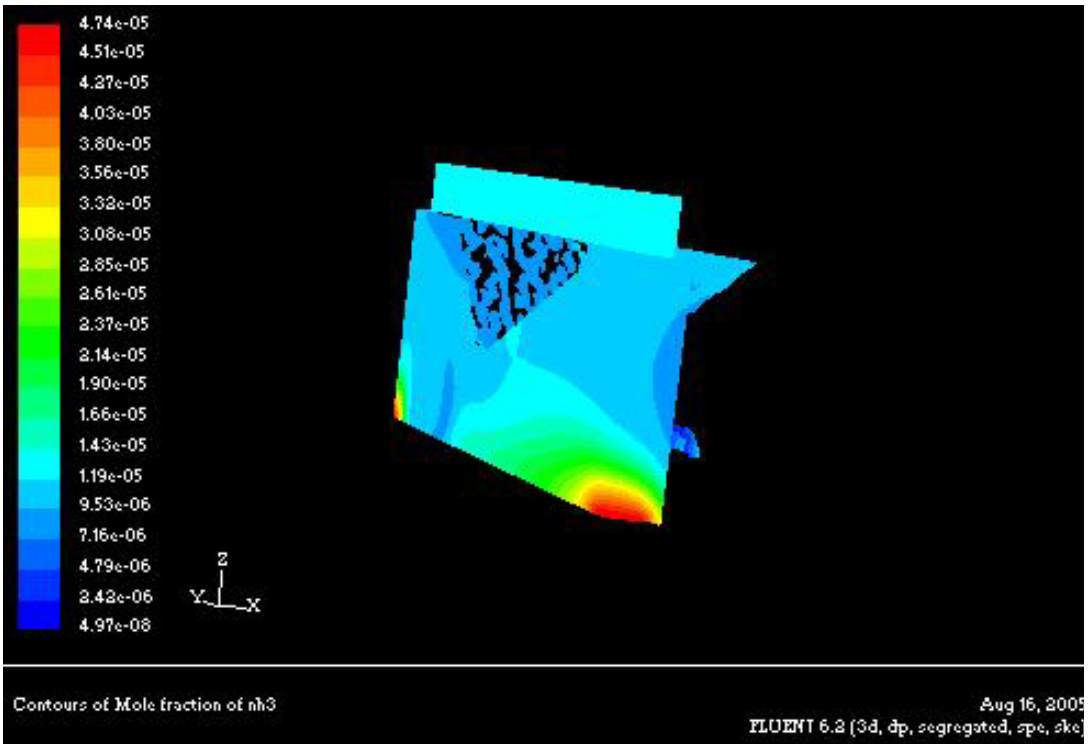

Figure B-34. Contours of NH_3 for CC in X-Y-Z plane (60 ACPH)

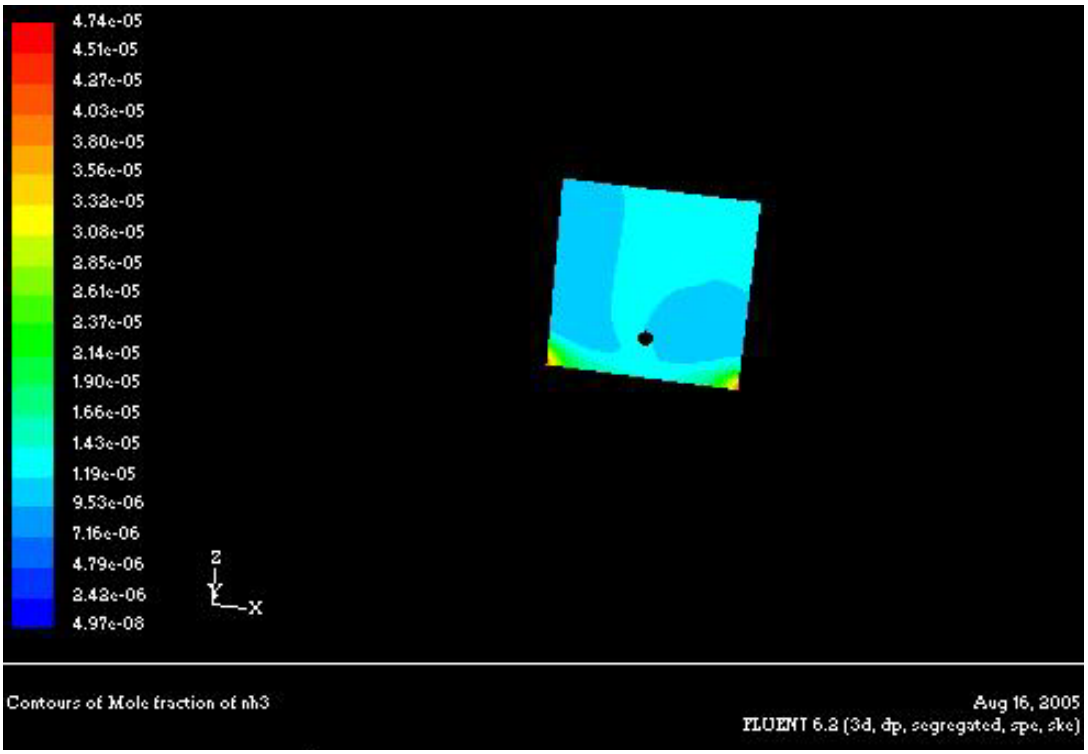

Figure B-35. Contours of NH_3 for CC in Z-X plane (60 ACPH)

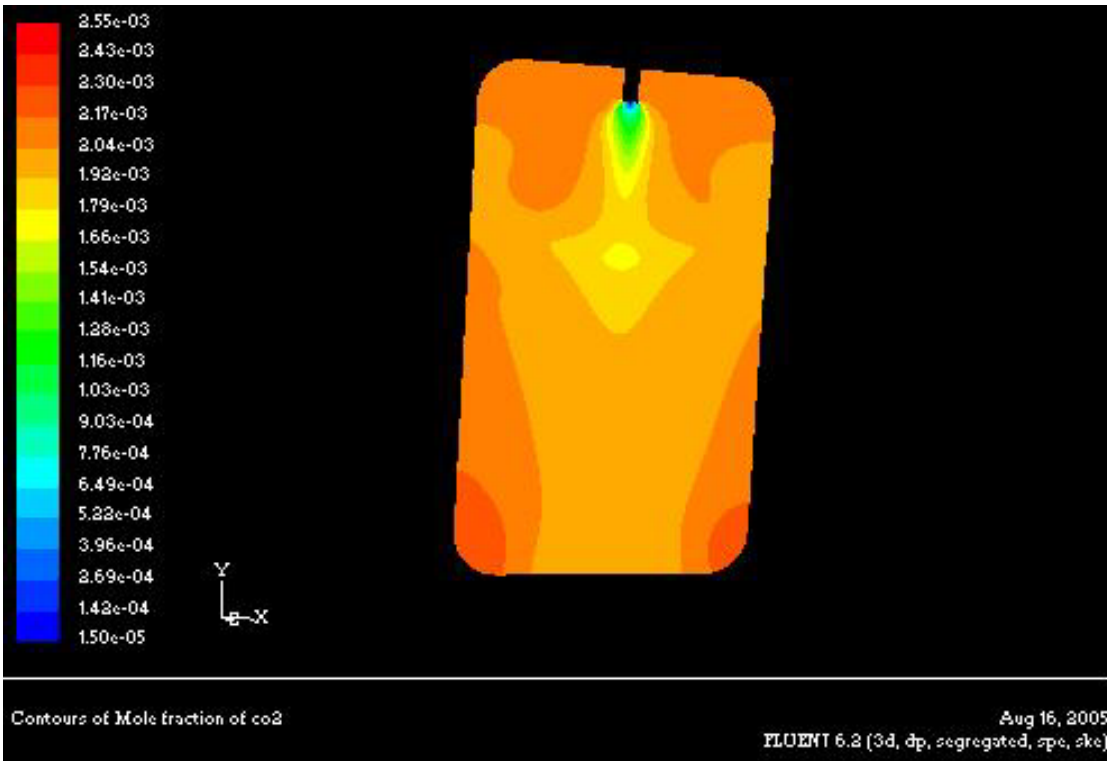

Figure B-36. Contours of CO_2 for CC in X-Y plane (40 ACPH)

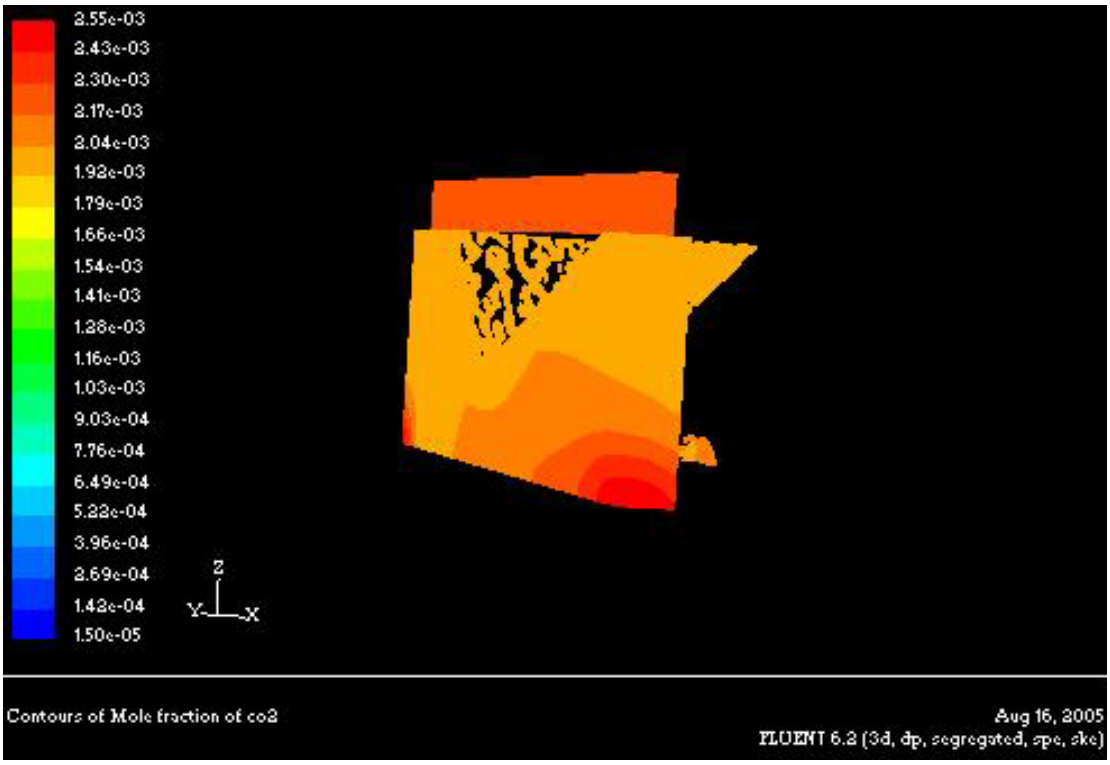

Figure B-37. Contours of CO_2 for CC in X-Y-Z plane (40 ACPH)

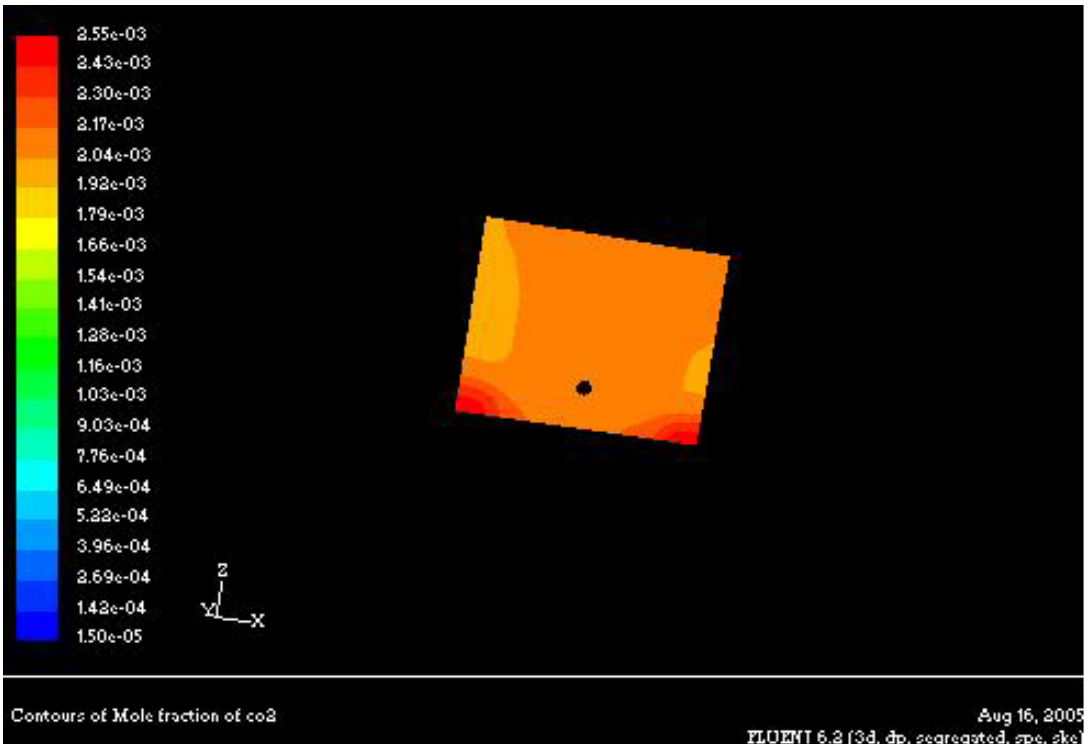

Figure B-38. Contours of CO_2 for CC in Z-X plane (40 ACPH)

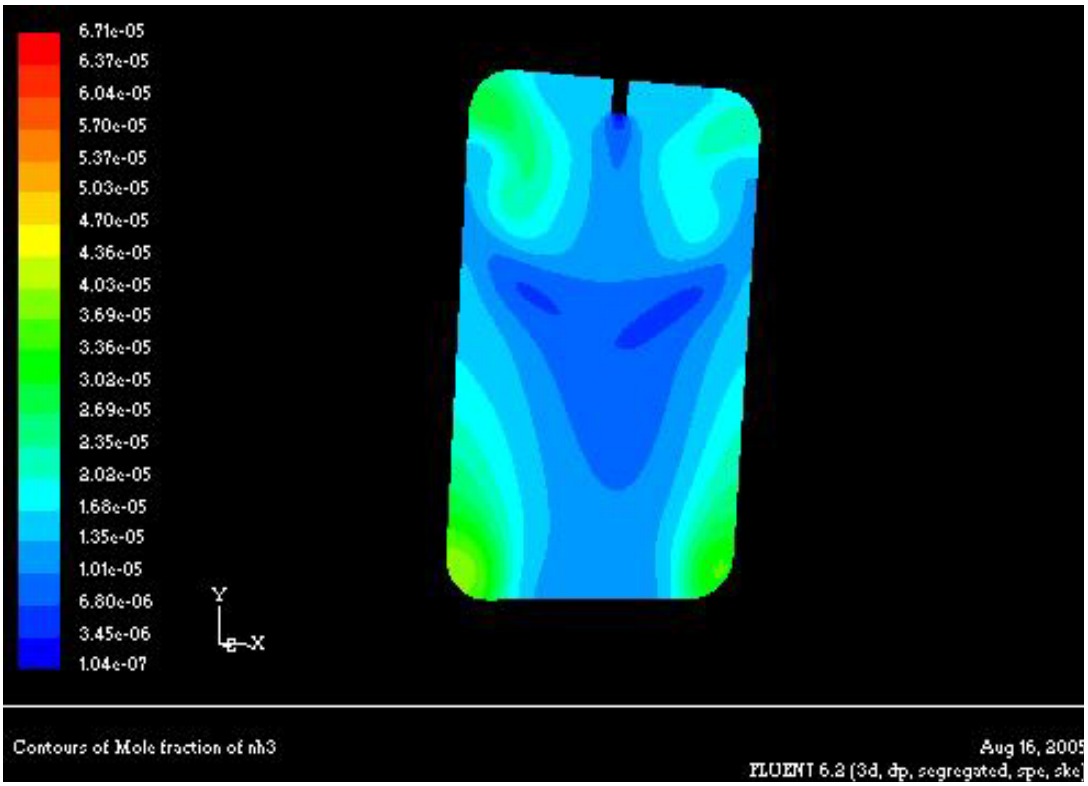

Figure B-39. Contours of NH_3 for CC in X-Y plane (40 ACPH)

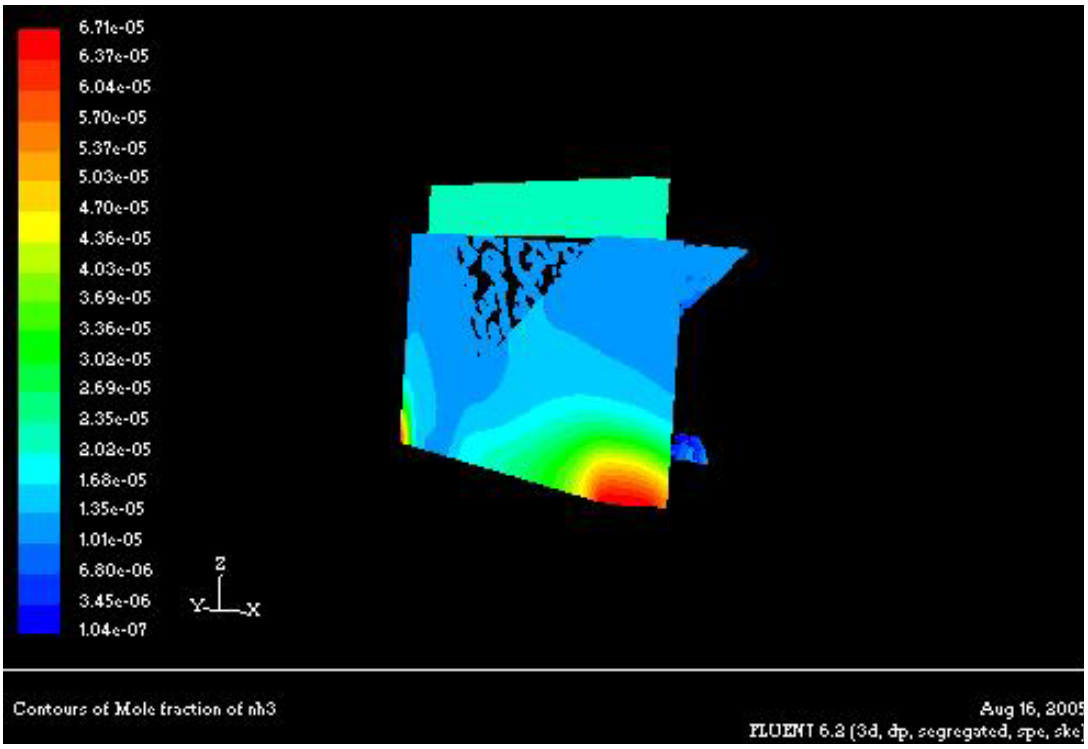

Figure B-40. Contours of NH_3 for CC in X-Y-Z plane (40 ACPH)

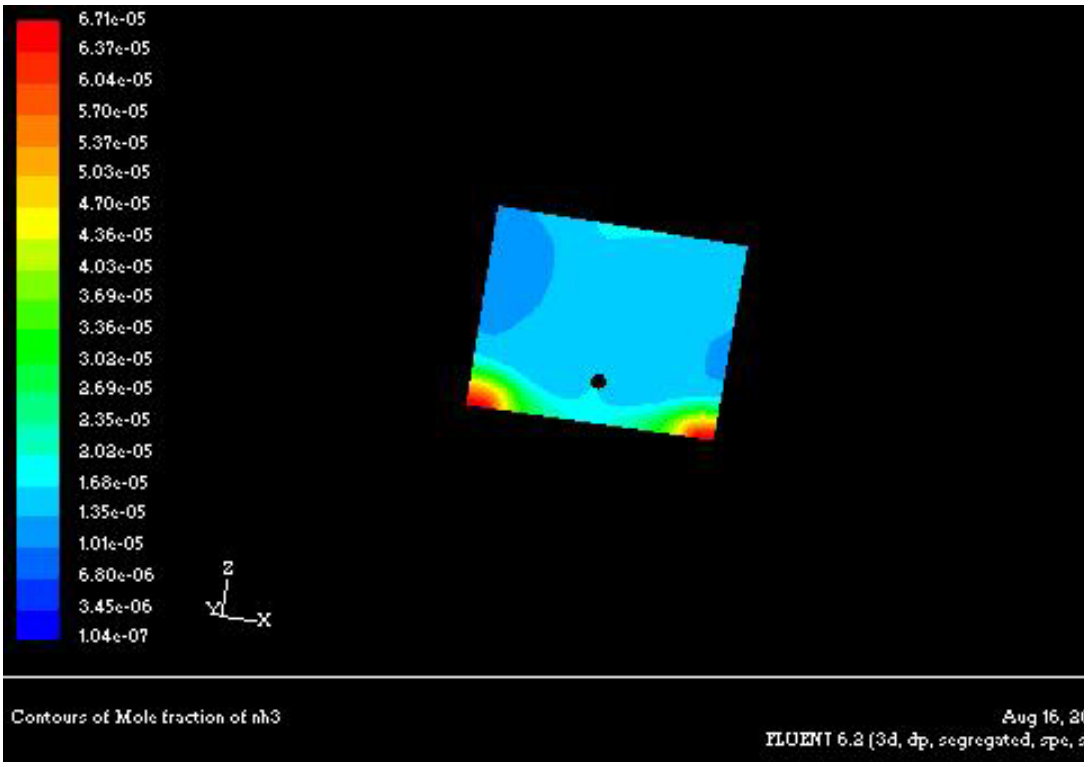

Figure B-41. Contours of NH_3 for CC in Z-X plane (40 ACPH)

APPENDIX C
CALCULATIONS FOR POWER CONSUMPTION AND SAVINGS

As the flow rate of air decreases from 100 to 60 to 40 to 20 ACPH the power consumed by the ventilation fan also decreases. As typical ventilated rack contains 140 cages, so the change in power consumed for 140 cages can be estimated:

The mass flow rate in cubic feet per minute for 100 ACPH $Q_1 = 0.460079$ ft^3/min

Q_1 for 140 cages= 64.411 ft^3/min

The power at 100 ACPH is P_1

The volume flow rate in cubic feet per minute for 60 ACPH $Q_2 = 0.276047$ ft^3/min

Q_2 for 140 cages= 38.647 ft^3/min

The power at 60 ACPH is P_2

Savings at 60 ACPH is S_1

The volume flow rate in cubic feet per minute for 40 ACPH $Q_3 = 0.184032$ ft^3/min

Q_3 for 140 cages= 25.764 ft^3/min

The power at 40 ACPH is P_3

Savings at 40 ACPH is S_2

The volume flow rate in cubic feet per minute for 20 ACPH $Q_4 = 0.092016$ ft^3/min

Q_4 for 140 cages= 12.882 ft^3/min

The power at 20 ACPH is P_4

Savings at 20 ACPH is S_3

The volume flow rate in cubic feet per minute for 30 ACPH $Q_4 = 0.138024$ ft^3/min

Q_5 for 140 cages= 19.323 ft^3/min

The power at 30 ACPH is P_5

Savings at 30 ACPH is S_4

As air change rate is reduced from 100 to 60 ACPH based on the fan law the change in power consumed can be calculated:

$P_1/P_2= (Q_1/Q_2)^3$

We get $P_2= .216P_1$

Similarly

$P_3= 0.063P_1$

$P_4= 0.007P_1$

$P_5= 0.027P_1$

The savings that can be obtained per year by reducing the airflow rate from 100 ACPH to 20 ACPH can be calculated:

$S_3= (P_1-0.007P_1)$

$S_3= 0.993P_1$

Assuming \$0.08 per kilowatt-hour, savings per year can be calculated:

$S_3= 24*365*.993P_1*0.08$

$S_3= \$695.9P_1$ per year

Similarly

$S_1= \$549.4P_1$

$S_2= \$656.6P_1$

$S_4= \$681.9P_1$

APPENDIX D
CALCULATIONS FOR VERIFICATION OF MASS FLOW RATE

For 100 ACPH for Center of Cage case
The most prevalent CO_2 concentration in the cage is in the range of 850-970 ppm.
Assuming the CO_2 coming out of the cage to be C_o= 970 ppm
The volumetric flow rate is F= 0.000217 cubic meters per second
Concentration of CO_2 entering the cage C_i= 350 ppm
C_o-C_i= 970-350= 620 ppm
For 620 ppm the mass flow rate = 620*.000217*44*/(1000000*22.4) = 2.632e-07 kg/s.
Actual mass flow rate= 3.58e-07 kg/s.
Using this mass flow rate and back calculating CO_2 in the cage:
C_o-C_i = 3.58e-07*22.4*1000000/(.000217*44)= 840 ppm
C_o= 840+350= 1190 ppm
% Error in amount of CO_2 leaving the cage= (1190-970)*100/1190= 18.5%
It can be seen that the amount of CO_2 assumed to be leaving the cage is less than amount of CO_2 that should actually leave the cage. This error is due to the fact that the most prevalent concentration is used for the calculation. There are some areas in the cage near the latrines where CO_2 concentration is more than the assumed concentration.

For 60 ACPH for Center of Cage case
The most prevalent CO_2 concentration in the cage is in the range of 980-1130 ppm.
Assuming the most prevalent CO_2 concentration in the cage C_o= 1130 ppm
The volumetric flow rate is F= 0.00013 cubic meters per second
Concentration of CO_2 entering the cage C_i = 350 ppm
C_o-C_i= 1130-350= 780 ppm
For 780 ppm the mass flow rate= 780*.00013*44*/(1000000*22.4)= 2.00e-07 kg/s.
Actual mass flow rate= 3.58e-07 kg/s.
Using this mass flow rate and back calculating CO_2 in the cage:
C_o-C_i= 3.58e-07*22.4*1000000/(.00013*44)= 1400 ppm
C_o= 1400+350= 1750 ppm
% Error in amount of CO_2 leaving the cage= (1750-1130)*100/1750= 35.5%
It can be seen that the amount of CO_2 assumed to be leaving the cage is less than amount of CO_2 that should actually leave the cage. This error is due to the fact that the most prevalent concentration is used for the calculation. There are some areas in the cage near the latrines where CO_2 concentration is more than the assumed concentration.

For 40 ACPH for Center of Cage case
The most prevalent CO_2 concentration in the cage is in the range of 1920-2300 ppm.
Assuming the most prevalent CO_2 concentration in the cage C_o= 2300 ppm
The volumetric flow rate is F= 0.0000869 cubic meters per second
Concentration of CO_2 entering the cage C_i= 350 ppm

$Co-C_i$= 2300-350= 1950 ppm
For 1950 ppm the mass flow rate= 1950*.0000869*44*/(1000000*22.4)= 3.32e-07 kg/s.
Actual mass flow rate used for the analysis was 3.58e-07 kg/s.
Using this mass flow rate and back calculating CO_2 in the cage:
C_o-C_i= 3.58e-07*22.4*1000000/(.0000869*44)= 2098 ppm
C_o= 2098+350= 2448 ppm
% Error in amount of CO_2 leaving the cage= (2448-2300)*100/2448= 6.0%
The error in this case is 6%, which is very small as compared to errors at 100 and 60 ACPH. The CO_2 concentrations agree with the concentration calculated using the mass flow rate of CO_2 used for the simulation.

For 20 ACPH for Center of Cage case
The most prevalent CO_2 concentration in the cage is in the range of 3500-4400 ppm.
Assuming the most prevalent CO_2 concentration in the cage Co= 4400 ppm
The volumetric flow rate is F= 0.0000434 cubic meters per second
Concentration of CO_2 entering the cage C_i= 350 ppm
C_o- C_i= 4400-350= 4050 ppm
For 4050 ppm the mass flow rate= 4050*.0000434*44*/(1000000*22.4)= 3.427e-07 kg/s.
Actual mass flow rate= 3.58e-07 kg/s.
Using this mass flow rate and back calculating CO_2 in the cage:
C_o-C_i= 3.58e-07*22.4*1000000/(.0000434*44)= 4200 ppm
C_o= 4200+350= 4550 ppm
% Error in amount of CO_2 leaving the cage= (4550-4400)*100/4550= 3.0%
The error in this case is 3%, which is very small as compared to errors at 100 and 60 ACPH. The CO_2 concentrations agree with the concentration calculated using the mass flow rate of CO_2 used for the simulation.

APPENDIX E
CASES THAT DID NOT WORK

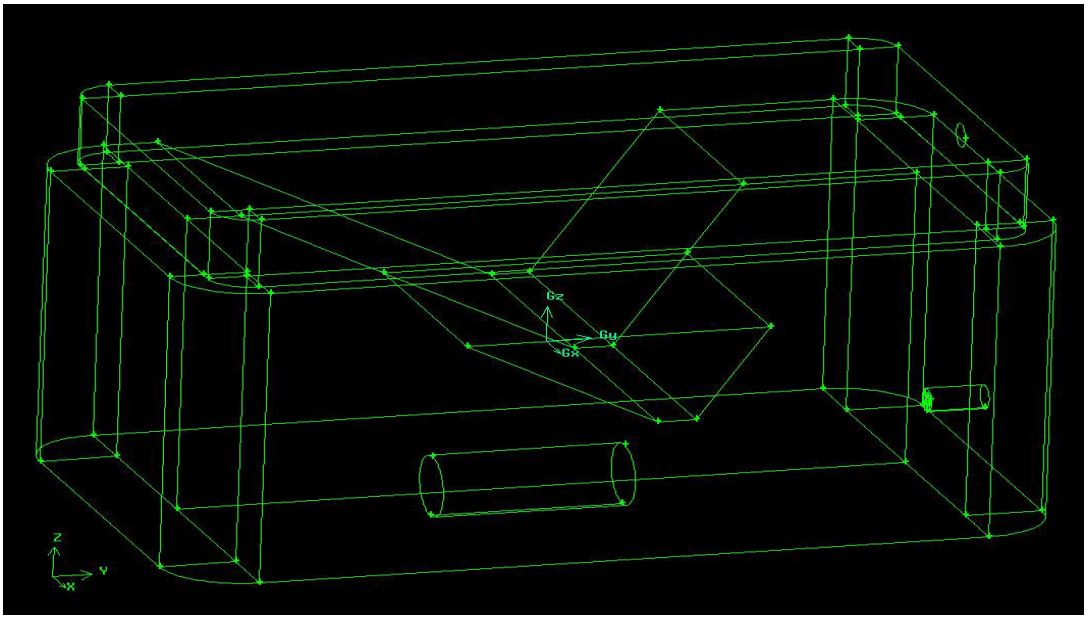

Figure E-1. Single mouse in Y- direction

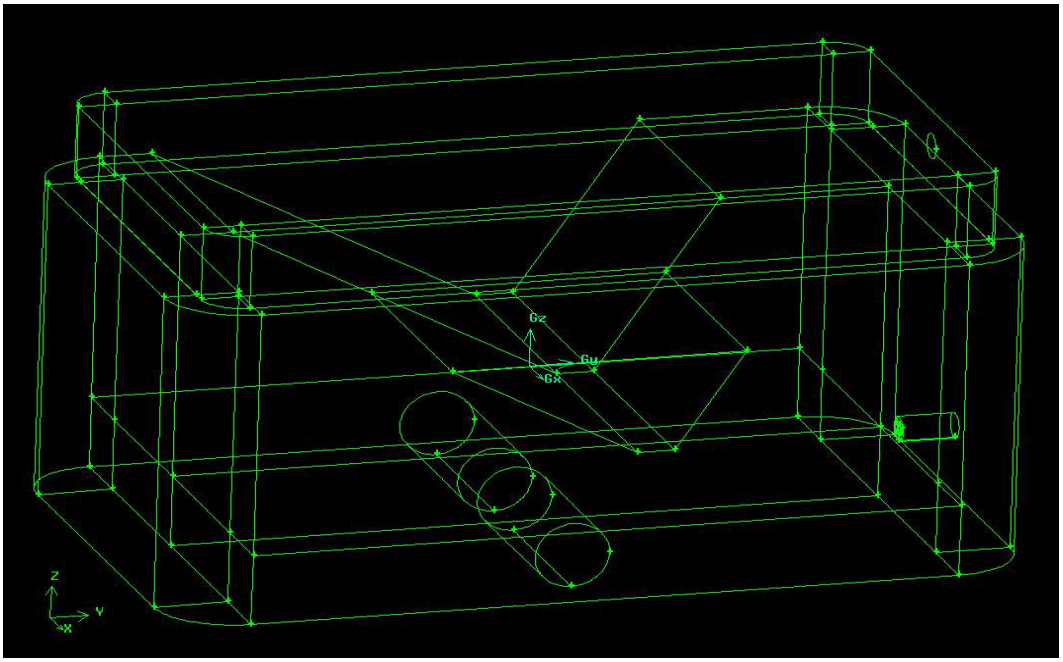

Figure E-2. Two mice in the center of cage in X- direction

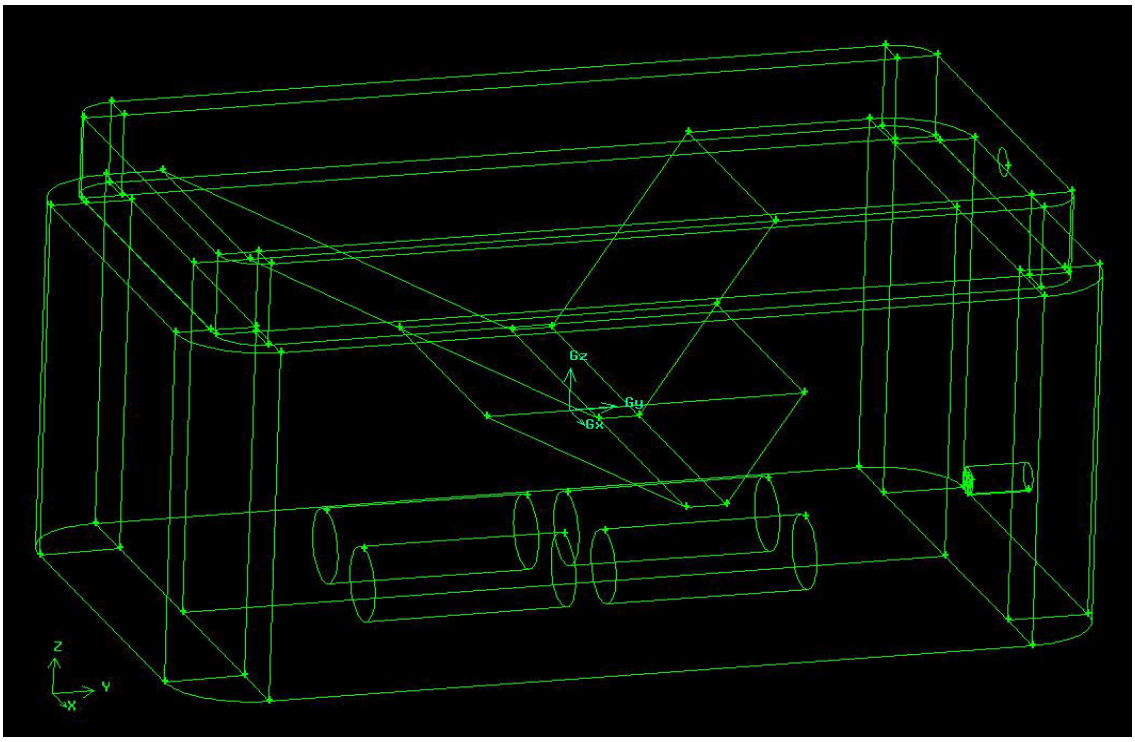

Figure E-3. Four mice in the center of cage in Y- direction

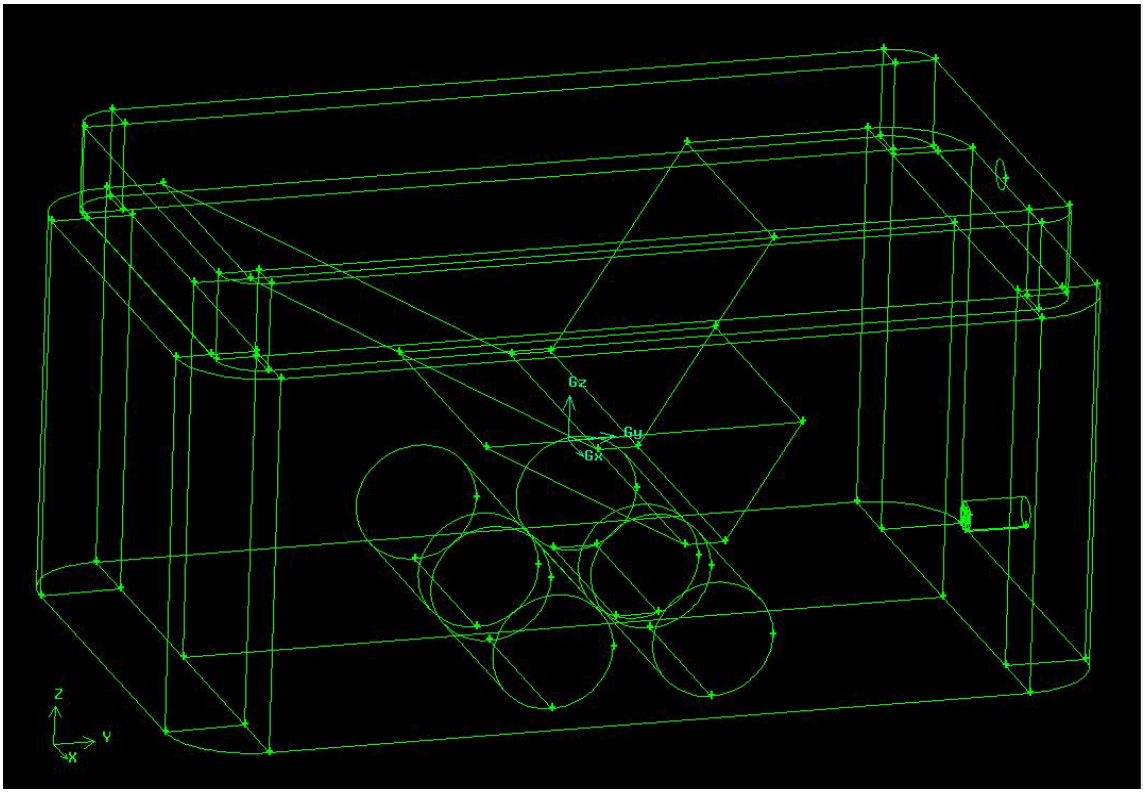

Figure E-4. Four mice in the center of cage in X- direction

APPENDIX F
GOVERNING EQUATIONS

The species concentrations at various points are determined by solving the mass, momentum and energy equations numerically (Turbulent Reacting Flows, by P.A. Libby, F.A. Williams).

The Mass Conservation equation is given as,

$$\frac{\partial \rho}{\partial t} + \frac{\partial}{\partial x_k}(\rho v_k) = 0 \qquad \text{F-1}$$

The momentum conservation equation is given as,

$$\frac{\partial}{\partial t}(\rho v_i) + \frac{\partial}{\partial x_k}(\rho v_k v_i) = -\frac{\partial p}{\partial x_i} + \frac{\partial}{\partial x_k}\tau_{ik} + g_i \qquad \text{F-2}$$

Where g_i is given by

$$g_i = -\rho g \delta_{i3} \qquad \text{F-3}$$

The shear stress τ_{ij} in the equation is expressed as,

$$\tau_{ij} = \mu\left(\frac{\partial v_i}{\partial x_j} + \frac{\partial v_j}{\partial x_i} - \frac{2}{3}\frac{\partial v_k}{\partial x_k}\delta_{ij}\right) \qquad \text{F-4}$$

The conservation of species equation is given as,

$$\frac{\partial}{\partial t}(\rho Y_i) + \frac{\partial}{\partial x_k}(\rho v_k Y_i) = -\frac{\partial}{\partial x_k}J_{ik} + w_i \qquad \text{F-5}$$

From Fick's Law, the turbulent flow mass diffusion equation is given by

$$J_{ij} = -\rho D_i \frac{\partial Y_i}{\partial x_j} \qquad \text{F-6}$$

Now Z_i is given by

$$Z_i \equiv \sum_{j=1}^{N} \mu_{ij} Y_j \qquad \text{F-7}$$

$$\sum_{i=1}^{M} Z_i = 1 \qquad \text{F-8}$$

As the chemical elements are conserved, we have for each element

$$\sum_{j=1}^{N} \mu_{ij} w_j = 0 \qquad \text{F-9}$$

Thus the conservation equation for elements is given by

$$\frac{\partial}{\partial t}(\rho Z_i) + \frac{\partial}{\partial x_k}(\rho v_k Z_i) = \frac{\partial}{\partial x_k} \sum_{i=1}^{N} \rho \mu_{il} D_l \frac{\partial Y_i}{\partial x_k} \qquad \text{F-10}$$

If $D_i = D$ then

$$\frac{\partial}{\partial t}(\rho Z_i) + \frac{\partial}{\partial x_k}(\rho v_k Z_i) = \frac{\partial}{\partial x_k} \rho D \frac{\partial Z_i}{\partial x_k} \qquad \text{F-11}$$

Turbulent flow was considered for the numerical analysis of the model and k-ε method was used to solve the model. The following transport equations are used in the k-ε model (FLUENT Inc., 2005)

$$\mu_T = c_\mu \overline{\rho} \frac{\widetilde{k}^2}{\widetilde{\varepsilon}_k} \qquad \text{F-12}$$

$$\frac{\partial}{\partial x_k} \rho\kappa + div(\rho k U) = div[(\mu + \frac{\mu_t}{\sigma_k}) grad k] + 2\mu_t Ei_j Ei_j - \rho\varepsilon \qquad \text{F-13}$$

$$\frac{\partial}{\partial x_k} \rho\varepsilon + div(\rho\varepsilon U) = div[(\mu + \frac{\mu_t}{\sigma_\varepsilon}) grad \varepsilon] + C_{1\varepsilon} 2\mu_t E_{ij} E_{ij} - C_{2\varepsilon} \rho \frac{\varepsilon^2}{\kappa} \qquad \text{F-14}$$

LIST OF REFERENCES

Fluent Incorporated, 2005. Fluent 6.2 Documentation, Lebanon, NH.

Hasegawa, Masakazu, Kurabayashi, Yuzuru, Ishii, Toshinori, Yoshida, Kazuya, Uebayashu, Nobukazu, Sato, Norimitsu, Kurosawa, Tsutomu, 1997. "Intra-Cage Air Change Rate on Forced-Air-Ventilated Micro-Isolation System-Environment within Cages: Carbon Dioxide and Oxygen Concentration," Experimental Animal Sciences, Vol 46(4), 251-257.

Hoglund, A.U., Renstrom, A., 2001. "Evaluation of Individually Ventilated Cage Systems for Laboratory Rodents: Cage Environment and Animal Health Aspects," Animals, Vol 35, 51-57.

Institute of Laboratory Animal Resources, 1996. Guide for the Care and Use of Laboratory Animals, National Academy Press, Washington, DC.

Krohn, Thomas C., Hansen, Axel K., 2002. "Carbon Dioxide Concentrations in Unventilated IVC Cages," Laboratory Animals, Vol 36, 209-212.

Krohn, Thomas C., Hansen, Axel K., Dragsted, Nils, 2003A. "The Impact of Cage Ventilation on Rats Housed in IVC Systems," Laboratory Animals, Vol 37, 85-93.

Krohn, Thomas C., Hansen, Axel K., Dragsted, Nils, 2003B. "The Impact of Low Levels of Carbon Dioxide on Rats," Laboratory Animals, Vol 37, 94-99.

Libby, P.A., Williams, F.A., 1993. Turbulent Reacting Flows, Academic Press, San Diego, CA.

Memarzadeh, F., Harisson, P. C., Riskowski, G. L., Henze, T., 2004. "Comparison of Environment and Mice in Static and Mechanically Ventilated Isolator Cages with Different Air Velocities and Ventilation Designs," Contemporary Topics in Lab Animal Science, Vol 43(1), 14-20.

Pandey, A., 2005. "Computational Fluid Dynamics Study of Ventilated Cages for Laboratory Animals," Master's Thesis, University of Florida, Gainesville, FL.

Reeb, C. K., Paigen, B., Beamer, W. G., Bronson, R. T., Churchill, G. A., Schweitzer, I. B., Myers, D. D., 2001. "The Impact of Reduced Frequency of Cage Changes on the Health of Mice Housed in Ventilated Cages," Laboratory Animals, Vol 35, 58-73.

Smith, E., Stockwell, J.D., Schweitzer, I., Langley, S.H., Smith, A. L., 2004. "Evaluation of Cage Micro-Environment of Mice Housed on Various Types of Bedding Materials," Contemporary Topics in Lab Animal Science, Vol 43(4), 12-7.

White, W.J., 2001. "A Guide to Research Rodent Housing," http://www.criver.com/research_models_and_services/research_models/rm_td_biosecurity_housing.pdf, accessed Gainesville, August 2005.

BIOGRAPHICAL SKETCH

Jatin Lamba was born on June 9th, 1980, in Faridabad, Haryana, India. He completed his high school from Faridabad. He started his bachelor's in engineering in Bharati Vidyapeeth College of Engineering in Pune, Maharashtra, India. However he transferred to Pittsburg State University after two years of engineering and then graduated from Pittsburg State in May 2003. He then enrolled in the University of Florida in the fall of 2003 to pursue his master's in mechanical engineering.